DEVELOPMENT OF SIDEROPHORE-BASED NOVEL DIAGNOSTIC SYSTEMS FOR BACTERIAL INFECTIONS

A DISSERTATION
SUBMITTED TO THE FACULTY OF
UNIVERSITY OF MINNESOTA
BY

Thakshila Madushani Wickramaratne

IN PARTIAL FULFILLMENT OF THE REQUIREMENTS
FOR THE DEGREE OF
DOCTOR OF PHILOSOPHY

Dr. Philippe Buhlmann

August 2015

Acknowledgements

The work described here would not have been successful without Dr. Valerie Pierre. I would like to thank her for being a wonderful adviser to me for years. Not only as a research adviser, but also as an instructor of Inorganic Chemistry course where I was a teaching assistant, I learned a lot of things from her.

I would like to thank Dr. Phil Buhlmann for all his support and guidance along the path to finish my PhD dissertation. Amidst a very busy schedule as the Director of Graduate Studies, he never hesitated to read my thesis several times and give me constructive feedback. I have no words to express my gratitude towards him for holding my hand and being beside me at all times when I needed him. I would also like to thank Dr. Bill Tolman, the Chair of the Department of Chemistry, for making sure that I progress towards the completion of my thesis with peace in my mind.

I would also like to thank past and present Pierre group members. Dr. Eric Smolensky was a very cheerful person all the time and he was very helpful in giving good comments for my oral exam. Dr. Katie Peterson helped me a lot in proof reading and correcting my writing and giving very good suggestions for improvement. Also she was the one who trained me on column chromatography where I became an expert at the end. Katie was very good at giving constructive feedback for presentations as well. Jennifer Koezly was a great co-worker with whom I worked together on biological studies of a project. Dr. Kriti Srivastava, Sarah Harris, Evan Weitz were all friends who were there to share both happiness and frustrations. Brian Hanson and James Herndon were two skillful undergraduates who worked with me for short time periods. Thank you all for your help and support.

I should also thank Dr. Aidan McDonald who was my very first mentor in the Que lab. I did learn a lot of organic and inorganic synthesis techniques from him. Dr. Matthew Cranswick and Dr. Kathy van Heuvalen are two other wonderful colleagues whom I highly appreciate. They all have a very high level of understanding in Chemistry. Matt and Kathy were mentors, friends and I can even say they were like family members. I would also like to thank all my teachers from elementary school until today, who taught me at least a single letter or who gave me a single piece of advice to live a better life.

Finally, I have no words to thank my family and friends. Especially my husband who spent all these long years in my PhD with me while he was in the PhD program as well. I would not have completed my degree without his help and encouragement. He never wanted to distract me by any means and he was always behind me to make sure that I am always safe. Also my parents who gave me birth as a human being and brought me up with lots of love and care. Although I cannot pay off the debt for them with my PhD, I am sure it will make them happy and proud. My brother, father-in-law and sister-in-law always had faith in me and their encouraging words were always helpful, especially at hard times. There are thousands of logs between the two rails of a rail road. Likewise my PhD train was driven with the direct or indirect help of a lot of people. Although I cannot mention all of their names here, I would like to pay my sincere gratitude to you all.

Dedication

This thesis is dedicated to my loving parents and husband

Abstract

While the type of bacterial infection depends on many factors, such as the geographical region, personal hygiene and the efficiency of the personal immune system, such infections are very common throughout the world. Infections spread very rapidly mainly because bacteria have enough time to spread as the correct diagnosis takes a lot of time. Therefore, a point-of-care diagnostic system for bacterial infections would be very helpful in reducing the number of infected people as well as the cost to treat the infected patients.

Bacteria possess chelating molecules called siderophores, in order to meet their iron needs. They secrete siderophores in large quantities and once those chelate iron, bacteria can absorb them again. The diagnostic systems introduced in this thesis target the secreted siderophores as well as their uptake.

The method that focuses on siderophore secretion involves a novel technology that uses a lanthanide probe and an aptamer probe, which we call lanthanide-apta-switch. A proof-of-concept demonstration has been performed using a mercury-selective structure-switching aptamer which showed very promising results. We anticipate that this technology can be used to detect siderophores using a siderophore-selective structure-switching aptamer.

The diagnostic method we developed, based on siderophore uptake, involves a probe that is an analogue of natural siderophores of bacteria which is then conjugated to a fluorescent dye. Preliminary results showed that our probe is taken-up by bacteria within 5 min. of incubation and the limit of detection is 10^5 CFU/mL. According to our results both diagnostic systems seem good candidates for point-of-care devices.

Table of Contents

List of Tables

List of Figures

List of Schemes

Abbreviations

ABC	ATP binding cassette
ATP	adenosine triphosphate
BSA	bovine serum albumin
CAS	chrome azurol S
CASAD	CAS agar diffusion assay
CDC	Centers for Disease Control and Prevention
CRE	carbapenem-resistant Enterobacteriaceae
DADE	decanoic acid diester
DEC	diarrheagenic *Escherichia coli*
DIPEA	*N,N*-diisopropylethylamine
DMA	dimethylacetamide
DMF	dimethylformamide
DMSO	dimethyl sulfoxide
DNA	deoxyribonucleic acid
DOTA	1,4,7,10-tetraazacyclododecane 1,4,7,10-tetraacetic acid
dsDNA	double-stranded DNA
EIA	enzyme immune assays
EIAC	enteroinvasive *Escherichia coli*
ELFA	enzyme-linked fluorescent immunoassay
ELISA	enzyme-linked immunosorbent assay
EPEC	enteropathogenic *Escherichia coli*
ESI	electrospray ionization

ETEC	enterotoxigenic *Escherichia coli*
FDA	Food and Drug Administration
FISH	fluorescence in situ hybridization
FTIR	fourier transform infra-red spectroscopy
GTP	guanidine triphosphate
GUD	β-D-glucuronidase
HAIs	healthcare-associated infections
HATU	1-[Bis(dimethylamino)methylene]-1*H*-1,2,3-triazolo [4,5-b]pyridinium 3-oxid hexafluorophosphate
HDTMA	hexadecyltrimethylammonium bromide
HR	high resolution
LAMP	loop-mediated isothermal amplification
LOD	limit of detection
LR	low resolution
MALDI	matrix-assisted laser desorption ionization
MRI	magnetic resonance imaging
mRNA	messenger RNA
MS	mass spectrometry
NAAT	nucleic acid amplification tests
NASBA	nucleic acid sequence based amplification
NGAL	neutrophil gelatinase-associated lipocalins
NMEC	neonatal meningitis-associated *Escherichia coli*
NMR	nuclear magnetic resonance

O-CAS	overlaid CAS
PBS	phosphate buffered saline
PCR	polymerase chain reaction
PDMS	polydimethylsiloxane
PeT	photoelectron transfer
PET	positron emission tomography
PNA	Peptide nucleic acid
POC	point-of-care
PVD	pyoverdine
QC-PCR	quantitative competitive PCR
RNA	ribonucleic acid
RP-HPLC	reverse phase high pressure liquid chromatography
rRNA	ribosomal RNA
RT-PCR	reverse transcription PCR
SDS	sodium dodecyl sulfate
SERS	surface-enhanced Raman scattering
SPR	surface plasmon resonance
ssDNA	single-stranded DNA
STEC	shiga-toxin-producing *Escherichia coli*
TBDTs	TonB-dependent outer membrane transporters
TRENCAM	*N,N′,N″*-(nitrilotris(ethane-2,1-diyl))tris(2,3-bis(benzyloxy) benzamide)
UPEC	uropathogenic *Escherichia coli*

US	United States
UTI	urinary tract infection
UV	ultra violet
WHO	World Health Organization

1 THESIS OVERVIEW

Bacterial infections are common all over the world. One of the reasons why bacterial infections are so common is poor diagnosis, which leads to overprescribing of antibiotics, which can cause increases in the spread of multidrug resistant bacteria. Currently available Food and Drug Administration (FDA) approved diagnostic methods for bacterial infections are too time consuming and therefore in order to minimize the spread of bacteria, a point-of-care (POC) diagnostic method is required.

The current study focuses on two aspects of bacterial siderophores: secretion and uptake processes. Both of these are aimed towards diagnosis of bacterial infections, specifically *E. coli* infections, by targeting the detection of a pathogen specific natural product, siderophores. Chapter 2 in this thesis provides a comprehensive discussion of the significance of this study, currently available diagnostic methods for bacterial infections, siderophore excretion and uptake by bacteria and currently available siderophore detection methods.

Our first approach, the detection of bacteria via detection of excreted siderophores is discussed in Chapter 3. The mode of action of our novel probe is shown in Figure 1.1. The probe features a phenanthridine coordinated to a DOTA-type ligand that chelates europium, which in turn is conjugated to a structure-switching aptamer. The aptamer is then hybridized with its complementary strand, the reporter strand. When phenanthridine is not intercalated in double-stranded DNA, excitation light energy is transferred to europium, which then emits in the visible region (probe is 'on'). However, when the probe is in the aptamer/reporter strand duplex form, the phenanthridine is intercalated in

between the DNA base pairs, preventing the energy transfer to the europium, which results in quenching of luminescence (probe is 'off'). Upon recognition of siderophore analyte by the aptamer, a conformational change in the aptamer is induced and the reporter strand is released. As a result, phenanthridine is no longer intercalated between the DNA duplex, and luminescence is 'turned on'. This working hypothesis and advantages of using lanthanides and structure-switching aptamers are discussed in this Chapter 3.

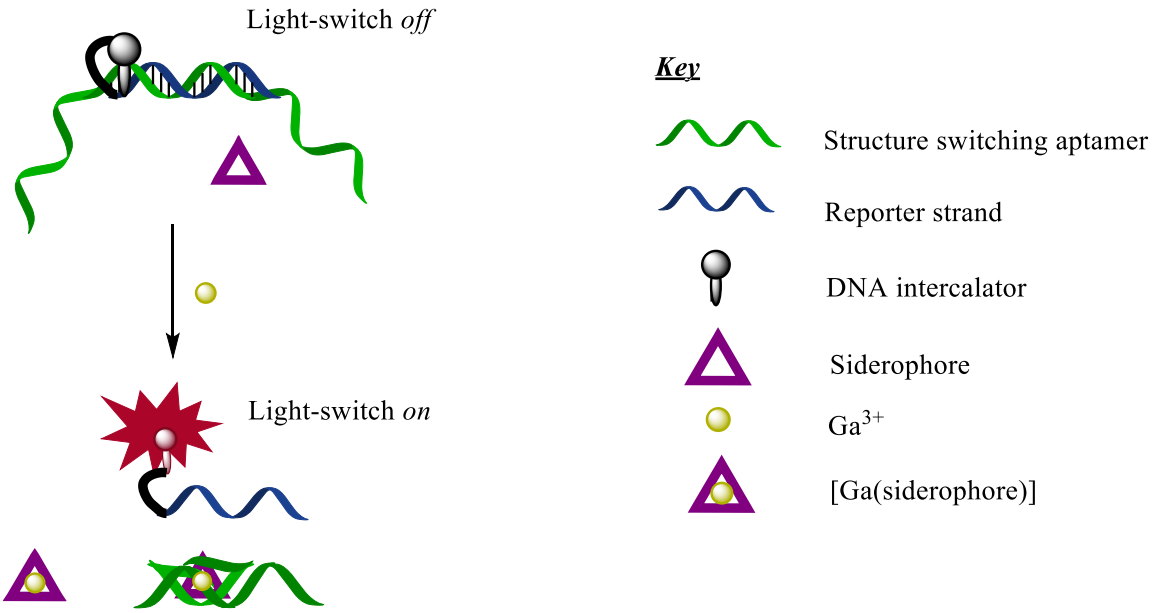

Figure 1.1 Mode of action of light-switch probe

A proof of principle for the lanthanide-apta-switch using a mercury-selective structure-switching aptamer together with a europium-based probe is demonstrated in Chapter 4. The positive responses obtained with a very high turn-on of our probe to mercury strengthens the hypothesis described in Chapter 3.

Our second approach is a Trojan horse approach which is two-fold. This approach is discussed in Chapter 5. First, an enterobactin model complex can be conjugated with a

fluorescent dye, or, second, an enterobactin model complex can be conjugated with a DNA intercalator. The model complex is synthesized with a modification to a previously reported enterobactin analogue (Figure 1.2).

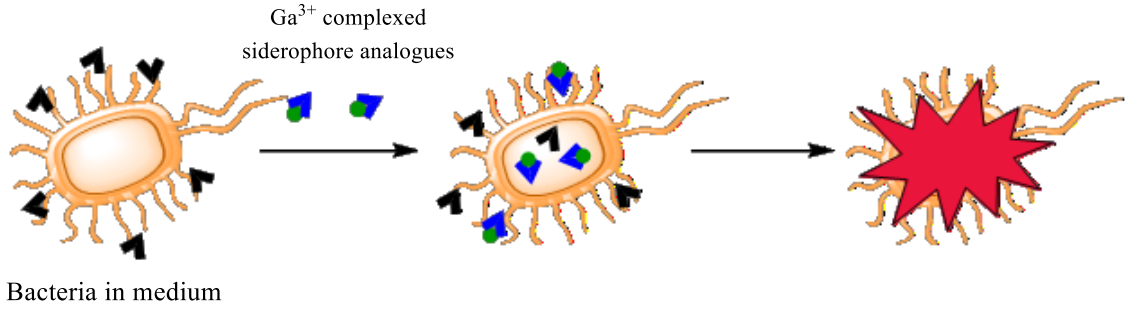

Figure 1.2 Siderophore Trojan horse approach

The enterobactin analogue *N,N′,N″*-(nitrilotris(ethane-2,1-diyl))tris(2,3-bis(benzyloxy) benzamide) (TRENCAM) is modified so as to contain a free acid group that can be conjugated with an amine by standard amide coupling. In one approach this model complex is conjugated to a commercially available dye, tamra cadaverine. In order to obtain better results, the model complex can also be conjugated to Alexafluor 488 and as another approach it can also be conjugated to ethidium bromide which is a known DNA intercalator. The first one is hypothesized to be taken-up by bacteria and luminesces under the fluorescence microscope, once the compound is inside the cells. The second is hypothesized to be taken-up by bacteria and, once inside the cell, if it reaches the cytoplasm, the DNA intercalator would stack in between bacterial DNA base pairs and luminesce.

2 AN INTRODUCTION TO DIAGNOSIS OF BACTERIAL INFECTIONS

2.1 Significance of Diagnosis of Bacterial Infections

Bacteria are ubiquitous. In the human body there are ten times more bacterial cells than human cells. Since human life evolved with bacteria, they live either on skin or within the body in the mouth or gut. Not all bacteria are infectious. Harmless and beneficial bacteria are known as commensal bacteria.[1] They are provided with a good food supply and a perfect temperature to live. In bacterial infections, pathogenic foreign bacteria invade the body and are virulent. The Global Burden of Disease Study 2013, shows statistics for the number of bacterial caused deaths.[2] For example, 1.29 million deaths were due to tuberculosis caused by various strains of mycobacteria including *Mycobacterium tuberculosis,* and 1.11 million deaths were due to diarrheal and respiratory tract infections caused by various types of bacteria.[2] Other than outbreaks of bacterial infections and contagious tranfers from infected people in the community, infections can be acquired in hospitals, in which case they are termed healthcare-associated infections (HAIs). Apart from a few viral infections, almost all the HAIs are bacterial infections.[3]

However, most of the bacterial infections remain poorly diagnosed. When immediate treatment is required, patients are often treated merely based on descriptions of symptoms, which leads to an overprescription of antibiotics. This in turn, contributes to the spread of multidrug resistant bacteria. Accurate diagnostic methods, such as bacterial cultures, have the significant drawback of requiring days to be performed, while the disease should be treated immediately. Thus, bacterial culture methods are not very

useful in point-of-care (POC) settings. Therefore, a rapid, accurate point-of-care diagnostic technology for bacterial infections that renders a good sensitivity and specificity is an unmet need in the medical community.

2.1.1 Pathogenic Bacteria in the US

2.1.1.1 Bacterial diseases

Bacteria, including clinically relevant strains, are typically classified into two groups: Gram positive or Gram negative. These bacteria also differ in many other characteristics, such as presence of an outer membrane, production of toxins, and cell wall composition. For example, Gram negative bacteria have two membranes while Gram positive bacteria have only one.

Disease causing bacteria, or pathogens, infect the habitat of commensal bacteria, which initiates a "bacterial battle" where the good bacteria compete with the pathogens and help the human immune system. Almost all pathogenic bacteria are contagious. Both Gram positive and Gram negative bacteria are among them (Table 2.1). They are transmitted to the body by a variety of carriers: raw food, pets and pests, infected people, water and soil.[4] Pathogenesis can occur when the immune system and commensal bacteria fail to fight with pathogenic bacteria. Some pathogens have a lot of variation in whether they cause the disease or not, depending on the person. For example, a pathogen can cause a disease but not make someone sick unless accompanied by other factors (like genetic influences or toxin exposures).[5] In addition, an infectious pathogen might not cause a disease in one person, but it can cause a disease in another person whom that

person associated with. Sometimes even after the pathogen has entered the body, symptoms of a disease will not show up for even several months.

Bacteria that cause disease are virulent and are able to establish themselves within the host due the production of virulence factors.[6] Virulence factors include cell surface proteins, fimbriae or pili that help bacterial attachment without being flushed off, flagella that mediate bacterial motion, cell surface carbohydrates and proteins that protect bacterial internal structures, hydrolytic enzymes, bacterial toxins and means of invasion.[7] Therefore, virulence factors make it possible for pathogenic bacteria to cause disease.

Table 2.2.1 Bacterial infections and their recent statistics

Bacteria	***Disease***	***USA incident estimates[a]***	***Global incident estimates[a]***
Extended-spectrum β-lactamase producing Enterobacteriaceae (Gram negative)	Bloodstream infections	140,000 cases and 1,700 deaths annually[8]	-
Carbapenem-resistant Enterobacteriaceae (CRE) includes *Klebsiella* spp. (Gram negative)	Bloodstream infections, Pneumonia, Urinary tract infections, Septicemia	9,000 cases and 600 deaths annually[8]	-
Haemophilus influenza (Gram negative)	Pneumonia, Bacteremia Meningitis, Epiglottitis, Septic arthritis, Cellulitis, Otitis media, Purulent pericarditis	5,540 cases and 700 deaths in 2013[9]	8.13 million cases, 371,000 child deaths in 2000[10]
Salmonella typhi (Gram negative)	Typhoid fever	5,700 cases and 620 hospitalizations	-
Shigella spp. (Gram negative)	Bloody diarrhea, Fever, Abdominal pains	13,352 new cases in 2011[11]	164.7 million cases annually[12]
Non-typhoidal *Salmonella* (Gram negative)	Bloody diarrhea, Fever, Abdominal cramps	1,200,000 cases and 38 deaths annually[8]	93.8 million cases and 155,000 deaths annually[13]

Bacteria	***Disease***	***USA incident estimates[a]***	***Global incident estimates[a]***
Acinetobacter spp. (Gram negative)	Pneumonia, Bloodstream infections	12,000 cases and 500 deaths annually[8]	-
Pseudomonas aeruginosa (Gram negative)	Pneumonia, Bloodstream infections Urinary tract infections, Surgical site infections	51,000 cases and 440 deaths annually[8]	-
Legionella spp. (Gram negative)	Pneumonia	3,362 cases and 335 deaths in 2012[14]	70 cases per 1,000,000[15]
Campylobacter spp.(Gram negative)	Bloody diarrhea, Fever, Abdominal cramps, Temporary paralysis	1.3 million cases, 13,000 hospitalizations and 120 deaths annually[8]	-
Neisseria meningitides (Gram negative)	Meningococcal meningitis, Meningococcemia	759 new cases in 2011[11]	1-3 cases per 100,000 annually[16]
Neisseria gonorrhoeae (Gram negative)	Gonorrhea	321,849 new cases in 2011[11]	88 million new cases in 2005[17]
Bordetella pertussis (Gram negative)	Pertussis (Whooping cough)	18,719 new cases in 2011[11]	249,556 cases in 2012[18]

Bacteria	***Disease***	***USA incident estimates[a]***	***Global incident estimates[a]***
Clostridium difficile (Gram positive)	Life-threatening diarrhea	250,000 hospitalizations and 14000 deaths annually[8]	-
Methicillin-resistant *Staphylococcus aureus* (Gram positive)	Bloodstream infections, Pneumonia, Surgical site infections	75,309 cases and 9,670 deaths in 2012[19]	-
Streptococcus pneumonia (Gram positive)	Pneumonia, Bacteremia, Meningitis	33,500 cases and 3,500 deaths in 2013[20]	14.5 million cases and 826,000 deaths in 2000[21]
Group B *Streptococcus* (Gram positive)	Neonatal Sepsis, Bacteremia, Pneumonia, Meningitis	28,500 cases and 1,750 deaths in 2013[22]	-
Vancomycin resistant *Enterococcus* spp. (Gram positive)	Bloodstream infections, Surgical site infections, Urinary tract infections	66,000 cases and 1300 deaths annually[8]	-
Group A *Streptococcus* (Gram positive)	Strep throat (mild), Impetigo (mild skin disease), Cellulitis, Pneumonia, Necrotizing fasciitis, Streptococcal toxic shock syndrome (STSS)	11,500 cases and 1,100 deaths in 2013[23]	~500,000 deaths annually[24]

Bacteria	***Disease***	***USA incident estimates[a]***	***Global incident estimates[a]***
Mycobacterium tuberculosis (Gram positive)	Tuberculosis	10,528 new cases in 2011[8, 11]	5,776,838 cases in 2012[18], 1.29 million deaths in 2013[2]
[a]Recent estimates from 2000 - 2013			

2.1.1.2 Significance

According to the Global Burden of Diseases Study report of 2013, a significant amount of deaths were caused by bacterial diseases (Table 2.2).[2] Bacterial diseases can be outbreaks, which affect a large number of people at once, or infections transmitted by some environmental source or personal contact, which affect a limited number of people. In addition to those, when patients are admitted to hospitals for surgical or medicinal treatments, they can acquire bacterial infections mainly through equipment or from contagious patients. According to the Centers for Disease Control and Prevention (CDC) statistics, the annual direct cost of HAIs to US hospitals in 2007 ranged from $35.7 billion to $45 billion.[25] Out of all 504 healthcare-associated infections reported in 2011, *Clostridium difficile* contributes to 61 infections while *Staphylococcus aureus* contributes to 54.[3] *Klebsiella pneumonia* contributes to 50 and *Escherichia coli* contribute to 47 infections.[3] Thus, bacterial diseases play a major role in public health as well as healthcare-associated infections in the United States. While these statistics show how severe bacterial infections can be, they also tell us how important can a reliable fast diagnostic system be.

Table 2.2.2 Number of deaths in 2013 due to selected bacterial infections[2]

Bacterial Infection	*Number of deaths (millions)*
Lower respiratory tract infections	2.65
Tuberculosis	1.29
Diarrheal diseases	1.26
Meningitis caused by bacteria	0.21
Syphilis	0.14
Whooping cough	0.06

2.1.1.3 Bacterial antibiotic resistance

Antibiotic resistance is a growing problem worldwide today. In the US, at least two million people acquire antibiotic-resistant infections annually, from which at least 23,000 people die.[26] It has been estimated that antibiotic-resistant infections can account for an excess of $20 billion direct healthcare costs out of annual total economic costs.[8] The main reason for the emergence of antibiotic resistance all over the world is mainly due to the overuse of antibiotics.[8] Another reason for the growth of antibiotic resistance is the transmittance of bacterial strains that have developed resistance from people or from food. The fight against antibiotic-resistant bacteria includes several parallel actions: preventing infections and the spread of resistance, tracking resistant bacteria, developing novel strategies to improve the efficacy of current antibiotics, investigating new generations of antibiotics with new targets and developing new diagnostic tools for resistant bacteria.[8,27] However, when addressing the issue of antibiotic resistance, the length of time it takes pathogens to develop resistance towards these antibiotics is an

important factor to consider. For instance, *E. coli* developed penicillin resistance in under one year.[28] Since resistance can develop rapidly in comparison to the drug development process, it is necessary to be able to detect and track resistant bacteria.

In addition to resistance towards single antimicrobial drug class, multidrug resistance also developed over time. Multidrug resistance is defined as resistance towards ≥ 3 antimicrobial drug classes.[28,29] As mentioned earlier, the type of infection depends on the bacterial strain and, therefore, therapeutic options also vary. A study that has been conducted by Food and Drug Administration (FDA) to test the antimicrobial drug resistance of *E. coli* isolated from human and food animals revealed that *E. coli* of animal origin are more resistant than those of human origin.[28] However, when data from 1950-1959 and 2000-2002 are compared, multidrug resistance has increased from 7.2% to 63.6%.[28] Therefore, the rapidity of development of antimicrobial resistance also signals for a need of efficient diagnostic methods for bacteria without leaving room for development of resistance towards drugs.

2.2 Currently available diagnostic methods for bacteria

2.2.1 Criteria for detection

The World Health Organization (WHO) has set criteria for diagnostic devices for resource-limited settings which is abbreviated as ASSURED: Affordable by those who are at risk of infection, Sensitive which provides only a few false negative results, Specific which provides only a few false positive results , User-friendly that the device should be able to use by people with a little training, Rapid identification at the first visit and robust to use without a need for storage, Equipment free which means the device

should not require large electricity dependent instrumentation and Deliverable for the needed ones.[30-32] In addition to the WHO criteria, providing rapid response to small test sample volumes is also expected.[32,33]

Since commensals and other harmless facultative anaerobic bacteria are present in the environment, humans, and animals, the detection of pathogens depends on the sample type. Generally fecal contamination is suspected if, food, or an environmental sample like water or soil is found to contain *E. coli*; however, it does not mean that if tests are negative, *E. coli* are absent.[34] Detection depends on several factors like the limit of detection of the assay, spatial density of the sampling sites and frequency of sampling.[34] Sample complexity also matters for the assay and the criteria for detection. Clinical samples are far more complex media than water. An assay that is very sensitive in water may not be sensitive, or even cannot be used, in blood or urine. For instance Wildeboer et al. reported an efficient and sensitive fluorescence detection method that detected *E. coli* at 7 CFU/mL in water using a 30 min assay.[35] This method is an enzyme based technique which uses the hydrolyzing ability of a biomarker of *E. coli*, β-D-glucuronidase (GUD) to hydrolyze 4-methylumbelliferone β-D-glucuronide and release fluorescent 4-methylumbelliferone.[35] Although GUD has been identified in *E. coli* and *Shigella* spp., it is believed that a few more microorganisms other than coliforms may exhibit this enzyme activity, in which case the assay would not be specific.[36] Furthermore, the use of this technique in biological media has not been demonstrated. An alternative detection method is FDA approved *s*pecies-specific peptide nucleic acid probes that utilize a fluorescence in situ hybridization (FISH) assay to identify cultures of *E. coli* in blood samples. These assays require two and half hours, and the limit of detection (LOD) is

10^5 CFU/mL.[37] Both of these methods present significant progress toward the detection of bacteria, but they are hindered by being less specific and requiring positive cultures respectively.

In addition, the interpretation of results for clinical samples highly depends on the specimen: whether it is collected from a sterile or non-sterile body site, quantity, and type of pathogen present.[38] For instance, if a urine sample culture has been identified to contain two infectious pathogens and one has a colony count of $>10^5$ CFU/mL, that infection is considered as a urinary tract infection (UTI).[39] The threshold value for pneumonia causing pathogens in bronchoalveolar lavage is considered to be $> 10^4$ CFU/mL.[40] Whereas in blood, the threshold value of *Staphylococcus pneumoniae* that causes pneumococcal disease is as low as 10 CFU/mL.[41,42] However, for blood, cerebrospinal fluid, and pleural fluid, positive cultures with any organism together with other symptoms is considered as an infection. In the diagnosis of diarrheal infections, obviously, the samples to be tested first would be stool samples. Stool is a complex matrix to study as it already contains a lot of commensal microbes.[43] Even if the lab results show the absence of pathogens, it does not necessarily mean that pathogens are not present. There can be other possible interpretations like the appropriate pathogen has not been tested, the amount of pathogen present is lower than the limit of detection of the assay or it might be a new pathogen causing the disease for which a diagnostic test has yet to be developed.[43]

Since there are both pathogenic and non-pathogenic types of strains, imaging techniques are important to identify localized colonies as well as to identify and classify different strains. However, in sterile samples the presence of any bacterial strain is

unacceptable. In an infection though, accurate identification aid the prescriptions of proper drugs capable of controlling the disease. Since bacterial detection techniques are now moving away from time consuming cultures and towards rapid detection techniques, it is important to be able to detect small colonies accurately. Therefore, it is an important field and needs improvements because still it is far from aforementioned ideality.

2.2.2 FDA approved diagnostic methods

Currently available FDA cleared bacterial diagnostic methods include microscopy, bacterial cultures, methods based on nucleic acid amplification tests (NAAT) and enzyme immune assays (EIA) (Figure 2.1).[33,38,44] Although the accuracy of most of these methods is almost over 90%, they have their own limitations and are not suitable for point-of-care (POC) diagnosis. The disadvantages of these methods for POC applications are summarized in Table 2.3.

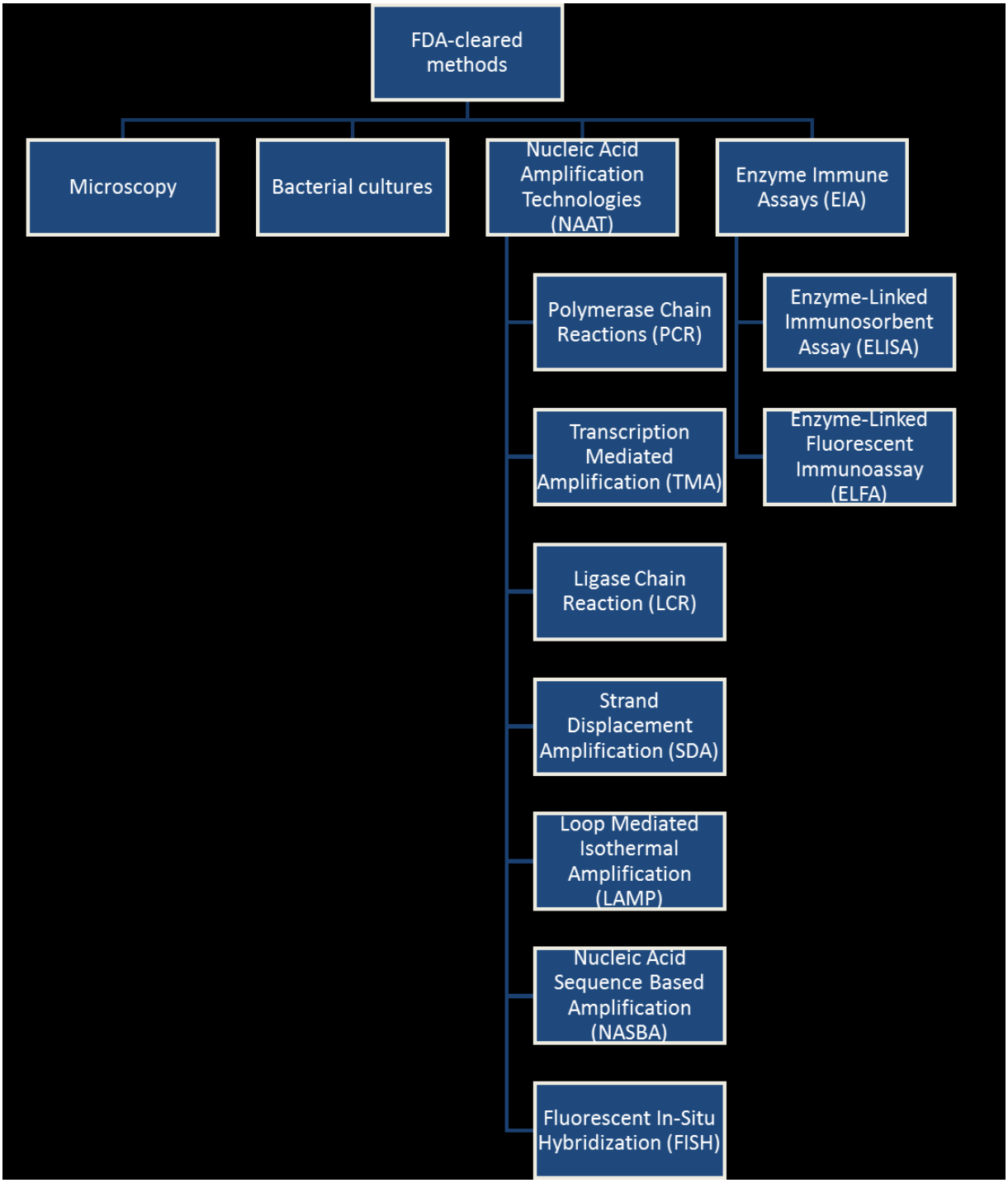

Figure 2.1 FDA-cleared conventional bacterial diagnostic methods (adapted from references 38, 45)

Table 2.2.3 Evaluation of conventional bacterial diagnostic methods for point-of-care applications according the ASSURED criteria.

	Microscopic tests	***Bacterial cultures***	***Nucleic-Acid Amplification Tests (NAAT)***	***Enzyme Immune Assays (EIA)***
Affordability	✓			✓
Sensitivity		✓	✓	✓
Specificity		✓	✓	✓
User-friendliness	✓			
Rapidity and Robustness	✓			
Equipment neediness	✓			✓
Deliverability for needed ones	✓	✓		
References	32, 38, 44-46	32, 44	32, 47-50	32, 51

2.2.2.1 Microscopy

Microscopy is a simple, inexpensive, rapid and user-friendly technique.[38,45] However, it needs well-trained technicians to avoid contaminations from other bacteria and thereby avoid false positives.[32] Data interpretation of microscopy is subjective, and the technique has a limited sensitivity.[44] For example, the sensitivity of acid-fast bacilli smear microscopy compared to culture technique in detection of *Microbacterium tuberculosis* is only 45-80% and also it cannot distinguish between *Microbacterium tuberculosis* and other Mycobacteria.[46] In urinary tract infections, if microscopic urine examination or urinalysis confirms the presence of pus or white blood cells, it is considered as an indication of UTI, however, this pyuria test is merely a laboratory finding and not considered as a diagnostic test, as it does not detect bacteria.[52,53]

2.2.2.2 Bacterial cultures

Bacterial cultures are considered to be the gold standard detection method because of their high sensitivity and specificity. In addition to that, cultures have an additional advantage of developing colonies those can be utilized for further tests.[54] However, it has several drawbacks like expense, requirement of stringent transport conditions, multiple post-cultural preparation steps, laborious training and skilled labor, constant supply of electricity and reagents, and others.[32,33] Also, the sensitivity and selectivity can be affected by laboratory conditions, transportation methods, storing conditions, sample volume, specific bacterial strain, *etc*. For example, Fan *et al*. reports an application of pour-plate quantitative culture technique to evaluate catheter sepsis that has a specificity of 100% ; however, it requires longer incubation time and has a poor

sensitivity of 78% attributed to false negatives as a result of minimal volumes of blood to test.[55-57] Hence, they are not useful in POC settings. Furthermore, culture plates can take 48-72 h for the whole process to confirm the presence of a pathogen and 5 days to confirm the absence, which is too long.[48,58,59] This time frame depends on the bacterial strain too. For example, *Mycobacterium tuberculosis* culture testing can even take 1-4 weeks.[38] The time to results is the major disadvantage of bacterial cultures; an analysis time of several days allows the bacterial infection to worsen.

2.2.2.3 Nucleic Acid Amplification Technology (NAAT)

As the name implies, nucleic-acid amplification technology (NAAT) is an amplification technique based on molecular detection. As shown in Figure 2.1, NAAT includes numerous techniques that utilize the amplification ability of probe, signal, or target. NAATs started to replace bacterial cultures, particularly because they can detect unculturable bacteria, difficult to culture bacteria, slow culture bacteria or dangerous to culture bacteria like *Bacteroides forsythus*, *Bordetella pertussis*, *Mycobacterium tuberculosis* and *Coxiella burnetii* respectively.[44,47,60] In NAAT techniques, a strain-specific or species-specific bacterial DNA sequence and two primers are carefully selected so that they perfectly match the target DNA.[47] Once target DNA is chosen, it is denatured, annealed to the primers and elongated. Conventional polymerase chain reaction (PCR) techniques require at least 35-40 PCR cycles to obtain adequate sample to analyze by gel electrophoresis.[47] The second generation PCR technique, real-time PCR technique (Figure 2.2) was developed with an added modification of molecular beacon probes, which is faster and more efficient than conventional PCR and also renders higher

reproducibility.[47] As shown in Figure 2.2, selected DNA is denatured, followed by the annealing of primers, and the probe with fluorophore and the quencher. Probe extension is blocked by the 3' phosphate group. Once DNA synthesis is extended from the primer by polymerase, the probe is displaced and cleaved separating the fluorophore and the quencher. The result is an increase in fluorescence with polymerization.

The limit of detection (LOD) of real-time PCR assay developed by Jordan *et al.* for *E. coli*, group B *Streptococcus* and *Listeria monocytogenes* in whole blood were 40, 50 and 2000 CFU/mL respectively.[48] As opposed to days for culture plates, PCR tests can be performed in 3-4 h.[32,48] In these nucleic acid based assays, isolation and purification of target molecules is required which can be considered as the main disadvantage.[61] PCR assays are also expensive, need sophisticated instrumentation like a thermocycler. False positive signals and carry-over of exogenous contaminants can result in the case of poor operating practices.[47] Since PCR merely detects DNA, they cannot distinguish between viable cells and nonviable cells, which should be a major concern.[54] The real-time PCR technique developed by Fortin *et al*. reported a LOD of 1 CFU/mL for *E. coli* O157:H7 after 6 h of incubation, which is a good sensitivity but still inadequate for POC settings.[49]

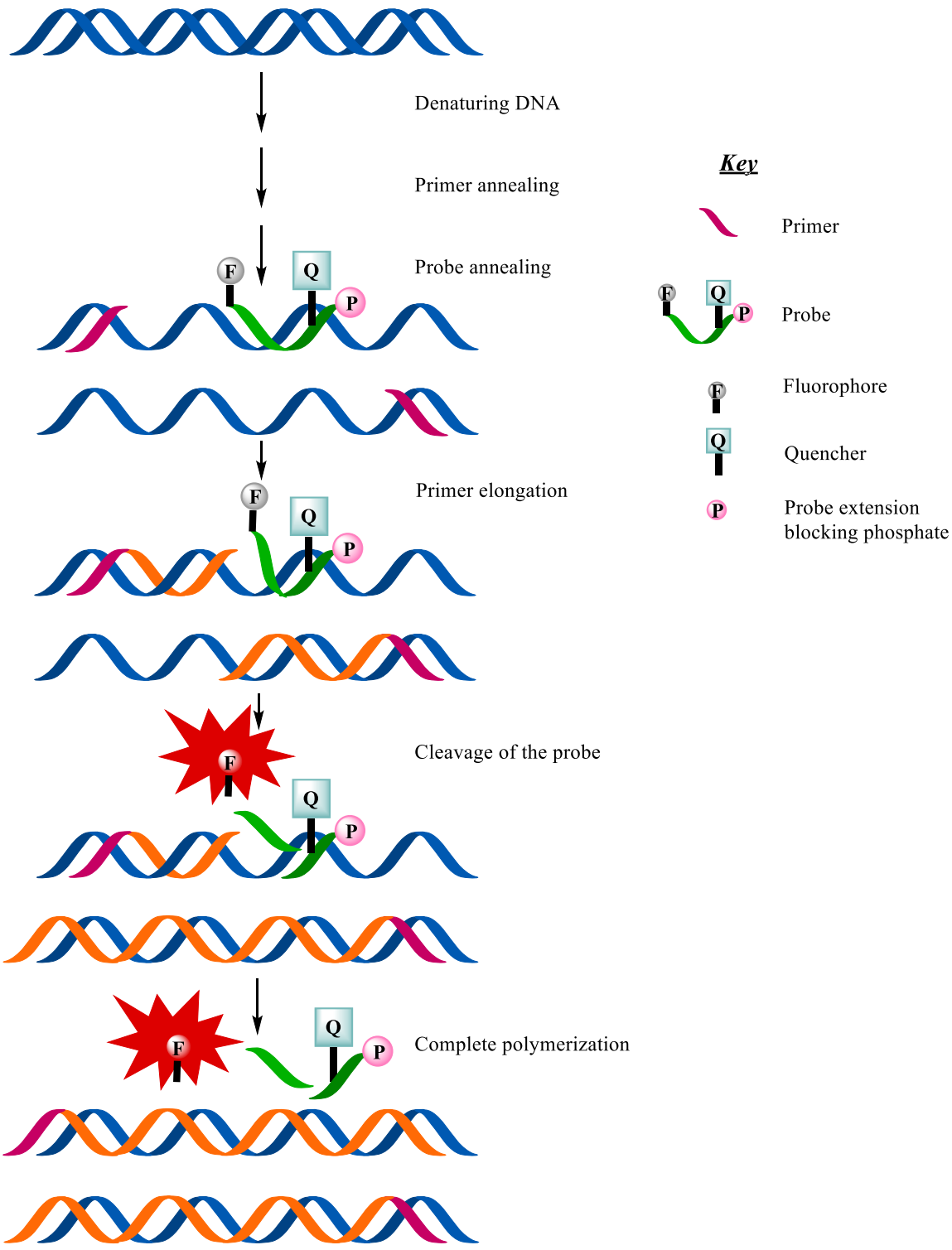

Figure 2.2 Real-time PCR technique (adapted from reference 47).

Multiplex PCR was demonstrated to identify four diarrheagenic *E. coli* (DEC) species simultaneously: enterotoxigenic *E. coli* (ETEC), enteropathogenic *E. coli* (EPEC), enteroinvasive *E. coli* (EIAC) and shiga-toxin-producing *E. coli* (STEC).[50] It eliminates the tedious counting of ambiguous colonies, which is a cumbersome step in plate culture methods and has the advantages of being rapid, easy, cost effective, sensitive, and specific.[50] Although, that study has been done using food and stool samples, they report limit of detections only for food samples. Also their study is not solely PCR; it is a combination of PCR and plate cultures. The PCR method was applied to randomly picked colonies they isolated from agar plates, which might lead to false negatives for some pathogens if those colonies were not chosen. Even though this method boasts cost effectiveness, and ease of diagnostic method, it requires gel electrophoresis and skilled technicians to perform tests which makes it not suitable for primary-care settings. If they omit the culturing step, they could easily obtain faster results but they might need relatively a large sample size.

Other NAAT techniques use different techniques for the denaturing process of DNA, several primers and different amplification aspects.[62] Loop-mediated isothermal amplification (LAMP) is one such powerful technique that provides high selectivity, specificity and efficiency. Therefore, LAMP is an FDA-approved diagnostic method for *Clostridium difficile* detection, where 98% sensitivity and selectivity were obtained compared to cultures and the detection time was one hour.[63,64]

To overcome the viability issue, quantitative competitive PCR (QC-PCR) and reverse transcription PCR (RT-PCR) which detects mRNA instead of DNA is used.[65] However, these assays also require selecting appropriate oligonucleotides and optimizing

conditions to maximize sensitivity and specificity and therefore, technical expertise is required in order to eliminate false positives.[32, 50,54] Altering reactions and conditions in such a way that multiple pathogens could be detected is a smart way to utilize the PCR assay to make it more efficient and economical.[50] However, then specificity cannot be achieved for a certain species.

Fluorescent in-situ hybridization (FISH) is another molecular technique that usually targets a sequence in DNA or 16S ribosomal RNA. For bacterial detection, oligonucleotide probes are synthesized with a fluorophore and hybridized to 16S rRNAs of bacteria which are fixed to a glass slide. Hybridized slides are then examined under a fluorescent microscope. FISH has been successfully used in diagnosis of *Pseudomonas aeruginosa*, *Burkholderia cepacia*, *Stenotrophomonas maltophilia*, *Haemophilus influenzae*, and *Staphylococcus aureus.*[66] The limit of detection of these pathogens from FISH has been 4×10^5 CFU/mL with a sensitivity of 90% and specificity of 100% compared to cultures.[66] Most of the NAAT techniques demonstrate specificity comparable to bacterial cultures although they vary in sensitivity.

2.2.2.4 Enzyme Immune Assays (EIA)

In order to address the affordability and time consumption issues in cultures, serological methods such as enzyme immune assays (EIA), which detect antibodies or bacteriophages in serum were developed.[32,61] FDA approved EIAs include enzyme-linked immunosorbent assay (ELISA, Figure 2.3) and enzyme-linked fluorescent immunoassay (ELFA).[67] EIA based assays are relatively less expensive and do not need sophisticated instrumentation.[32] Since these tests can be performed in batches, EIAs are faster than

blood cultures and require 3-4 h for the whole process.[32] For instance, antibody-based EIA method can be performed as high throughput multiplex immunoassays. This technique, however, is hindered by the expense of production and limited shelf life of antibodies.[68] Also the sensitivity of the assay highly depends on the affinity and avidity of antibodies.[61] In order to overcome these disadvantages, antibodies were replaced by bacteriophages. For example, Shabani *et al.* developed a method to detect *E. coli* using T4 bacteriophages.[69] Phages are easy to isolate and proliferate, and they have a relatively long shelf life.[61] However, phage contamination could cause false results which can occur by inadvertent production and propagation of phages.[61]

As shown in Figure 2.3, in an ELISA, a microtitre plate is first coated with a bacterial antigen suspension and incubated. The antigen suspension is aspirated, washed, and the remaining sites are blocked with a non-reacting protein. Antibody-enzyme conjugates that recognize a bacterial antigen are added and incubated. After washing the enzyme substrate is added. The enzyme is allowed to act for some time, and then the reaction is quenched. Finally, the absorbance is measured in a spectrophotometer.[51] Although (ELISA) is highly sensitive and specific, it also requires multiple preparatory steps, higher sample volumes and refrigeration.[58] Processing and amplification of sample are also needed for ELISA when detection of rare bacteria is performed which is another drawback.[58] For the diagnosis of some disease causing pathogens like *Chlamydia trachomatis*, *Listeria* spp. ELFA has been identified as a better diagnostic technique than ELISA where it uses a fluorogenic substrate.[51] Even though ELISA and ELFA assay have specific advantages, the methods are still far from being a candidate for a POC diagnosis.

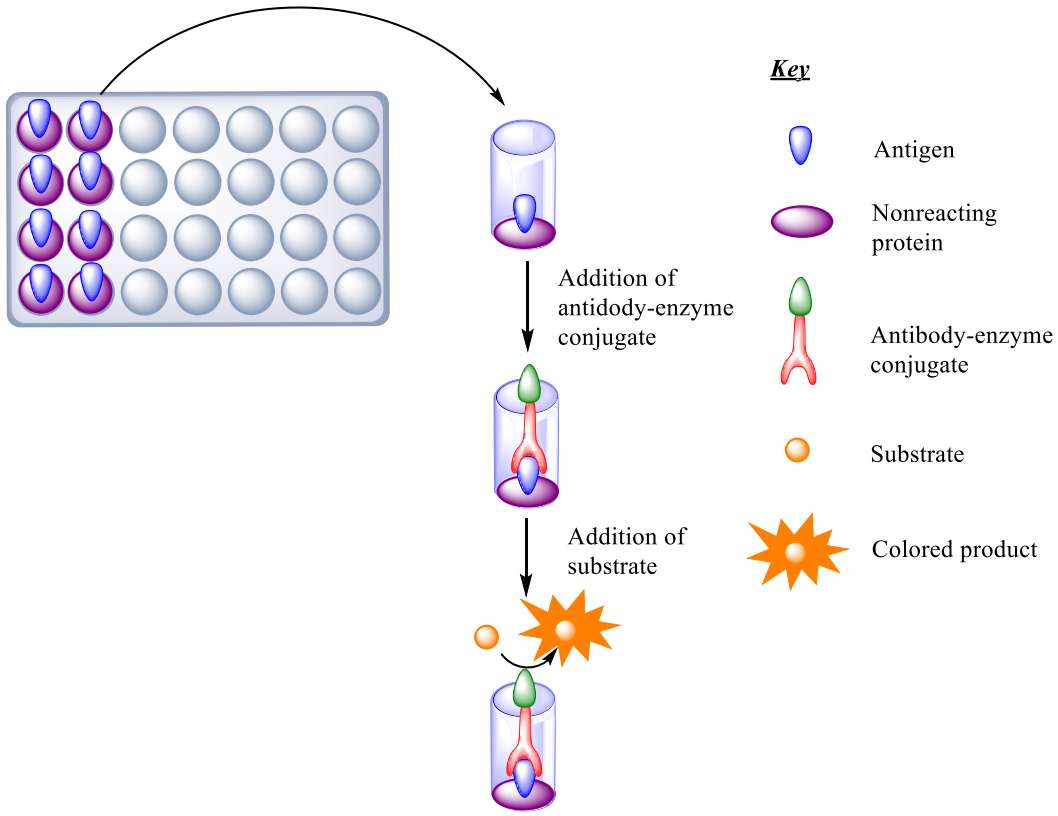

Figure 2.3 Enzyme-Linked Immunosorbent Assay (ELISA) (adapted from reference 51)

Although NAAT and EIA techniques developed demonstrate higher sensitivities and specificities, when compared with culture-based techniques, they cannot be generalized as such because those depend on the bacterial species too. Also they need positive cultures to begin with, which means they are species identification methods rather than rapid diagnostic methods. Although the detection technique itself is not time consuming, requirement of bacterial cultures raises the question of whether or not these methods are actually *rapid*.

An application of immunosorbant assays that has entered the clinic are immunochromatographic assays or dipstick/lateral flow detection systems. These are used in POC settings and are based on antigen-antibody lattice formation or assessing nitrites converted from urine nitrates by certain bacteria. Dip stick methods offer 100% specificity; however, poor sensitivity (29%) compared to cultures.[70] Lateral flow immunoassay developed by Vollmer *et al*. had a sensitivity of 10^3-10^5 CFU/mL for Gram negative bacteria and 10^4-10^5 CFU/mL for Gram positive bacteria.[71] Although these lateral flow immunoassays are rapid and user friendly techniques, data interpretation can be difficult if faint bands are observed.

2.2.3 Other techniques that have been tested for bacterial diagnosis in clinical samples

As discussed above, all FDA approved methods suffer from limitations. When new methods are developed, the increase in sensitivity is compromised by the expensive, requirement of sophisticated equipment or trained personal to handle, or limited shelf life. Therefore, to overcome these drawbacks, in recent years a vast development of biosensors have taken place. Biosensors are devices that convert a biological response into a measurable electrical signal (Figure 2.4). They are composed of a biological species/system which is termed a bioreceptor and a transducer that recognizes the molecular species and generates a measurable signal. Then that signal is amplified and sent to a data processor where the output can be displayed in a readable form.[44,72,73] Depending on the various bioreceptors and transducers used, a large number of biosensors (Figure 2.5, Figure 2.6) have been developed that can diagnose an assortment

of bacterial infections. Since the biological target plays a major role in diagnostic devices, classification based on types of bioreceptors has been developed in addition to the classification based on transducers.

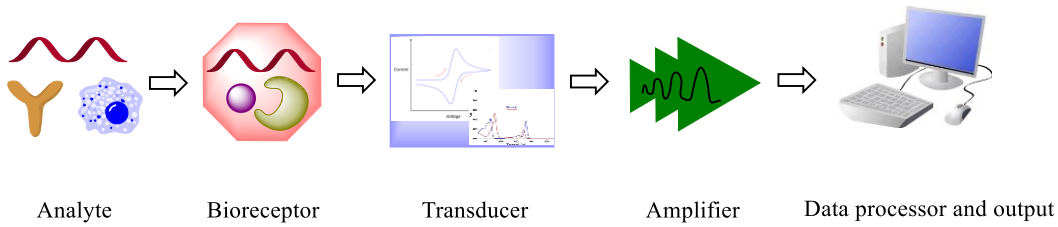

Figure 2.4 Schematic diagram of a biosensor (adapted from references 44, 72, 73)

Although many biosensors have been developed, most of those methods such as the method developed by Li *et al*. for detecting *Pseudomonas aeruginosa* by antibody coated gold nanoparticle based immunochromatographic lateral flow biosensor, the method developed by Gill e*t al.* for detecting *Mycobacterium aeruginosa* by nucleic acid sequence based amplification (NASBA) gold nanoparticle system have not been tested for clinical samples. The method developed by Ho *et al*. for detecting *Salmonella typhimurium* by immunoliposome tagged antigen antibody system have intriguing limits of detection, however, that has also not been tested for clinical samples.[74-76] Since transformation of detection methods from environmental samples to clinical samples involves several concerns such as difference in complexity of the test sample it is very important to develop novel methods that can detect bacteria in clinical samples.

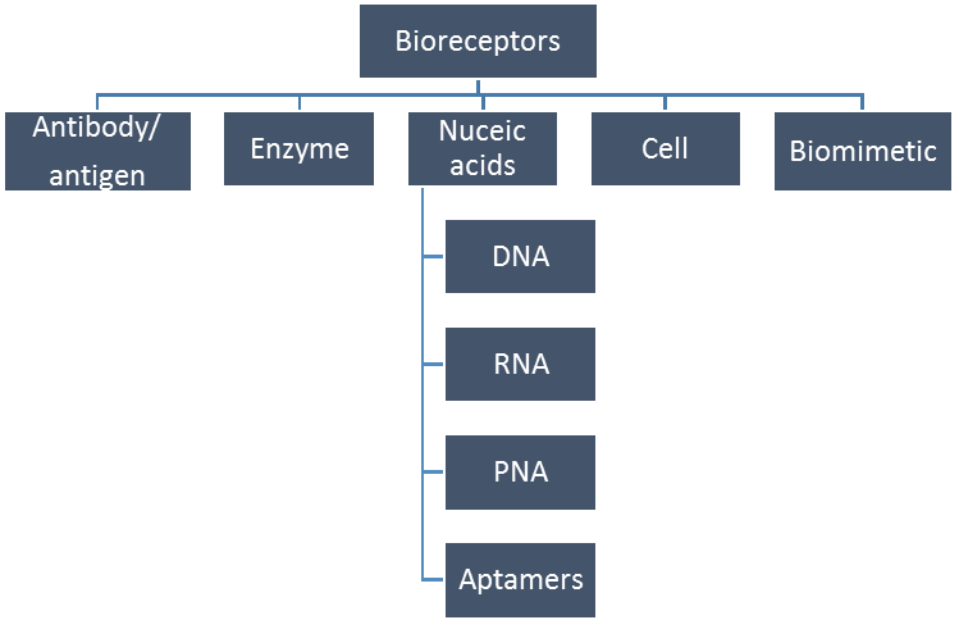

Figure 2.5 Biosensors –Classification based on bioreceptors (adapted from 44,72,73)

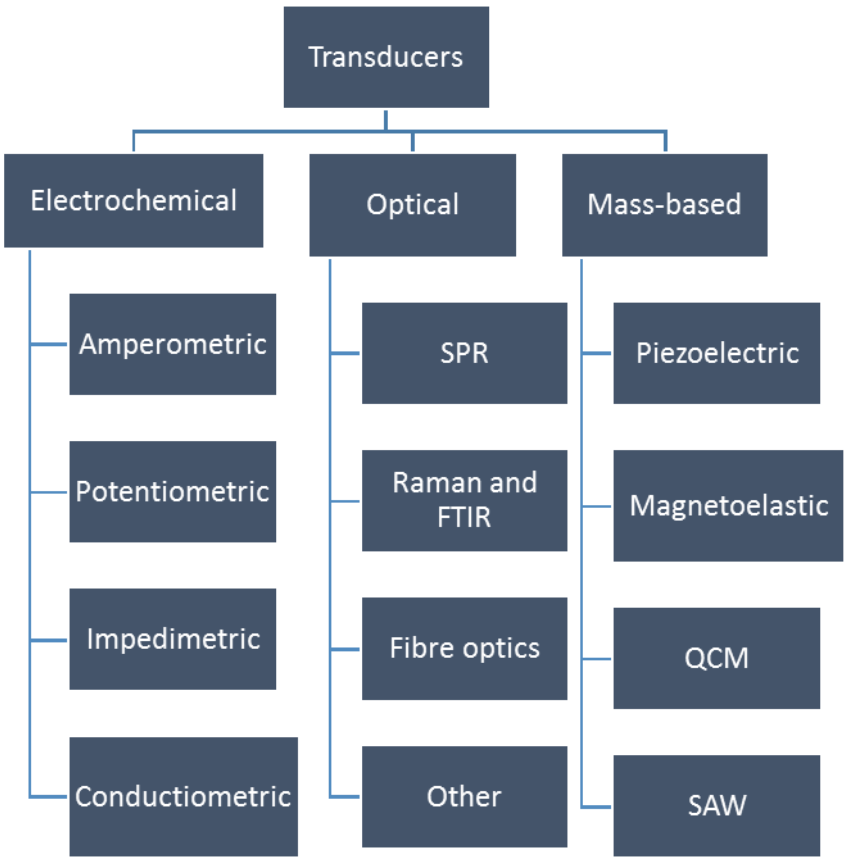

Figure 2.6 Biosensors-Classification based on transducers (adapted from 44,72,73)

Recently developed biosensors that have been tested for clinical samples are summarized in Table 2.4. Nevertheless, none of those techniques have been completely be able to fulfill the FDA requirement (ASSURED) to use in low-resource settings.

Table 2.4 Biosensors that have been tested for clinical samples

Bacteria	***Probe type***	***Sample type***	***LOD (CFU/mL)***	***Analysis time (min)***	***Technique***	***Reference***
E. coli	Primer	Blood	10^6	60	Surface-modified pillar-packed microchip	77
E. coli	RNA	Blood	10^4	20	Electrochemical sensor array	78
E. coli	RNA	Blood	4×10^2	2	Nanoliter wells using electrochemistry	79
E. coli	RNA	Serum/Urine	3×10^6	30	Screen-printed gold electrodes Microfluidic device	80
E. coli O157:H7	DNA	Blood	10^3	180	Evanescent wave fibre-optic biosensor	81
E. coli O157:H7	Antibody	Blood	10^4-10^5	5	AC electrokinetics facilitated biosensor cassette	82
		Feces	10^4-10^5	40		
Uropathogenic *E. coli*	RNA	Urine	10^3	30	Amperometry –Electrochemical sensor assay	83
Uropathogenic *E. coli*	RNA	Urine	10^4	45	Amperometric detection of nucleic acid hybridization	84
Uropathogenic *E. coli*	DNA	Serum/Urine	-	45	Interdigitated microelectrode based Impedance sensor	85
Uropathogenic *E. coli*	Whole cell	Urine	7	60	Gold microelectrode based impedance sensor	86

Bacteria	***Probe type***	***Sample type***	***LOD (CFU/mL)***	***Analysis time (min)***	***Technique***	***Reference***
Pseudomonas aeruginosa	Peptide	Blood	10^5	25	Microfluidic chip	[87]
Methicillin-resistant *Staphylococcus aureus*	Primer	Body fluids	-	3.3	SERS spectroscopy detection	[88]
S. aureus	Whole cell	Mucus	10^7	60	MALDI-MS assisted by titanium dioxide nano particles	[89]
Vibrio cholera	DNA	Feces	25 ng/ μL	65	RCA and microchip electrophoresis	[90]
Mycobacterium spp.	Breath	Breath	10^4	15	^{13}C labeled urea breath test	[91]
M. tuberculosis	RNA	Sputum	10	<60	NASBA and gold nanoparticles	[75]
Staphylococcus pneumoniae	DNA	Blood	10^3	-	Genetyping workflow	[42]
S. pneumoniae	DNA	Blood/urine	10^3	10	Amperometric magnetosensors coupled to asymmetric PCR	[92]
Salmonella typhimurium	DNA	Blood/Feces	Could detect 10^5	5	Paper microfluidic and smartphone based fluorescence microscopy	[93]
Multiplex detection Uropathogens	DNA	Urine	10^4	60	Electrochemical sensor	[94]

Bacteria	***Probe type***	***Sample type***	***LOD (CFU/mL)***	***Analysis time (min)***	***Technique***	***Reference***
Multiplex detection *P. aeruginosa* *S. aureus*	Whole cell	Sputum	5×10^2 – 5×10^3	3	Immuno-disc sensor with antibody-gold nanoparticle system	74
Multiplex detection *Bacillus anthracis* *E. coli O157:H7* *F. tularensis* *Listeria* spp. *Salmonella* spp. *Shigella* spp. *Yersinia pestis*	Antibody	10% Serum/Nasal wash	 10^5 10^5 /10 10^6 $10^4/10^2$ $10^5/10^6$ 10^5 10^5	<120	Microflow cytometry	95
Multiplex detection *E. coli* *S. saprophyticus*	PNA	Urine	10^5	2	Nanostructured electrochemical biosensor	96

2.3 Siderophores and bacterial virulence

As discussed above, over the past few decades numerous methods have been developed for the detection of bacteria. However, sensitive, selective, affordable, rapid and robust detection methods suitable for point-of-care settings is still an unmet need. Therefore, targeting nutrient uptake pathways of bacteria as a detection method would be a thought-provoking strategy. The iron uptake pathway is such an important pathway that therapeutic applications have been developed which target it.[97,98]

2.3.1 Iron uptake/ need for Iron

Not only for higher organisms, but also for almost all of the microorganisms, iron is an essential element for growth. Under physiological conditions iron exist either as Fe^{2+} or Fe^{3+}, however under aerobic conditions Fe^{2+} converts into Fe^{3+} and exists as an insoluble ferric-oxihydroxide polymer.[99,100] Iron is involved in microbial membrane bound respiration as it plays a key role in many enzymes involved in energy generative processes such as the Krebs cycle, oxidative phosphorylation and electron transport.[100,101] It is also important in other biological process such as in photosynthesis, gene regulation, oxygen transport and as a cofactor of ribonucleotide reductase which is an important redox enzyme in DNA synthesis.[102] Therefore, bacteria usually require approximately 10^{-6} M internal iron concentration.[103-105] In the human body, transferrin, the human serum iron transport protein, maintains the free ferric ion concentration at $\approx 10^{-24}$ M in order to regulate iron and minimize the toxic effects of free ferric ions. Due to the insolubility of iron in aerobic conditions and unavailability of free iron, microorganisms who invade human body have a highly iron-stressed environment.[99] Therefore, in order to survive in

such iron-deficient media, bacteria have developed several iron-uptake mechanisms. These include scavenging iron through the excretion and reuptake of siderophores, and, acquiring iron from heme and heme-containing molecules and aquiring iron from transferrin, lactoferrin or ferritin / assimilate ferrous ions.[101,106]

Many bacteria and fungi sequester their needed iron by excreting siderophores which are high affinity, low molecular weight (< 1000 Da) iron chelators. The siderophore iron uptake pathway is the most common one found in Gram negative bacteria. Some Gram positive bacteria also use the siderophore iron uptake systems.[106] Table 2.5 shows a list of bacterial pathogens and their corresponding siderophores. Note that the data in this table are generalized; secreted and taken-up siderophores can vary depending on the specific strain of bacteria.

Studies have shown that some pathogenic bacterial strains can also use other methods mentioned above as well to uptake iron.[107-109] Iron sources of Gram negative bacteria include ferric-siderophores, heme and human iron proteins like lactoferrin and transferrin.[110] Iron acquisition from heme and heme-containing molecules can also be seen in both Gram negative bacteria such as some pathogenic *E. coli* strains, *Bordetella* spp. and Gram positive bacteria such as some *Staphylococcus* spp. and *Bacillus* spp.[106] Some bacteria can directly uptake heme while some bacteria secrete hemophores, which are heme-binding proteins to acquire iron. *Niesseria* spp. and *Haemophilus* spp. have been found to utilize a heme uptake pathway as their iron acquisition mechanism. Interestingly, siderophore production has not been found in these bacetria.[106] Although human iron proteins serve as iron sources, specific receptors that directly extract iron from them are not very common in Gram negative bacteria. Several pathogenic bacteria

such as *Niesseria* spp. and some pathogenic enteric *E. coli* strains have also been shown to have receptors for iron uptake from host proteins transferrin and lactoferrin.[109,111] Ferrous ion uptake systems are believed to present in many Gram positive and negative species including some non-pathogenic *E. coli* strains, *Bordetella* spp., *Legionella* spp. etc.[106]

Table 2.5 Secreted and taken-up siderophores of pathogenic bacteria

Pathogenic bacterial species	***Principal siderophores secreted and taken-up***	***Other siderophores that are taken-up but not synthesized***	***Reference***
Enterobacteriaceae - *Escherichia* spp. - *Shigella* spp - *Klebsiella* spp. - *Enterobacter* spp. - *Citrobacter* spp.	Mainly enterobactin and aerobactin. yersiniabactin and salmochelin (*E. coli* Nissle 1917, *E. coli* O26:H11, *E. coli* 4-85, *E. coli* 85207, *E. coli* 85201, *E. coli* 83972, *K. pneumoniae* K2, *K. rhinoscleromatis* 475, *K. ozaenae* 10 79, *K. planticola* CIP 100 751, *K. oxytoca* 2 82, *C. diversus* 3 89, *C.* koseri)	yersiniabactin, salmochelin, ferrichrome, rhodotorulic acid, coprogen, 2,3-dihydroxybenzoic acid	112-124
- *Yersinia* spp.	yersiniabactin, enterobactin, aerobactin (some)	enterobactin, desferal, schizokinen, ferrioxamine	125,126
-*Salmonella* spp.	salmochelin, enterobactin, aerobactin	corynebactin, myxochelin C	120,127
Haemophilus spp.	No siderophore production identified	ferrichrome	128
Acinetobacter spp.	acinetobactin, fimsbactin (some)	anguibactin, enterobactin	129,130

Pathogenic bacterial species	***Principal siderophores secreted and taken-up***	***Other siderophores that are taken-up but not synthesized***	***Reference***
Pseudomonas spp.	pyoverdine, pyochelin	enterobactin, aerobactin, cepabactin, mycobactin, carboxymycobctin, ferrichrome 3, desferrioxamines, desferrichrysin, desferricrosin, coprogen	[27,117]
Legionella spp.	legiobactin		[131]
Neisseria spp.	No siderophore production identified	enterobactin, salmochelin, aerobactin	[132]
Bordetella spp.	alcaligin	desferrioxamine, ferrichrome, enterobactin	[133]
Clostridium spp.	Phenolate type siderophore is suspected	Not identified yet	[134]
Staphylococcus spp.	staphyloferrin A, staphyloferrin B, staphylobactin, aureochelin	ferrichrome, enterobactin, aerobactin, desferal, actinoferrin	[135-139]
Streptococcus spp.	equibactin, desferrioxamine		[140,141]

Pathogenic bacterial species	***Principal siderophores secreted and taken-up***	***Other siderophores that are taken-up but not synthesized***	***Reference***
Bacillus spp.	bacillibactin, 2,3-dihydroxybenzoic acid	enterobactin, petrobactin, ferrichrome, schizokinen	[142,143]
Mycobacterium spp.	mycobactins, carboxymycobactins, exochelins	exochelins	[119, 144,145]

2.3.1.1 Siderophores

Gram negative and Gram positive bacterial strains, some fungal species and some plants excrete siderophores that can extract Fe^{3+} from precipitates and other host proteins.[102,146-148] Although nearly 500 siderophores have been identified so far that vary in overall structure, they all contain functional groups that bind Fe^{3+}.[149] Usually iron coordinating atoms of siderophores are hard Lewis bases, such as oxygen ligand groups, that form stable complexes with the hard Lewis acid, Fe^{3+}. Depending on the functional moiety of the oxygen donor for ferric coordination, siderophores are divided into three main categories: 1) catecholates and phenolates, 2) hydroxamates and 3) hydroxycarboxylates.[102, 149-150] Structures of the siderophores mentioned in this thesis are shown in Figure 2.7 and Figure 2.8. Most Gram negative pathogens produce their own siderophores. For example, *E. coli* is found to secrete two types of siderophores, enterobactin and aerobactin, to uptake iron.[109] It has also been shown that some virulent strains that belong to enterobacteriaceae family secrete yersiniabactin and salmochelin.[107,151] In addition to uptaking siderophores that they synthesize, some strains can uptake xenosiderophores produced by other strains of bacteria. For instance, *E. coli* can utilize iron bound to exogenous siderophores such as ferrichrome, ferrioxamine B, rhodotorulic acid.[148] Similarly, the principal siderophores produced by *Pseudomonas* spp. are pyoverdine and pyochelin, but these organisms can utilize a wide variety of xenosiderophores such as enterobactin, cepabactin, mycobactin, carboxymycobctin, ferrichrome 3, deferrioxamines, desferrichrysin, desferricrosin and coprogen.[117]

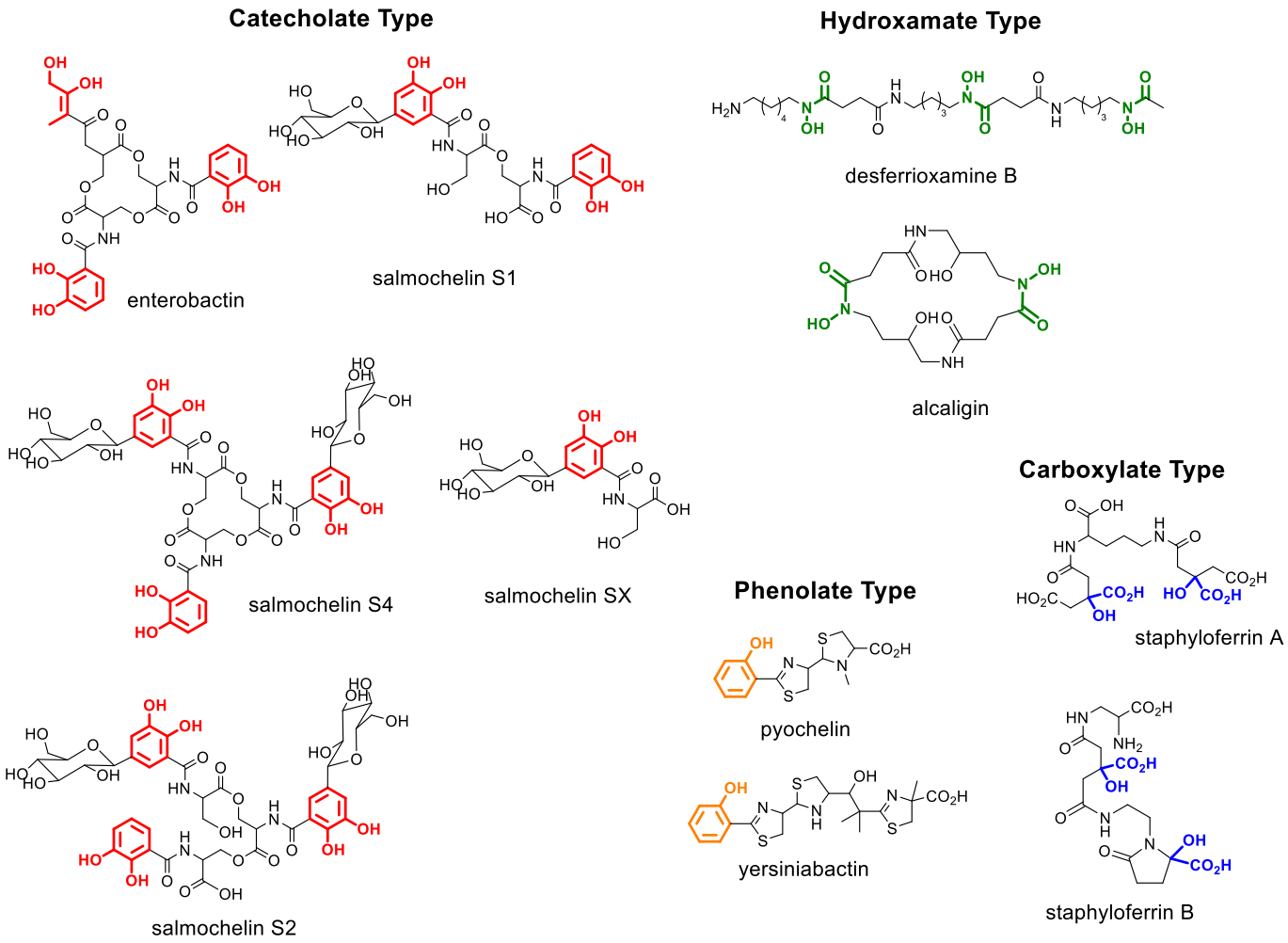

Figure 2.7 Siderophore types (I)

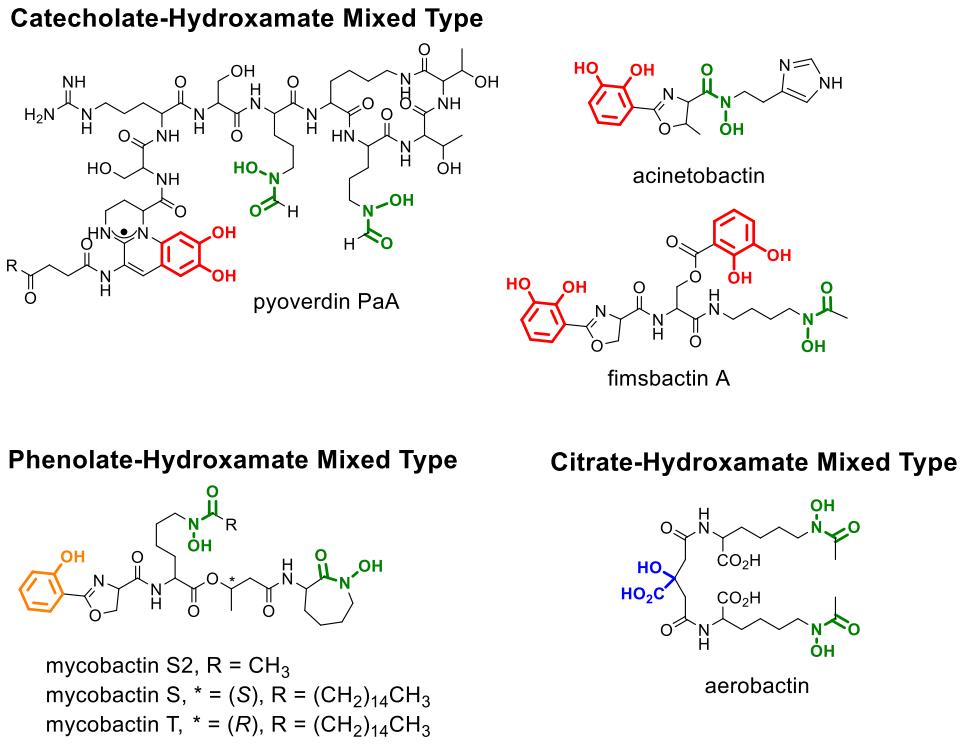

Figure 2.8 Siderophore types (II)

When coordination of iron with the siderophore is considered, depending on siderophore class, different iron : siderophore ratios are observed.[101] These highly stable ferric siderophore complexes contain oxygen donor ligands that generally hexacoordinate Fe^{3+} in an octahedral geometry.[150] Even if the siderophore does not have six atoms to coordinate, hexacoordinated systems are formed either with water molecules occupying the remaining open coordination sites or with higher Fe: ligand ratios.[150] As shown in Table 2.6, most of the siderophores can be either tetradentate or hexadentate and this denticity affects the affinity constants.[119] The ability of siderophores to complex iron is given in p[M], which is the free Fe^{3+} concentration when total [Fe^{3+}] = 1 μM and [siderophore] = 10 μM.[121] These affinity constants, expressed in p[M], for siderophores at

pH 7.4 are given in Table 2.6. According to the values of p[M], enterobactin makes the most stable Fe-siderophore complex while rhizoferrin makes the least stable complex.

Table 2.6 Values of p[M] and denticities of siderophores

Siderophore	***pFe^{3+}***	***Denticity***	***Reference***
enterobactin	35.4	6	119,152
aerobactin	23.3	6	119, 153
alcaligin	23.0	6	154
ferrichrome	25.2	6	155
rhodotorulic acid	21.8	4	119, 152,156
ferrioxamine B	26.5	6	155
rhizoferrin	19.7	6	152
amonabactin T	26.0	4	119,157
desferrioxamine B	25.0	6	119,154
desferrioxamine E	26.6	6	119
desferriferrichrome	25.0	6	119
desferriferrichrome A	25.2	6	119
pyoverdine	27.0	6	158

As illustrated in Figure 2.9, the affinity of siderophores for Fe^{3+} is highly dependent on the pH. Chelation efficiency of enterobactin significantly increases more than that of aerobactin at pH > 6; however, at pH < 4.3, the Fe^{3+} binding affinity of aerobactin is greater than that of enterobactin.[121] The pH dependence of Fe affinity

illustrates that at ~pH 4.3, all: enterobactin, aerobactin and desferrioxamine B are equally effective. In the range of pH 5-6, enterobactin is the most efficient Fe-chelator, followed by aerobaction and then desferrioxamine. Above pH 6, desferrioxamine out ranks aerobactin in iron binding abilities because areobactin's affinity for iron remains constant in the pH range of 5.5-9. Moreover, the pKa of donor atoms is an important factor to be considered. Catecholates have pKa 6.5-8 and hydroxamates have pKa ranging 8-9. However, since carboxylates have pKa 3.5-5, they act as efficient siderophores for bacteria those live in acidic conditions.[150]

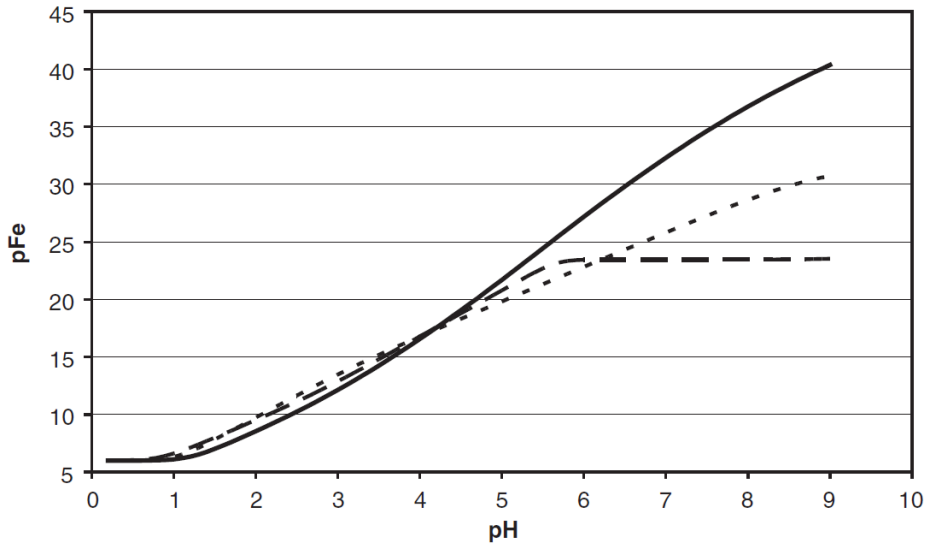

Figure 2.9 pFe vs pH for enterobactin (solid line), aerobactin (dashed line) and desferrioxamine B (dotted line – reproduced with permission from 121)

2.3.1.2 Scavenging iron by excreting siderophores

As mentioned earlier, siderophore-mediated iron transport systems are the most common and well defined iron acquisition mechanism of bacteria.[102] Iron acquisition by siderophores involves several steps: siderophore synthesis in the cytoplasm, siderophore secretion, ferric-siderophore uptake, ferric-siderophore internalization and iron release in the cytoplasm.[159] These transport systems involve outer membrane receptors, periplasmic binding proteins and ATP binding cassette transporters.[99,102,160] The siderophore-mediated iron transport system is depicted in Figure 2.10.

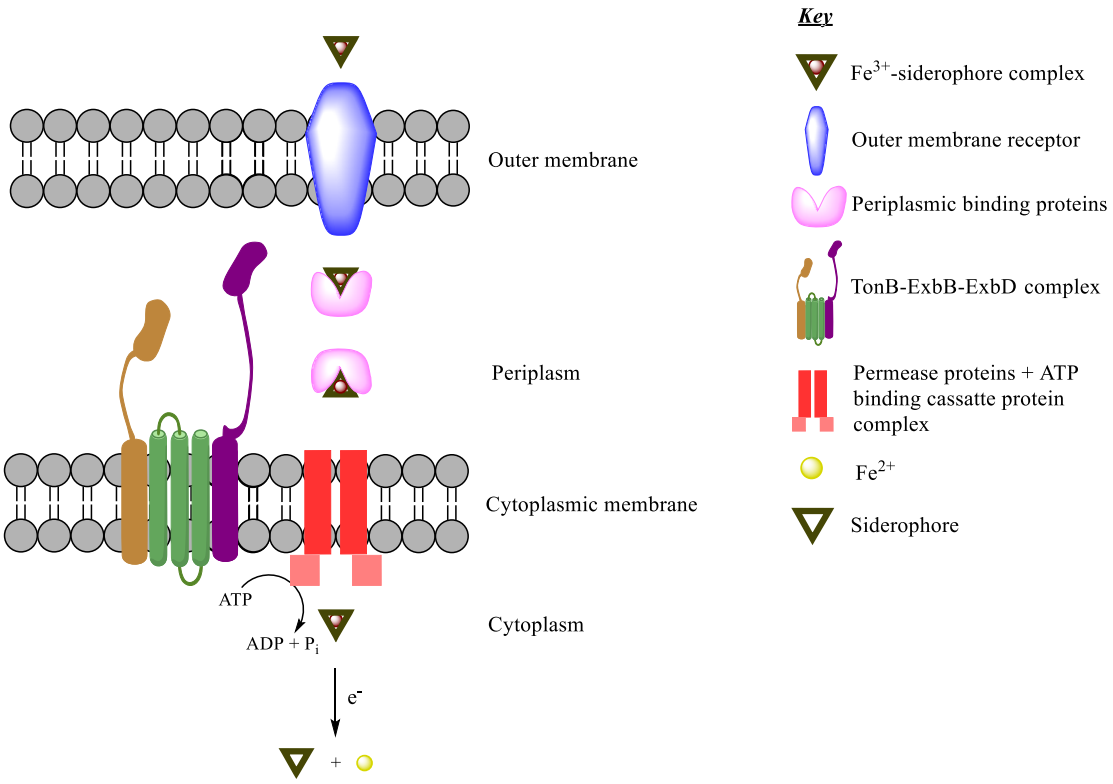

Figure 2.10 Siderophore-mediated iron uptake system in Gram negative bacteria

Siderophore uptake process starts when Fe^{3+}-siderophore complex reaches the outer membrane receptor (Figure 2.10). Outer membrane receptors, such as those found

in *E. coli*, are highly specific proteins that can bind Fe^{3+}-siderophore complexes with binding affinities of < 0.1 μM.[104] Usually bacteria possess several outer membrane receptors for both exogenous and endogenous siderophores.[160] For example in *E. coli*, FhuA, FecA and FepA are the outer membrane receptors for hydroxamate, citrate and enterobactin respectively.[102] Outer membrane receptors also allow binding of bacteriophages and thereby the entry of toxins to the bacterial cell.[104] Therefore in order to prevent the entry of toxins inside the cells, expression of siderophores receptors is usually induced upon iron starvation.[160]

Although binding of siderophores to the outer membrane receptor does not require energy, release and transport of ferric siderophores across the outer membrane is an energy dependent process.[104] The proton motive force created by the cytoplasmic membrane is coupled to the outer membrane by TonB-ExbB-ExbD protein complex.[99] TonB and ExbD have only one transmembrane domain which is located at the periplasm, while ExbB has three transmembrane domains and it is located at the cytoplasm.[102] These TonB-dependent outer membrane transporters (TBDTs) interact with TonB by a conserved hydrophobic 7-10 residue region, called TonB box, which is proximal to the N-terminus.[99] However, the exact energy transfer pathway between units of the TonB-ExbB-ExbD complex or from the complex to TBDTs is yet to be determined.[99] This complex is subjected to Fur regulation, which means that the abundance of the complex can increase upon iron starvation.[106, 161]

Periplasmic siderophore binding proteins deliver siderophores to the cytoplasmic membrane transporters.[102] Similar to outer membrane receptors, periplasmic binding proteins are also specific for shuttling their specific siderophore type. For example,

E. coli periplasmic binding proteins, FhuD, FecB and FepB are responsible for shuttling hydroxamates, citrates and catecholates respectively. Once ferric siderophores are in the periplasm, they are delivered to the cytoplasm across the cytoplasmic membrane via another energy driven process that involves ATP hydrolysis which is consumed by the ATP binding cassette (ABC) transporter protein complex.[102, 104]

The mechanism by which iron is extracted from the internalized ferric siderophore complex is not clearly understood.[160] However, iron must dissociate from the complex. This process is believed to either be facilitated by the reduction of ferric to ferrous by enzymes, which would reduce the affinity of the siderophore for iron, or enzymes that degradation the siderophore and release of iron.[162] The low pH environments encountered by bacteria support the redox-based mechanism of Fe release.

It is also important to note that the siderophore iron uptake system in Gram positive bacteria is very similar to that of Gram negative bacteria, except for the absence of outer membrane receptors.[163] As illustrated in Figure 2.11, in Gram positive bacteria Fe^{3+}-siderophore complex is received by membrane-anchored binding protein and then it is shuttled through an ABC transporter protein complex.

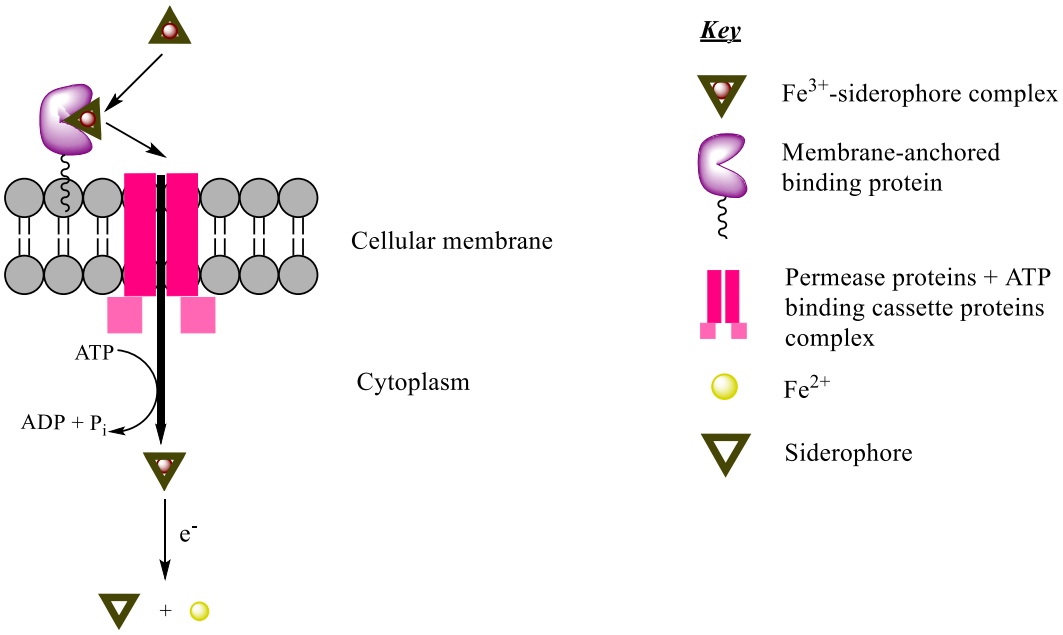

Figure 2.11 Siderophore- mediated iron uptake system in Gram positive bacteria

2.3.2 Siderophores and their virulence

There is evidence that shows a direct relationship between siderophore production and bacterial virulence.[115] This positive correlation can result in increase in colonization and increase pathogenesis.[164] Some siderophores, such as pyoverdines, can even regulate the production of other virulence factors.[165] Lamont *et al.* demonstrated that pyoverdine secreted by *Pseudomonas aeruginosa* can control the production of exotoxin A and PrpL protease which are virulence factors.[165] In addition, Vagarali *et al.* showed that siderophore production in pathogenic bacterial strains is more prevalent than non-pathogenic strains.[166] They tested 160 *E. coli* strains isolated from urine of UTI patients and 97.5% showed siderophore production whereas, out of 50 fecal *E. coli* strains, only 4% showed siderophore production.[166] When siderophores are produced since they are

produced in bulk, bacterial detection via targeting detection of siderophore production would be an interesting approach. Therefore, siderophores can be considered as non-invasive target molecules to diagnose infections.

Almost all *E. coli* strains, including pathogenic *E. coli*, secrete enterobactin (enterochelin) as their main siderophore.[145,148] In addition to enterobactin, few other siderophores, namely aerobactin, salmochelin and yersiniabactin are also found in many pathogenic *E. coli*.[150,159,167]

Enterobactin (Figure 2.7) was concurrently discovered in *E. coli* and *Salmonella enterica* by two groups of scientists in 1970; O'Brien and Gibson named it as enterochelin, and, Pollack and Neilands named it enterobactin.[168,169] Ferric enterobactin complex has a hexadentate triscatecholate geometry with a Δ configuration.[103,170,171] Enterobactin has three main domains: a trilactone backbone, amide linkage domain and metal binding catechol domain.[103] Enterobactin in the neutral state has an ortho-hydroxy proton of the catechol moiety hydrogen bonded to amide oxygen; however, upon metal binding deprotonation of ortho-hydroxy proton results in a *trans* conformation where the ortho-hydroxy oxygen is hydrogen bonded to the amide proton.[103] Studies have shown that amide linkage and an unsubstituted catechol moiety are required for recognition by Fep A, but the trilactone ring is not mandatory. This is supported by studies that have modified the trilactone ring, or even replaced it with other chemical entities, and still retained the ability to bind Fep A.[172,173] A good understanding of iron binding and uptaking mechanisms of siderophores is important in developing siderophore-based novel diagnostic probes.

Metal-ligand stability constants of siderophores are generally expressed as β_{mlh}, where m stands for metal, l for ligand and h for protons (Equation 2.1). For example the strongest *E. coli* siderophore enterobactin has a log β_{110} of 49 which is a measure of formation constant.[153,174]

Equation 2.1

$$mM + lL + hH \longrightarrow M_m L_l H_h$$

Following the discovery and structure studies of enterobactin, it was identified as a virulence factor .[175,176] Specifically, host immune proteins called neutrophil gelatinase-associated lipochalins (NGAL) or siderocalins, are known to bind, and possibly inactivate, enterobactin.[112,177] Therefore, in blood, NGAL bind and sequester ferric-enterobactin effectively.[103] However, bacteria have also been able to evolve another mechanism to overcome the threat by NGAL. That is to glucosylate their enterobactin using the enzyme IroB to salmochelins which can avoid the sequestration of NGAL.[112] Salmochelin (Figure 2.7) is the main siderophore secreted by *Salmonella* spp., but it is excreted and/or utilized by many bacterial species other than *Salmonella* spp. such as UTI strain CP9, neonatal meningitis-associated *E. coli* (NMEC) strain S88 and *Klebsiella pneumonia*.[159,178] Interestingly, genes that encode for IroB, the enzyme responsible for glucosylation of enterobactin is not found in all *E. coli* strains; hence salmochelin iron uptake systems are not common in *E. coli*. The outer membrane receptors for salmochelins have been identified as IroN which are specific for catecholate-type siderophore uptake.[179] The salmochelin siderophore system is one of the few siderophore schemes that is found to be more ubiquitous in pathogenic bacteria than commensal

bacteria.[180,181] It is characterized by the IroN receptor, and this system plays a key role in UTI pathogenesis.[180-182] Therefore, IroN helps bacteria to evade sequestration of enterobactin by host immune proteins.[112,183]

Aerobactin (Figure 2.8) was first isolated from *Aerobacter aerogenes* in 1969.[159] Unlike in the case of enterobactin, aerobactin biosynthetic genes have been mostly detected in pathogenic *E. coli* strains.[184,185] Aerobactin is a citrate-hydroxamate mixed-type siderophore (Figure 2.8). Garcia *et al*. demonstrated the contribution from aerobactin to iron uptake, using an *in vivo* UTI model.[186] Aerobactin is known to be one of the important urovirulence factors that cause the pathogenicity of uropathogenic *E. coli* (UPEC).[183,187,188] In addition, aerobactin is considered as a major virulence factor in *Klebsiella pneumonia*.[189] Aerobactin is highly effective in serum and bacterial growth can be stimulated even with a very low concentration.[190]

Yersiniabactin (Figure 2.7) is a phenolate-type siderophore and was first discovered in 1993.[125] Although yersiniabactin was first identified is *Yersinia* spp. it has also been found in pathogenic *E.coli* strains such as *E. coli Nissle 1917, E. coli O26:H11, UPEC 85972,* and some other bacterial species such as *K. pneumoniae* and *Citrobacter koseri*.[125,191] The formation constant, K_f associated with ferric-yersiniabactin complexation is 4×10^{36}.[192-194] the importance of the yersiniabactin iron acquisition system for the virulence of *Yersinia pestis* is proven.[125, 192,195,196] Specifically, it has been shown that the yersiniabactin system is the main iron uptake route from transferrin and lactoferrin.[192] Moreover, yersiniabactin has been identified as a major virulence factor associated with UTI.[186,197]

Pyoverdin and pyochelin (Figure 2.7 and Figure 2.8) are two siderophore types secreted mainly by *Pseudomanas* spp. depending on the severity of the iron stress, *P. aeruginosa* secretes either pyoverdin or pyochelin. Pyoverdin is a fluorescent siderophore and, depending on the bacterial strain, it has slight variations such as the number and composition of amino acids on the peptide backbone.[198] Even within the same species, different strains can secrete different versions of pyoverdin.[198] Pyoverdins chelate iron very strongly; the affinity constant, $\beta_{110.}$ for pyoverdin PaA secreted by one of the *Pseudomonas aeruginosa* strains is determined 30.8.[199] Not only is pyoverdins a virulence factor, it is also known to stimulate the production of other virulence factors.[200] Pyoverdin secreted by *P. aeruginosa* can evade NGAL and cause chronic infections in cystic fibrosis lungs.[201] Pyochelin on the other hand, is secreted by Gram negative bacteria such as *Burkholderia cepacia* complex.[202] As it is implied by the affinity constant of ferric complexes of phyochelin (β_{110} of 28.8), they are less stable than pyoverdin.[203] Like pyoverdin, pyochelin can also enhance other virulence factors and increase the lethality of virulent bacterial strains.[204]

Mycobactins (Figure 2.8) are a class of siderophores secreted by Gram positive *Mycobacterium* spp. The relationship between bacteria virulence and mycobactin secretion is also known.[205,206] Mycobactin structure is analogous to that of yersiniabactin and vibriobactin.[205] Although it has been found that *Mycobacterium* can uptake iron from heme *via* non-siderophore mediated mechanisms, the mycobactin iron uptake pathway has been identified as a main iron uptake pathway.[207]

2.3.3 Siderophore-targeted bacterial detection

2.3.3.1 Currently available siderophore detection methods

The virulent nature of siderophores make them a suitable analyte to detect pathogenic bacterial strains.[165] Furthermore, the presence of siderophore varients, such as glucosylated versions of enterobactin (salmochelins), used by some bacteria to bypass host defense strategies, illustrates the importance of a rapid method to detect siderophores preferably different classes of siderophores. Currently available siderophore detection methods can be categorized mainly into two classes: 1) Assays based on chemical properties, and 2) bioassays based on biological or functional properties.

Examples of chemical assays include the Arnow, Csaky, Atkin, and Rioux assays.[208-212] All of these assays are based on colorimetry, and therefore cannot be used for diagnosis as they are not sensitive enough. However, they are used to confirm the presence of siderophores. The Arnow assay, being the oldest assay, was not originally designed for siderophore detection.[208] In the Arnow reaction (Scheme 2.1), catechols give a yellow color upon addition of nitrite-molybdate reagent in acidic medium, and the solution turns red upon addition of base. The drawback of this assay, is that it can only be used for detection of catechol-type siderophores no other types of virulent siderophores. Other disadvantages that can lead to inaccurate results include the pH dependence of the wavelength used for product quantification and the time allowed for the color development.[209] Now, after other methods have been developed, the Arnow method is used only as reference method to detect catechol-type siderophores.

Scheme 2.1 Chemical reactions in Arnow assay for catechol detection

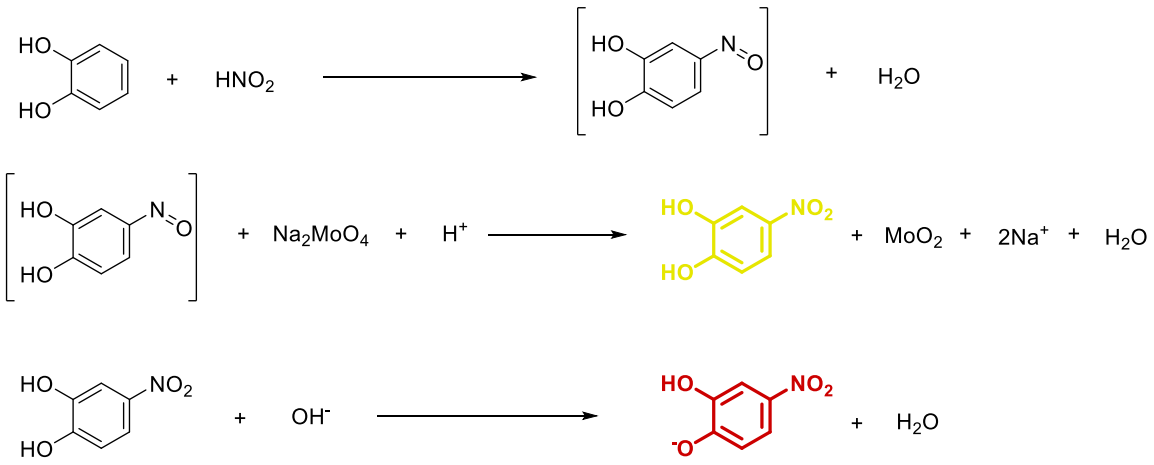

The Rioux assay is also a highly sensitive colorimetric method for the selective detection of catechol-type siderophores.[210] Treating the sample with ferric ammonium citrate in acidic medium, reduces ferric to ferrous and ferrous is detected by 1,10-phenanthroline (Scheme 2.2). This assay is performed under acidic conditions below pH 3. Although Rioux assay is seven times sensitive than Arnow method, the color development is time consuming and hence not the ideal method for detecting catechol-type siderophores. Since the Rioux assay involves a heating step, heat unstable siderophores will not be detected, which is a limitation in this method.

Scheme 2.2 Chemical reaction in Rioux assay for catechol detection

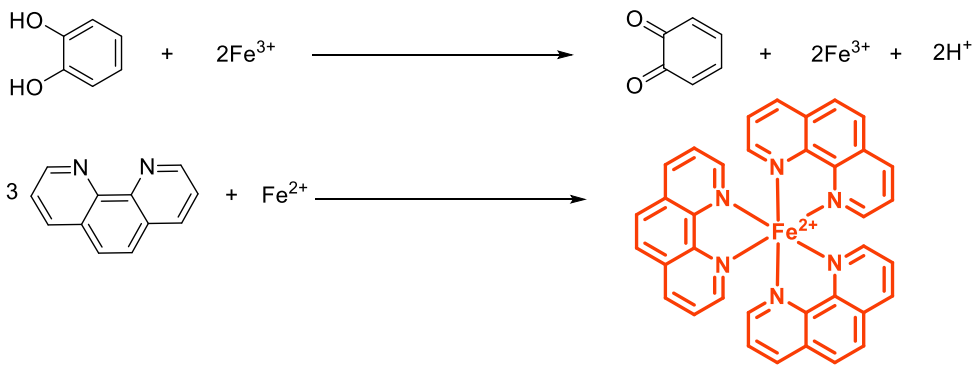

The Csaky assay is also colorimetric, but it is suitable only for hydroxamate-type siderophore detection.[211] In the Csaky assay, the sample is first treated with sulphanilic acid and iodine, followed by sodium arsenite and α-naphthylamine. The color indication gives an estimate for the amount of hydroxamate present. Similar to the Arnow method, this can only be used as a reference assay as it can only detect one type of siderophore. The Atkin assay was also developed to detect hydroxamate-type siderophores.[212] This method involves a ferric perchlorate assay and has the advantage of differentiating between mono-, di- or trihydroxamates by having characteristic extinction coefficients. Although this method is simple, it is not specific and lacks sufficient sensitivity. For example, the Csaky assay is 20 times more sensitive than Atkin assay.[212]

Currently, the chrome azurol S (CAS) assay is considered as the universal assay to detect siderophores.[213] This assay is based on biological and functional properties, and can detect all forms of siderophores. The CAS assay was originally introduced by Schwyn and Neilands in 1987, and since then it has been modified several times by other groups. In this method an indicator with an extinction coefficient of 10^5 M^{-1} at 630 nm is

employed. The indicator (Scheme 2.3) is composed of a ternary complex of chrome azurol S, Fe^{3+} and hexadecyltrimethylammonium bromide (HDTMA).

Scheme 2.3 CAS indicator

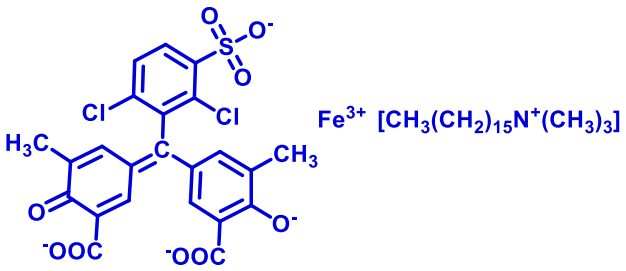

A strong iron chelator like a siderophore can remove iron from the complex thereby making a color change from blue to orange. This assay can be performed on agar plates and in conjunction with paper electrophoresis chromatography. Since it is a biological method, it is time consuming. Further, the detergent present in the CAS medium is highly toxic to bacteria and inhibits the growth of some bacterial strains. The utility of this assay lies in its ability to detect all siderophores regardless of their chemical identities. However, this presents a disadvantage of the method; it lacks the ability to differentiate among siderophore types.

In 1989, the CAS assay was modified by Ames-Gottfred *et al*.[214] They attempted incorporating a strain identification ability to the original CAS method. Since all the strong iron chelators could change the color from blue to orange upon addition of the dye, strains were vaguely identified by culture characteristics. Also the growth of some bacterial species was retarded in the CAS medium due the detergent component, HDTMA. In order to address this issue, they developed a method with varying carbon sources for the agar medium, which could, to a certain extent, select for the growth of particular bacteria strains. Although this is an improvement over the original method, it

relies on the growth characteristics of different strains and hence cannot be used as a universal method. Furthermore, agar plate preparation would be a cumbersome and time consuming step as agar media with different carbon sources are used.

To address the issue of high toxicity of the CAS detergent, Milagres *et al*. slightly altered the CAS method.[215] They prepared culture plates using half culture medium and half CAS-blue agar. Different siderophore types were also identified by development of different colors. For example, at neutral pH, monohydroxamates and trihydroxamates colored reddish-orange and orange respectively while, catechols colored reddish-purple. Although this method is an inexpensive and a reliable technique, culture preparation is time consuming. Also in order to identify the most appropriate culture medium for each bacterial strain, many trial and error experiments must be performed. Hence, this technique becomes extremely laborious, especially considering that only one strain per plate can be identified. Furthermore, quantitative detection is complicated by the rate of colonization of different strains.

CAS liquid assays are also used in siderophore detection which are more sensitive and quantitative than CAS solid assays. However, these methods are limited to chemically defined media and are thus not compatible with siderophores produced in biological media that is colored. Another disadvantage of the CAS liquid assay is its pH sensitivity, preventing its use at basic pH and therefore at basic pH it cannot be used.

In 2003, Machuca and Milagres modified the CAS agar plate method again, so that they could quantify siderophore production.[216] Moving forward with the method they developed earlier, they measured the rate of CAS reaction in millimeter per day. Further they studied the effect of variables such as pH and iron concentration on siderophore

production using a fungal strain. However, aforementioned limitations of culture plates do apply in this assay as well.

CAS agar diffusion assay (CASAD) is another method with a modification to the CAS assay which is actually a combination of CAS agar plate assay and CAS liquid assay.[217] This method produces highly reproducible results even in a wide pH range, from 5-9, and it permits quantification of siderophores. Furthermore, it is a simple and economic assay for siderophore detection in various biological fluids. However, the quantification depends on the size of the haloes around the holes in agar, which is neither an easy nor accurate way to interpret results. Plus, this method also requires long incubation times and cannot differentiate siderophores if more than one type is present.

Overlaid CAS (O-CAS) assay is a major improvement for the CAS assay.[218] Here the CAS method was optimized to yield an easy, rapid and non-toxic assay to detect siderophores. Using an overlay technique, more than one single siderophore producing microorganism could be identified. The growth inhibition problem is avoided in this technique by overlaying agarose gel after microbial growth. Use of agarose in low concentrations allows easy diffusion for the siderophores and thereby increasing the efficiency of the process. The ability to recover the microorganisms after the test is an advantage as they can be used in further tests. However, this method lacks the ability of quantification. Although the assay itself is fast, prior preparation steps which involve incubations require time.

The method specific limitations of the CAS bioassay, prompted the development of a novel siderophore assay. Very recently, Sankaranarayana *et al.* reported a new method based on fluorescence spectroscopy.[219] They used 4-methylumbelliferone-8-methyliminodiacetic acid (Calcein Blue) as the iron chelator of which the fluorescence is quenched upon chelation.[220] This assay can detect nanomolar levels of siderophores, which is a great advantage. Also it is 25 times more sensitive than the standard CAS assay. However, the LOD varies from bacterial species to species, but the authors generalize the LOD to be 10^6 cells/mL.[219] Fluorescence based assays are believed to be more advantageous than colorimetric assays because of higher sensitivity, cost effectiveness and rapidity.[221] Although this method renders all these advantages, differentiation of siderophores or strains is not possible as it only considers the iron extraction from Calcein Blue. Furthermore, although the assay is rapid in comparison to culture-based methods, the entire process still takes about 7-8 h.

When all the methods discussed above are considered, it is clear that the clinical community currently lacks an ideal method for siderophore detection. A simple, rapid, cost-effective, detection system capable of functioning in complex media such as body fluids and that allows quantitative determination of siderophores with a high sensitivity and selectivity is desired. All the assays based on agar plate cultures or broth cultures are laborious and time consuming. When moving towards point-of-care diagnosis systems, rapidity is very crucial. Also wide-spread application of a method can be expected only if the new technology it is simpler and less expensive than that currently available. In addition to assay time, improvements in other properties of siderophore assays are need.

For example all these discussed methods share the drawback of not being able to detect the cell viability. The chemical assays do allow for the detection of a specific siderophore, but they lack the required sensitivity for clinical applications. Fluorescence based assays have many advantages and seem to overcome the challenge of sensitivity. However, since it is known that even a single strain can produce several kinds of siderophores, a method that allows multiplex detection would be extremely advantageous.

2.3.3.2 Currently available siderophore detection methods based on their uptake

Two main types of detection methods that are based on siderophore uptake are reported to date with the purpose of detection and differentiation and include:

- Immobilized-siderophore chip assay
- Assay based on biotin-streptavidin conjugation strategy

Immobilized-siderophore chip methods were developed very recently in order to address mainly the rapidity, cell viability and selectivity issues of other chemical and biological methods.[222-224] This new class of methods directly detect the bacterial strain instead of their excreted siderophores. They utilize the siderophore uptake strategy of living bacterial cells to identify the strain as well as to differentiate debris from live cells. In 2010, Doorneweerd *et al*. demonstrated a novel ligand-patterned chip method (Figure 2.12) which is sensitive, selective and rapid for the detection of *Pseudomonas aeruginosa*.[222] They stamped a gold coated glass chip with a gallium pyoverdine complex conjugated to bovine serum albumin (BSA) using a polydimethylsiloxane (PDMS)

stamp. After exposing that chip to bacteria labeled with a membrane dye carbocyanine known as DiO, they observed the cells under a dark field fluorescence microscope.[222] The limit of detection (LOD) for this method was reported as 10^2 cells/mL.[222] Although this method detects only viable cells, labeling bacteria and construction of the chip are expensive, tedious and time-consuming. However, after application of bacteria on siderophore-patterned chip, the incubation time of one minute is sufficient to capture adequate amounts of bacteria for further study. Although this method works well for siderophores like pyoverdine, which are uptaken by *Pseudomonas* spp., when a siderophore like enterobactin is used several bacterial species would uptake it and hence, species specificity would not be possible. Thus this method is useful only with pathogen-specific siderophores.

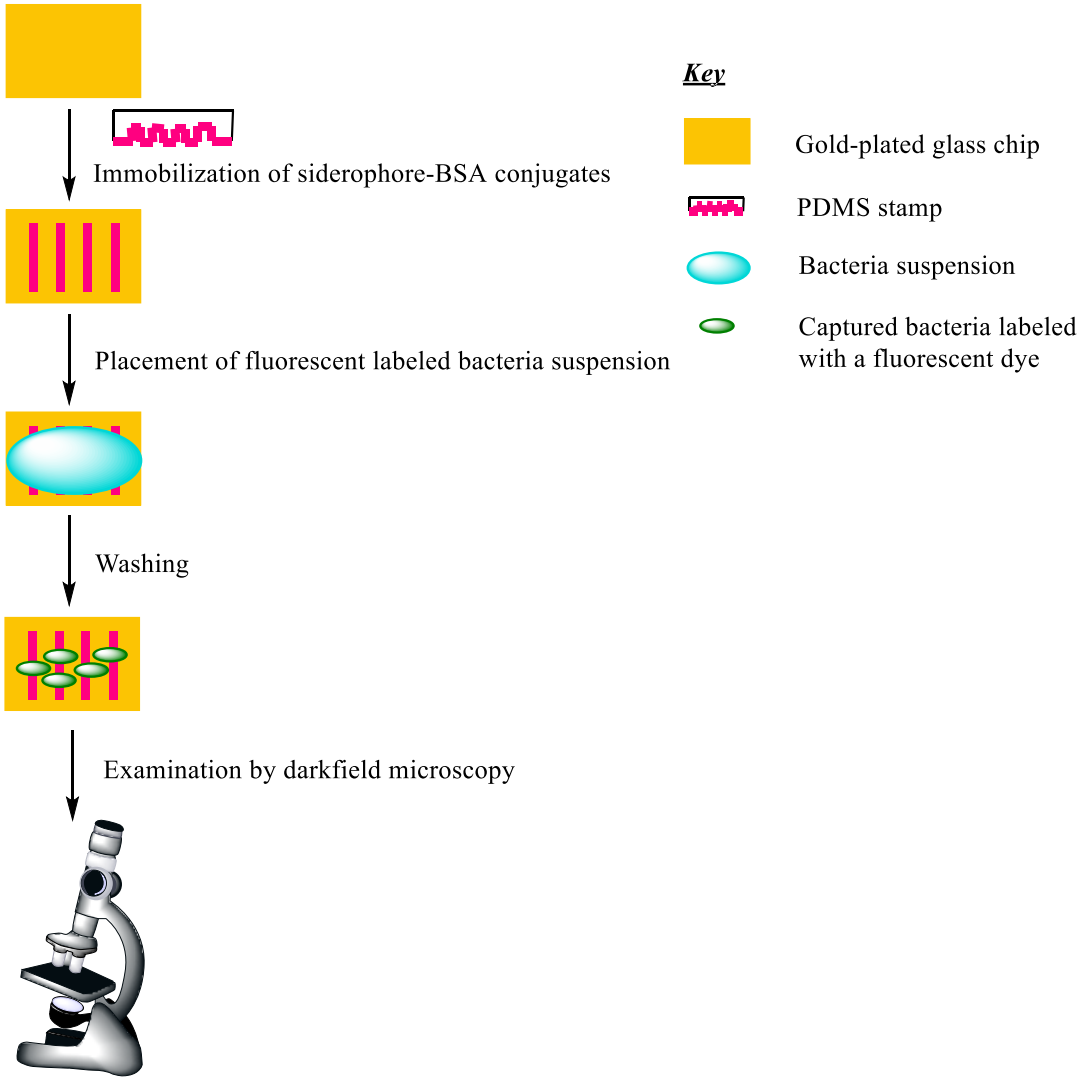

Figure 2.12 Siderophore-patterned gold-plated glass chip (adapted from 220)

In 2012, Kim *et al*. also used the same siderophore-immobilized chip method to detect *Yersinia enterolitica* with the siderophore ferrioxamine, They achieved a LOD of 10^3 CFU/mL.[223] The difference between Kim's method and Doorneweerd's method is that Kim stained the bacteria after capturing whereas, Doorneweerd suspended bacteria in a solution with a membrane dye before capturing them on the chip and assumed them to be live. Therefore, not only Kim could avoid the time consuming bacterial staining, but also it provided a clear demonstration for viable-nonviable differentiation. The major drawback of these methods is the short shelf-life of siderophore-BSA (bovine serum albumin) solutions due to the aggregation property of BSA upon longtime storage. However, once printed on chips, patterned chips were stable even at room temperature for a year given that conditions such as temperature do not exceed the protein denaturing temperature. These studies used ferrioxamine, which is not selective for *Yersinia*, and the authors claim that the problem of ability of some bacteria to uptake xenosiderophores could be avoided by using gold chips coated with pathogen-specific siderophores.

Wolfenden *et al*. simplified the method of Kim.[224] They covalently attached siderophores to a gold coated microscope slide which rendered a greater structural integrity, and they used self-assembled monolayers for surface functionalization that minimized non-specific interactions. In fact they report two methods: a direct method where they covalently attached the siderophores and obtained an LOD of 10^5 CFU/mL and an indirect method where they tethered siderophores to glass chip via a biotin-streptavidin linkage and obtained an LOD of 10^6 CFU/mL.[224] Later the same group reported an improvement of LOD of 10^4 CFU/mL for *E.coli* using the direct method by

increasing the effective surface area of interaction.[225] In addition, they quantified fluorescence imaging intensity with microscopy image software. However, the use of the same siderophore-BSA (ferrioxamine-BSA) conjugates to detect *E. coli*. further solidifies the argument claimed above. The authors claim the specificity of this approach only by comparing with sterile samples, which cannot be a good competition/selectivity study. They could have used other bacterial strains to test for the specificity. Knowing that ferrioxamine is a characteristic siderophore for *Streptomyces spp*., but not evaluating the chip for those bacteria is surprising.

Bugdahn *et al*. developed a biotin-streptavidin binding strategy (Figure 2.13) to identify siderophore-binding proteins.[226] Here, the siderophores are tagged with biotin and they are immobilized on agarose beads derivatized with streptavidin. After treating the biotinylated siderophores with $FeCl_3$ and incubating with streptavidin-derivatized agarose, an affinity chromatography isolated siderophore binding proteins from the crude cell lysate.[226] Although the intention was not bacterial siderophore detection, their biotin-streptavidin binding strategy is an interesting approach for siderophore detection. In fact the aforementioned method by Wolfenden *et al*. incorporated this biotin-streptavidin binding strategy to tether siderophores to the gold coated chips shows the importance of this technique.[224]

A limitation of these methods that rely on siderophore binding, is that some bacteria use exogenous siderophores (xenosiderophores) that are produced by other microorganisms. In that case these methods would provide false positives. However, a selective elimination method could be useful to identify the bacteria present.

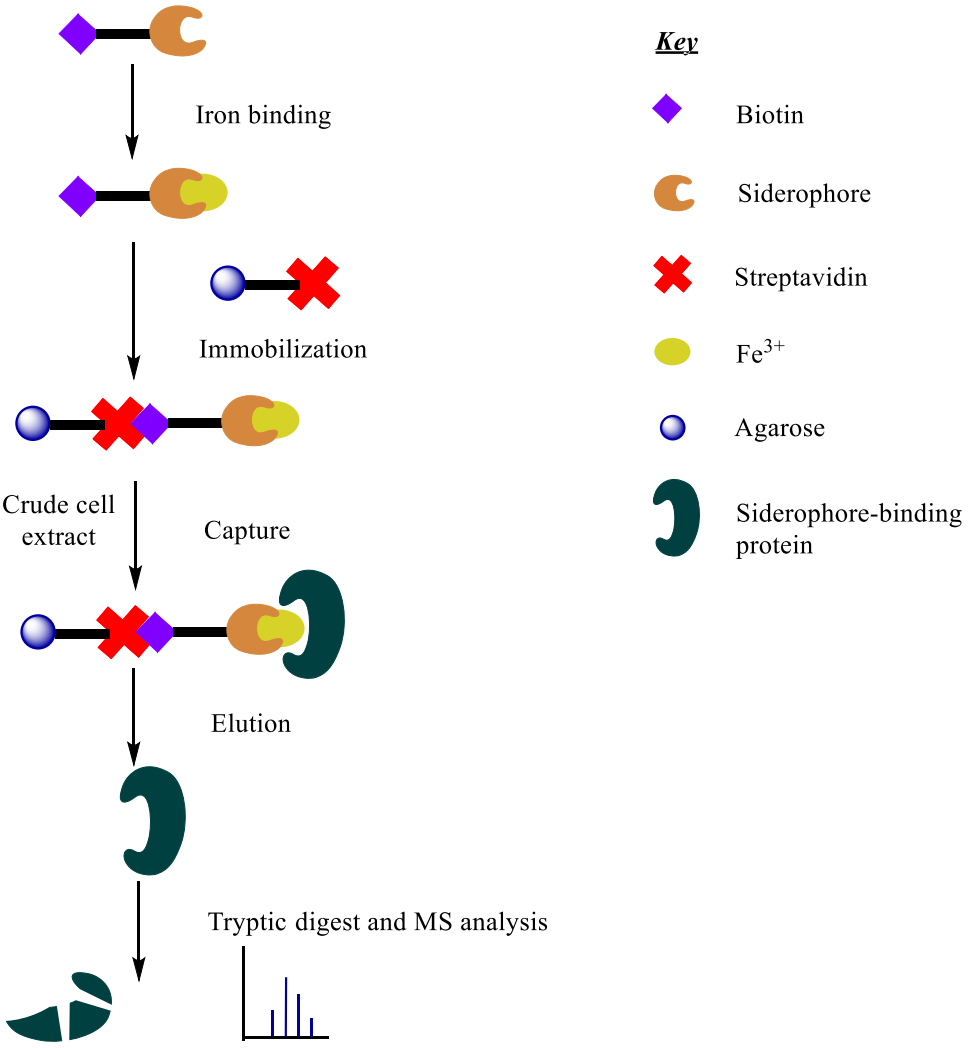

Figure 2.13 Identification of siderophore-binding proteins by siderophore immobilization (adapted from 224)

Given the importance of rapid identification of bacterial infections, targeting detection of siderophores is an interesting approach. Since siderophores are secreted to the media and also secreted in large quantities, if detection of siderophores is possible that would be very useful.

3 BACTERIAL DIAGNOSIS BY TARGETING DETECTION OF SECRETED SIDEROPHORES

3.1 Synopsis

A point-of-care (POC) diagnostic device for bacterial infections that meets the criteria set by WHO is an unmet need in the medical community. Regarding this concern, our first approach focuses on developing a novel technology for rapid diagnosis of bacterial infections by targeting siderophores. As a proof-of-concept demonstration, this novel technology was first applied to the detection of mercury ions using a mercury selective structure-switching aptamer based probe which is discussed in Chapter 4. This novel technology involves a probe that is a combination of an aptamer-based probe and a lanthanide-based probe. Hence, we named it as a lanthanide-apta-switch.

3.2 Introduction

The lanthanide-apta-switch we introduce features a phenanthridine coordinated to a DOTA-type ligand that chelates europium, which in turn is conjugated to an aptamer. The aptamer is then hybridized with its complementary strand, called the reporter strand. When phenanthridine is not intercalated in double stranded DNA, excitation light energy is transferred to the europium, which then emits in the visible region (probe is 'on'). However, when the probe is in the aptamer/reporter strand duplex form, the phenanthridine is intercalated in between the DNA base pairs preventing the energy transfer to the europium, which results in quenching of luminescence (probe is 'off'). Upon recognition of a metal coordinated siderophore by the aptamer, a conformational change in the aptamer is induced, and the reporter strand is released. As a result, phenanthridine is no longer intercalated between the DNA duplex, and luminescence is 'turned on' (Figure 3.1). Although bacteria secrete siderophores to sequester their ion need, the probe will work much better if gallium is present instead of iron. Therefore, a gallium salt is also introduced to the medium along with the probe. The reason for this is Fe^{3+} being a d^5 metal ion it tends to quench the luminescence of europium, but Ga^{3+} does not as it is a d^{10} ion.

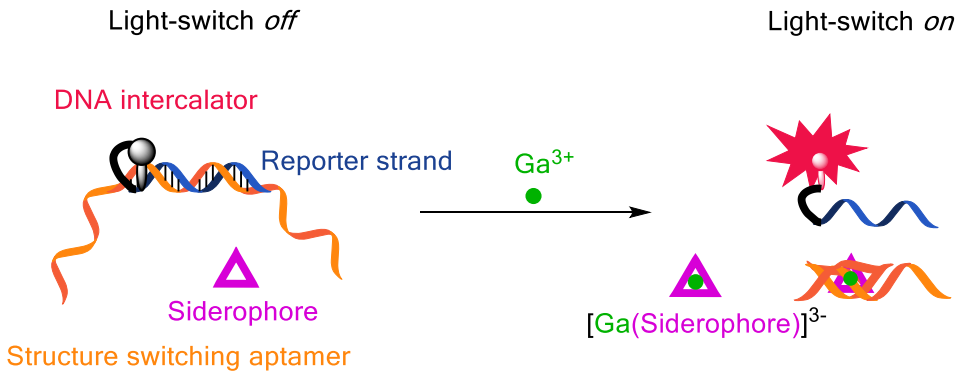

Figure 3.1 Mode of action of lanthanide-apta-switch

3.2.1 Aptamer-based luminescent probes and their advantages

Aptamers are single-stranded oligonucleotides that bind the target molecules with high affinity and high selectivity. Both DNA and RNA aptamers have been isolated from repeated rounds of *in vitro* selections, known as systematic evolution of ligands by exponential enrichment (SELEX).[227] Aptamers are increasingly used in medicine, nano-technology, microbiology and in other bioanalytical applications because they can be engineered in such a way to selectively bind the target molecules such as proteins or other small molecules like ATP or even metal ions with a high affinity.[227] They are easy to synthesize on a large scale, can be stored at room temperature and have long shelf lives.[228] Not all aptamers are structure-switching and the structure-switching capability highly depends on the length of the aptamer.[227,229] Aptamers that can fold into a ternary structure inducing a significant conformational change are termed as structure-switching aptamers.[229] For practical applications that use structure-switching aptamers often utilize molecular beacon approach where a fluorophore and a quencher are linked.[230-233]

However, this technology requires multiple, often difficult, bioconjugation steps. Our approach uses a light-switch DNA intercalator minimizing the bioconjugation steps.

3.2.2 Lanthanide-based luminescent probes and their advantages

3.2.2.1 Advantages of lanthanides

The probe featured in this Chapter and the 4th Chapter, employs a lanthanide ion which renders several advantages such as a large Stokes shift, narrow emission bands and a long luminescence lifetime.[234] The advantage of having a large Stokes shift is that a linear relationship is obtained between the probe response and the concentration of analyte avoiding self-absorption issues (Figure 3.2 a).[234] In lanthanide probes, an antenna is connected to a ligand coordinated lanthanide via a spacer group. The Stokes shifts between the absorption by antenna and the emission of lanthanide is quite large. For example, Stokes shifts of terbium and europium are larger than 200 nm, which is approximately ten times larger than that of the organic fluorescent dyes.[234] Narrow emission bands of lanthanides which are about 20 nm in width do not completely overlap with that of another lanthanide (Figure 3.2 b), which allows to the probes to be synthesized in such a way that several analytes could be detected simultaneously.[234,235] Furthermore, lanthanides have long luminescent lifetimes due to the forbidden nature of f-f transitions.[234] For example luminescent lifetimes of terbium and europium are in the millisecond range whereas those of organic dyes are in the nanosecond range.[234] This nature is important in obtaining quantitative analysis in complex biological media via time-gated measurements (Figure 3.2 c).[234] Therefore, with the time delay, the probe-only

response can be measured after allowing the background fluorescence to completely decay.[234]

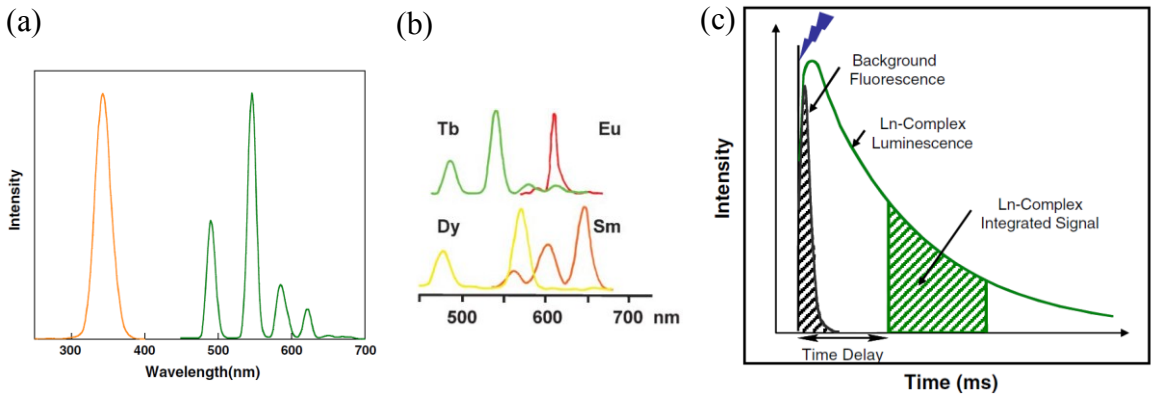

Figure 3.2 (a) An example of a lanthanide Stokes shift,[234] (b) non-overlapping emission bands of lanthanides,[235] (c) time-gated luminescence spectroscopy.[234]

3.2.2.2 Principles of lanthanide-based probes

In lanthanide-based probes Laporte forbidden f-f transitions of lanthanides are activated by an antenna that is coordinated to the lanthanide via a spacer group. Consider the lanthanide complex discussed in this chapter (Figure 3.3 a), once the antenna is excited, the energy is transferred to the lanthanide metal which then lumineses in the visible region. As depicted in the Jablonski diagram (Figure 3.3 b), the quantum yield of the lanthanide luminescence depends on several factors such as how efficiently the triplet excited state of the antenna is populated, the difference of energies between the triplet excited state of the antenna and the ^5D excited state of the lanthanide, the distance between the antenna and the lanthanide and the number of coordinated water molecules.[234]

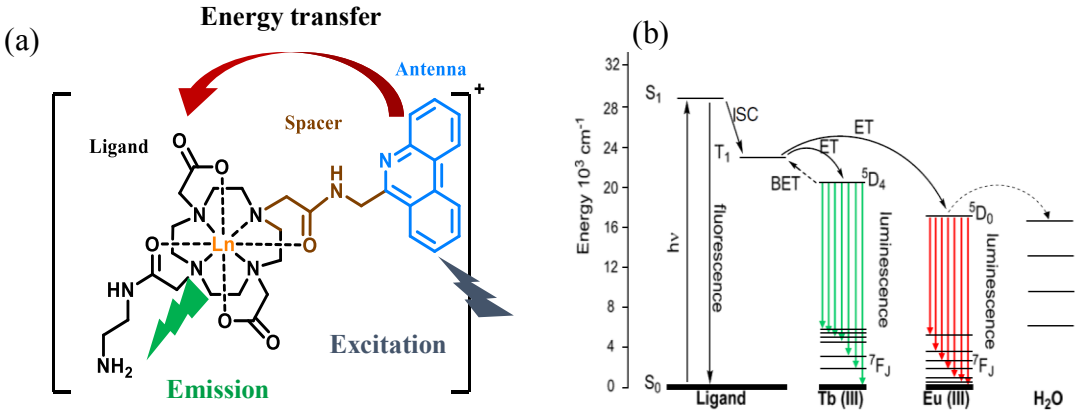

Figure 3.3 (a) Energy transfer of lanthanide based probe Eu-DO2A-Phen-Amine, (b) Jablonski diagram that shows the energy transfer process in lanthanide probes.[234]

4 TURNING AN APTAMER INTO A LIGHT-SWITCH PROBE WITH A SINGLE BIOCONJUGATION

4.1 Synopsis

We describe a method for transforming a structure-switching aptamer into a luminescent light-switch probe *via* a single conjugation. The methodology is demonstrated using a known aptamer for Hg^{2+} as a case study. The approach utilizes a lanthanide-based metallointercalator, Eu-DOTA-Phen, whose luminescence is quenched almost entirely and selectively by purines, but not at all by pyrimidines. This complex, therefore, does not luminesce while intercalated in dsDNA, but it is bright red when conjugated to a ssDNA that is terminated by several pyrimidines. In its design, the light-switch probe incorporates a structure-switching aptamer partially hybridized to its complementary strand. The lanthanide complex is conjugated to either strand *via* a stable amide bond. Binding of the analyte by the structure-switching aptamer releases the complementary strand. This release precludes intercalation of the intercalator in dsDNA, which switches on its luminescence. The resulting probe turns-on 12-fold upon binding to its analyte. Moreover, the structure switching aptamer ensures the selectivity, and the long luminescence lifetime of the probe readily enables time-gating experiments for removal of the background autofluorescence of the sample.

4.2 Introduction

Aptamers, single-stranded oligonucleotides that bind with high affinity and high selectivity to a selected target such as a protein, a small molecule or a metal ion, are increasingly used in therapeutics, diagnosis and detection.[236] Luminescent analogs have been prevalent for the latter two applications due to the widespread use of the technique. Indeed, significant work has already been published on the design of fluorescent aptamer-

based probes, most commonly and successfully with approaches involving molecular beacons[230-233] and aptamer-based G-quadruplex systems.[237-240] Unfortunately, this technology requires multiple, often difficult, bioconjugation steps and it remains ill adapted to multiplex detection and applications in complex aqueous or biological media. The first limitation with regards to synthesis can, in theory, be met with the use of light-switch DNA intercalators, molecules whose quantum yields vary greatly upon intercalation between base pairs. However, intercalators have so far only been used in "label-free" approaches, which consist of simply mixing the intercalators with the aptamer. In each case, most of the dyes are intercalated both in the absence and in the presence of the analyte. Consequently, the responses observed were small (typically 3-fold) and also turn-off.[241-250] The other two limitations, multiplex detection and also detection in a complex aqueous sample, could in theory be resolved with a lanthanide-based probe.[251] The narrow emission bands and long luminescence lifetimes of lanthanide complexes make them uniquely suited for multiplex detection and quantitative analysis in complex media *via* time-gated measurements. Herein we report such a light-switch lanthanide-based aptamer probe, with substantial turn-*on* and a long luminescence lifetime. Its synthesis, unlike most aptamer-based probes,[230-233] requires only one bioconjugation, whereas other systems need an individual conjugation for both the fluorophore and the quencher. The application of this methodology can readily be expanded to other substrates and for multiplex detection. The key to multiplex detection is simply to ensure that each aptamer probe for each analyte has a unique reporter strand sequence and makes use of a distinct lanthanide ion such as terbium or europium. However, we anticipate that our technology would work with thulium, dysprosium and

samarium as well. Since the emission spectra of lanthanide ions mostly do not overlap, they can be readily used for multiplex detection. Further, multiplex detection with lanthanide ions has been extensively reported by our group and others.[252-255]

In terms of design, we postulated that the first of the aforementioned three limitations, the number of bioconjugation steps, could be resolved *via* a single conjugation of a light-switch DNA intercalator to a structure-switching aptamer. Structure-switching aptamers change their structure upon binding to their cognate target, most often *via* the release of a shorter complementary strand.[256,257] Judicious conjugation of an intercalating dye to either strand of such an aptamer/complement duplex ensures that the dye is completely intercalated only in the absence of the analyte, but is not intercalated in the presence of the analyte (Figure 4.1). If the intercalating dye itself is a light-switch, then the aptamer probe will also be one. The probe is thus devised to have a higher response than label-free intercalator-based systems,[244] while at the same time limiting bioconjugation to a single DNA strand. Note that in this design, use of a dye that only luminesces while intercalated will result in a turn-*off* probe, while one that is quenched by stacking with base pairs will result in a turn-*on* probe. Since turn-*on* probes are generally preferred for practical applications, this design excludes the use of common light-switch intercalators such as dppz-based ruthenium[258] or osmium complexes,[259] platinum complexes[260,261] or organo-intercalators such as ethidium bromide.[262] Instead, we postulated that the desired response could be achieved with lanthanide complexes whose luminescence is nearly completely quenched upon intercalation in double-stranded DNA (dsDNA). A further advantage of using lanthanides is that they also solve the above mentioned other two limitations of current molecular beacons. The long luminescence

lifetimes of lanthanide complexes, typically in the millisecond range for Eu^{III} and Tb^{III}, enable facile time-gating experiments whereby the background autofluorescence of the sample is removed. Their narrow emission bands with limited overlap further enables simultaneous detection of multiple analytes in the same sample.

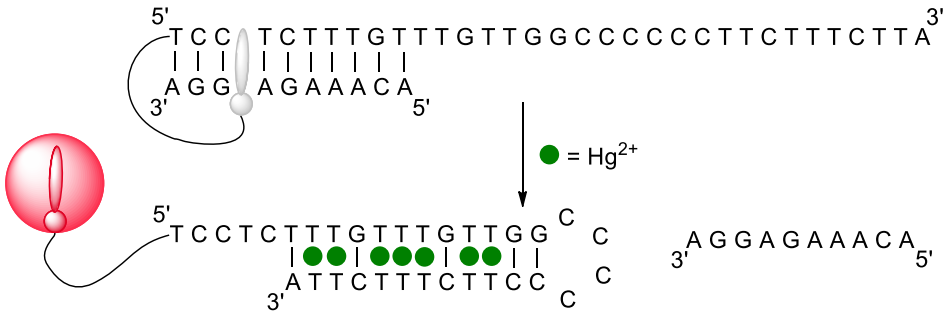

Figure 4.1 Proposed mode of action of aptamer light-switch, Eu-AptaSwitch (1). *In the absence of Hg^{2+}, the Eu^{III} complex intercalates in dsDNA. Photoelectron transfer from the purines to the phenanthridine antenna quenches the luminescence of Eu^{III}. Binding of Hg^{2+} by the aptamer releases the short complementary strand, thereby preventing intercalation of the Eu^{III} complex and turning on its luminescence.*

This design thus requires a lanthanide complex not only capable of intercalating in dsDNA, but whose luminescence is substantially affected by the oligonucleotide. Our group[252,263,264] and Parker's[265-268] have previously demonstrated that the luminescence of phenanthridine-based terbium and europium complexes can be nearly completely quenched upon intercalation in dsDNA. This effect, which is likely the result of photoelectron transfer from stacked purines to the excited state of the chromophore, was the basis behind the recent design of our probe for GTP and ATP detection.[252,264] Importantly, although both purines efficiently quench the lanthanide-centered emission of

this complex, neither of the two pyrimidines does. Our probe, Eu-AptaSwitch (**1**), was thus constructed by conjugating the phenanthridine-based lanthanide complex to the DNA strand of the structure-switching aptamer that is mostly composed of thymidines and cytidines (Figure 4.2). The shorter complementary strand is thus primarily composed of adenosines and guanosines. The probe was designed to function as follows (Figure 4.1). In the absence of the analyte, i.e. when the phenanthridine is intercalated in the dsDNA, the probe is in the *off* mode. Consequentially, photoelectron transfer (PeT) from the stacked purine bases quenches the lanthanide luminescence. Binding of the analyte by the aptamer releases the short complementary strand. At this point, intercalation and quenching of the phenanthridine by purines are no longer possible. Therefore, the luminescence of the lanthanide complex turns *on*.

Lanthanide complexes used for biological and medical applications must be thermodynamically stable and kinetically inert so as to minimize the risk of trans-metallation with Ca^{2+} and trans-ligation with endogenous ligands such as phosphates.[269] To this end, a macrocyclic polyaminocarboxylate was incorporated in our Eu-AptaSwitch (**1**). Although more difficult to synthesize than their linear analogs, macrocyclic DOTA-type chelates, such as the one used in this study, are more appropriate for detection of analytes in biological or environmental aqueous systems due to their kinetic inertness. Furthermore, the overall positively charged lanthanide complexes of DOTA tetraamide (DOTAm) ligands are kinetically more inert than DOTA analogues as a result of the decreased basicity of the nitrogen atoms.[270]

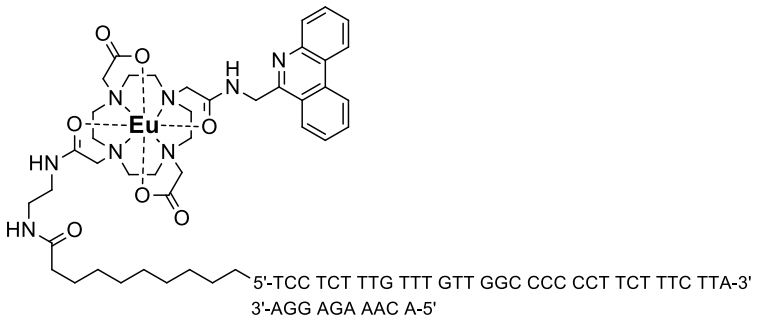

Figure 4.2 Chemical structure of Eu-AptaSwitch (1). *The Eu^{III} complex is conjugated to the aptamer via a C9 alkyl chain. The two oligonucleotides are annealed prior to use.*

As a proof of principle, we applied our concept to a structure-switching aptamer previously reported for Hg^{2+}.[271] This aptamer makes use of the ability of thymidines to coordinate Hg^{2+} in a T-Hg^{2+}-T fashion. Therefore, the lanthanide complex was conjugated to the thymidine-rich strand that binds Hg^{2+} as opposed to its shorter complementary strand. Note that in order to further increase the turn-*on* of the probe, some of the purine bases in the mercury-binding strand reported by Lu[271] were replaced by pyrimidines (third and fifth positions, A to C and G to C, respectively). Presumably, this design can be applied to any structure-switching aptamer, given that it is mostly composed of either purines or pyrimidines regardless of how the aptamer binds its analyte.

4.3 Results and Discussion

The molecular probe Eu-AptaSwitch (**1**) was synthesized according to Scheme 4.1 from three advanced intermediates: DO2A^{t}Bu (**2**),[272] the phenanthridine acetamide arm (**3**),[264] and the bridging arm (**5**). The syntheses of the former two were previously reported in the literature. Conjugation of the phenanthridine arm followed by that of the

bridging arm yielded the fully protected ligand (**6**). Treatment under acidic conditions deprotected the acids and the amine simultaneously, thereby yielding the free ligand which was metallated with Eu^{III} under slightly basic aqueous conditions. Note that as for any DOTA-type complex, long reaction times are needed to ensure full complexation of the lanthanide by the macrocycle.[273] Advantageously, the stability of the resulting amine-terminated complex enables subsequent conjugation to any molecule containing a carboxylate. For our intended application, the complex was reacted with the DADE-terminated aptamer on solid support. DADE (decanoic acid diester) is a commercially available pre-activated carboxyl linker that enables facile conjugation to the Eu^{III}-complex all the while being long enough for the phenanthridine to intercalate in the dsDNA (Figure 4.2). Cleavage of the bioconjugate from its solid support, followed by deprotection of the bases and purification by reverse phase high pressure liquid chromatography (RP-HPLC) yielded the Eu^{III} complex (**9**) that was annealed with the short complementary strand to yield the luminescent probe Eu-AptaSwitch (**1**). Notably, bioconjugation was only possible with a lanthanide complex containing an amine and a DNA terminated with an activated acid. Our multiple attempts at reversing the functional groups, that is, to conjugate a Eu complex with a pendant acid or activated acid to an amine-terminated oligonucleotide, were all unsuccessful, regardless of the coupling agent used. This also highlights the difficulty of conjugating metal complexes to DNA.[230-232,274-285] The synthesis described above should be applicable to the conjugation of other types of metal complexes to DNA for therapeutic and diagnostic purposes.

Scheme 4.1 Synthesis of Eu-AptaSwitch (1)[a]

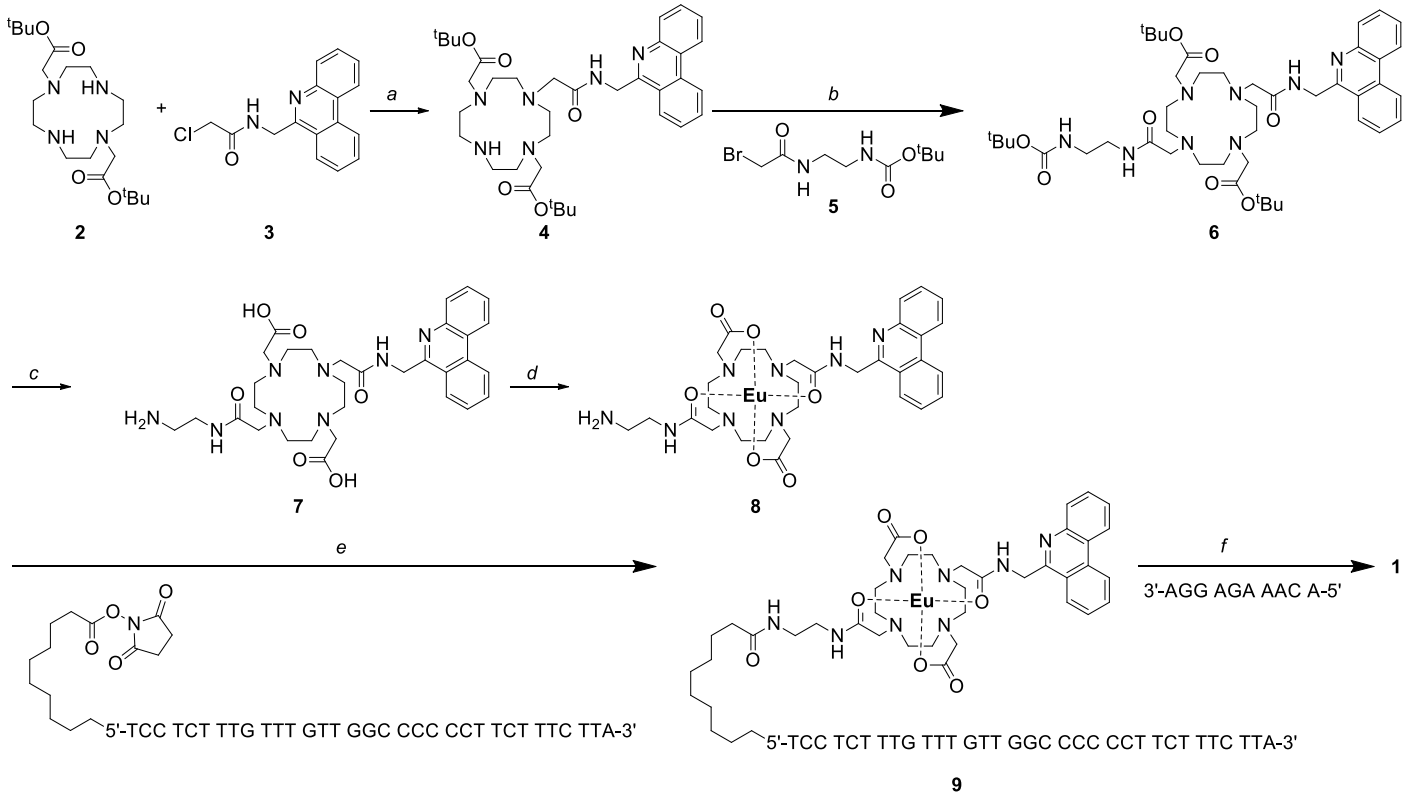

[a]Experimental conditions: (a) Et_3N, $CHCl_3$, 62 °C, 18 h; (b) Cs_2CO_3, CH_3CN, 82 °C, 18 h; (c) HCl, CH_3OH, rt, 5 d; (d) $EuCl_3 \bullet 6H_2O$, LiOH, H_2O, pH 8, 70 °C, 76 h; (e) conjugation of the aptamer to the DADE linker (on solid support) in phosphate buffer, pH 8, 15 h; deprotection: 30% NH_3, 65 °C, 5 h; (f) complementary strand, PBS, 95 °C for 15 min, slow cooling.

The time-gated emission profile of the probe in the absence and presence of its analyte is shown in Figure 4.3. As expected, annealing the Eu-DNA conjugate with the complementary strand quenches most of the metal-centered luminescence; the luminescence of the annealed Eu-AptaSwitch (**1**) is only 4% that of the ssDNA conjugate (**9**). This result is consistent with the intercalation of the phenanthridine in the dsDNA; resulting photoelectron transfer from the purine bases to the antenna quenches the lanthanide-based emission. Importantly, the luminescence of Eu^{III} is fully recovered upon addition of Hg^{2+}. This observation is in agreement with binding of Hg^{2+} by its structure-switching aptamer with concomitant release of the complementary strand such that the phenanthridine can no longer intercalate in dsDNA. Since PeT from purine bases to the antenna is no longer possible, luminescence of Eu^{III} is recovered. This design enables not only a complete recovery of the lanthanide emission, but also a substantial 12-fold turn *on* which is comparable to that of other light-switch probes. Notably, such a turn-*on* is readily observable with the naked eye upon illumination with a standard portable UV-lamp (Figure 4.4). The characteristic red luminescence of the Eu^{III} probe is only apparent in the presence of ten equivalents of Hg^{II}. This light-switch response thus bodes well for future application of this technology to the detection of other analytes without the need for a spectrophotometer. Moreover, the probe detects its analyte rapidly; the luminescence turn-*on* is observed in one minute after adding mercury at room temperature.

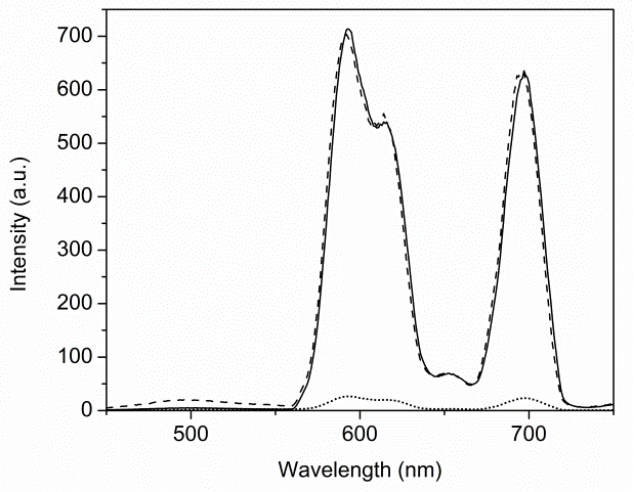

Figure 4.3 Time-gated emission profiles of Eu-DNA conjugate (9) (solid line), Eu-AptaSwitch (1) (dotted line), Eu-AptaSwitch•Hg^{2+}(dashed line). *Experimental conditions: [Eu-DNA conjugate] = [Eu-AptaSwitch] = 20 μM, [Hg^{2+}]= 250 μM, PBS buffer, pH = 7.0, T = 20 °C, time-delay = 0.1 ms, slit widths = 20 nm, excitation at 271 nm.*

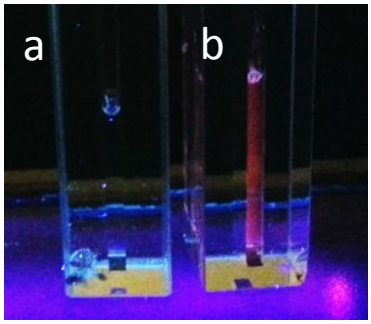

Figure 4.4 Luminescence of Eu-AptaSwitch (1) upon excitation with a portable UV lamp in the absence (a) and presence (b) of ten equivalents of Hg^{2+}. *Experimental conditions: PBS, pH 7.0, rt, $\lambda_{excitation}$ = 254 nm.*

Time-gated luminescence titration of Eu-AptaSwitch (**1**) in the presence of Hg^{2+} is shown in Figure 4.5. Turn-*on* in the presence of low concentration of mercury is shown in the inset. The very long lifetime characteristic of Eu^{III}-centered luminescence, a

requirement for time-gating experiments, is ideally suited for titration in complex aqueous media. Note that, as for Lu's probe,[271] the titration curve of Eu-AptaSwitch can be fitted with a Hill coefficient of 2, suggesting a cooperative binding of Hg^{2+} to the aptamer.

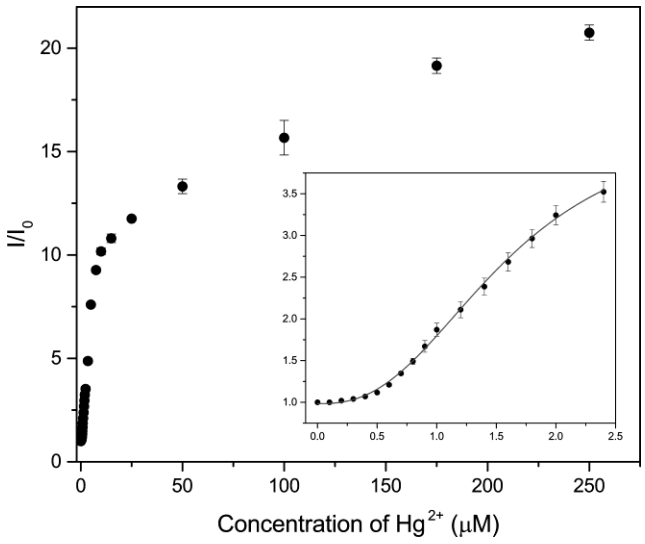

Figure 4.5 Time-gated luminescence of Eu-AptaSwitch (1) with increasing concentration of Hg^{2+}. *Experimental conditions: [Eu-AptaSwitch] = 20 μM, PBS buffer, pH = 7.0, T = 20 °C, time-delay = 0.1 ms, slit widths = 20 nm, excitation at 271 nm, emission integrated from 450 to 750 nm, error bars represent SD, n = 3. Inset: data points at low concentrations of Hg^{2+}.*

As shown in Figure 4.6, a competitive binding study was performed with 10-fold excess of some divalent metal ions. The metal ions tested were Mg^{2+}, Ca^{2+}, Zn^{2+}, Cd^{2+}, Mn^{2+}, Co^{2+}, Pb^{2+}, Ni^{2+} and Cu^{2+}. First, 250 μM metal ion solution was added individually to 20 μM probe solution and the luminescence was monitored. Then, 25 μM Hg^{2+} solution was added and the luminescence was measured again. Not only that the probe does not turn-*on* with any other competing divalent ions tested, but also the turn-*on* with

Hg^{2+} was not affected by these competing ions. This competitive binding study strongly suggests that Eu-AptaSwitch shows an excellent selectivity towards the detection of Hg^{2+}, and replacing two purines with pyrimidines in the Hg^{2+}-selective aptamer has not affected the selectivity of the aptamer.

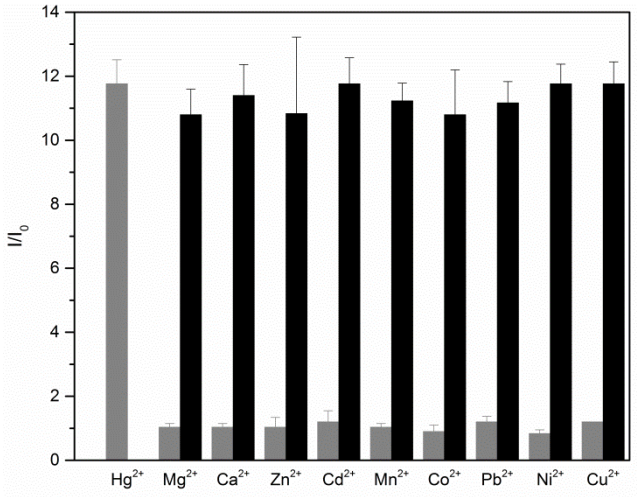

Figure 4.6 Selectivity of Eu-AptaSwitch (1). Gray bars represent the luminescence response after adding 250 µM metal ion (except Hg^{2+}, which is only 25 µM). *Black bars represent the luminescence response after adding 25 µM of Hg^{2+} to the probe containing 250 µM metal ion. Experimental conditions: [Eu-AptaSwitch] = 20 µM, PBS buffer, pH = 7.0, T = 20 °C, time-delay = 0.1 ms, excitation at 271 nm, emission at 592 nm, error bars represent SD, n = 3.*

The performance of the Eu-AptaSwitch probe was also tested in human serum. As shown in Figure 4.7, the probe turns *on* in serum, however, at a given concentration of Hg^{2+}, the luminescence intensity was low compared to that of the buffered aqueous solution. The serum, being a complex medium, this result was expected.

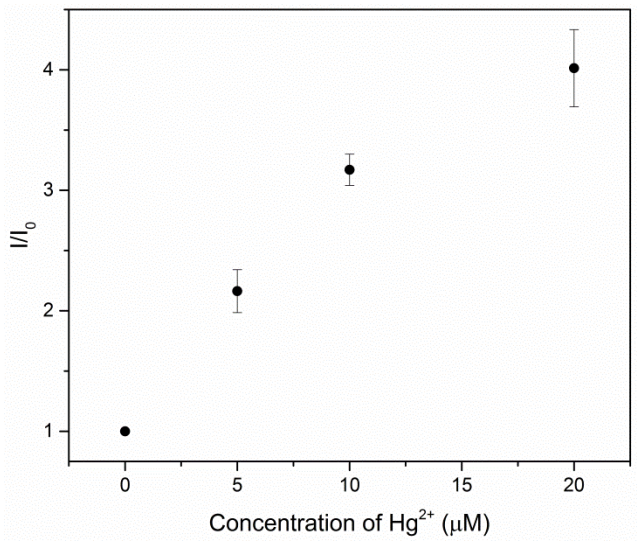

Figure 4.7 Time-gated luminescence of Eu-AptaSwitch (1) in human serum with increasing concentration of Hg^{2+}. *Experimental conditions: [Eu-AptaSwitch] = 20 μM, T = 20 °C, time-delay = 0.1 ms, excitation at 271 nm, emission at 592 nm, error bars represent SD, n = 3.*

4.4 Conclusions

In conclusion, a novel approach to the design of luminescent aptamer probes that makes use of a light-switch lanthanide intercalator is reported. Compared to beacon-type approaches, this approach only requires a single conjugation, and therefore enables a more facile synthesis. As opposed to the label-free approaches that also employ DNA intercalators, our approach yields not only a turn-*on* response but also a substantially greater response. Moreover, the structure switching aptamer ensures the selectivity of the probe, while the long luminescence lifetime and the narrow emissions of lanthanide metals are expected to facilitate multiplex detection in a single, complex aqueous sample.

4.5 Experimental Procedures

General Considerations.

Unless otherwise noted, starting materials were obtained from commercial suppliers and used without further purification. DNA was purchased from Trilink Biotechnologies. Water was distilled and further purified by a Millipore cartridge system (resistivity 18.2 MΩ). Flash chromatography was performed on Salicycle Silica Gel (230-400 mesh) or Brockmann activated aluminium oxide (neutral, 60 mesh). ^{1}H-NMR spectra were recorded on a Varian 300 or Varian 500 at 300 MHz or 500 MHz respectively, and ^{13}C NMR spectra on a Varian 300 at 75 MHz at the LeClaire-Dow Instrumentation Facility at the Department of Chemistry at the University of Minnesota, Twin-Cities. The residual solvent peak was used as an internal reference. Data for ^{1}H NMR are recorded as follow: chemical shift (δ, ppm), multiplicity (s, singlet; br s, broad singlet; d, doublet; t, triplet; q, quartet; m, multiplet), integration, coupling constant (Hz). Data for ^{13}C NMR are reported in terms of chemical shift (δ, ppm). Mass spectra (LR = low resolution; HR = high resolution; ESI = electrospray ionization) were recorded on a Bruker BioTOF II at the Waters Center of Innovation for Mass Spectrometry at the Department of Chemistry at the University of Minnesota, Twin-Cities. Liquid Chromatography-Mass Spectrometry, HPLC-ESI-MS were performed on an Agilent 1100 capillary HPLC-ion trap mass spectrometer (Agilent Technologies) at the Mass Spectrometry facility at the Masonic Cancer Center at the University of Minnesota. A Zorbax 300SB-C8 column (150 mm x 0.3 mm, 3.5 μm, Agilent Technologies) was eluted at a flow rate of 9 μL/min with a gradient of 15 mM ammonium acetate and 5-16 % acetonitrile in over 14 min and then up to 90 % over 2 min. The column was maintained

at 40 °C. The mass spectrometer was operated in the negative mode for the analyses of oligonucleotide conjugates. UV-Vis data was obtained on a Cary Bio 100 UV-Vis Spectrophotometer. Fluorescence data was acquired on a Varian Cary Eclipse Spectrophotometer using a quartz cell with a path length of 10 mm, excitation slit width of 20 nm and emission slit width of 20 nm at 20 °C.

Di-tert-butyl 2,2'-(4-(2-oxo-2-((phenanthridin-6-ylmethyl)amino) ethyl)-1,4,7,10-tetra azacyclododecane-1,7-diyl)diacetate (4).

Di-*tert*-Butyl 2,2'-(1,4,7,10-tetraazacyclododecane-1,7-diyl)diacetate (**2**) and 2-chloro-*N*-(phenanthridine-6-ylmethyl)acetamide (**3**) were synthesized according to previously published procedures.[252,272] A solution of 2-chloro-*N*-(phenanthridine-6-ylmethyl)acetamide (**3**) (101 mg, 0.355 mmol) in $CHCl_3$ (10 mL) was added to a solution of di-*tert*-butyl 2,2'-(1,4,7,10-tetraazacyclododecane-1,7-diyl)diacetate (**2**) (285 mg, 0.711 mmol) and triethylamine (59 μL, 0.48 mmol) in $CHCl_3$ (10 mL) under N_2 (*g*). The reaction mixture was heated to reflux under N_2 (*g*) for 20 h then allowed to cool to room temperature. The product was purified by chromatography over alumina eluting with a gradient of CH_2Cl_2 to 10% CH_3OH/90% CH_2Cl_2. The product was obtained as a yellow oil (200 mg, 87%). ^{1}H NMR (500 MHz, $CDCl_3$) δ 8.65 (d, *J* = 8.5 Hz,1H), 8.57 (d, *J* = 8.0 Hz, 1H), 8.36 (d, *J* = 7.5 Hz, 1H), 8.16 (m, 1H), 7.88 (t, *J* = 7.5 Hz, 1H), 7.73 (m, 3H), 5.14 (s, 2H), 2.91 (m, 22H), 1.30 (s, 18H); ^{13}C NMR (125 MHz, $CDCl_3$) δ 171.8, 170.5, 143.4, 133.0, 131.2, 129.6, 129.0, 128.1, 127.3, 126.5, 125.6, 124.5, 124.3, 122.7, 122.4, 81.5, 58.0, 54.6, 52.5, 49.8, 47.9, 43.1, 28.1; HRMS (ESI) calc for $[C_{36}H_{52}DN_6O_5]^+$ ($[M+D]^+$): *m/z* 649.4056, found: 649.4070.

Tert-butyl (2-(2-bromoacetamido)ethyl)carbamate (5).

A solution of K_2CO_3 (202 mg, 1.46 mmol) in water (20 mL) and a solution of bromoacetylbromide (132 μL, 1.51 mmol) in CH_2Cl_2 (20 mL) were simultaneously added over 30 min to a solution of *tert*-butyl (2-aminoethyl)carbamate (200. μL, 1.26 mmol) in CH_2Cl_2 (50 mL) cooled to 0°C. The reaction mixture was subsequently allowed to warm to room temperature and stirred for an additional 1.5 h. The reaction mixture was rinsed with water (2 × 50 mL) and saturated NaCl (*aq*) (1 × 50 mL), dried over magnesium sulfate, and filtered. The solvents were removed under reduced pressure to yield the product **5** as a white solid (315 mg, 90%). ^{1}H NMR (300 MHz, $CDCl_3$) δ 5.21 (s, 2H), 3.61 (t, J = 6.6 Hz, 2H), 3.06 (m, 2H), 1.39 (s, 1H); ^{13}C NMR (60 MHz, $CDCl_3$) δ 166.5, 156.5, 79.7, 53.2, 39.5, 41.2, 28.0; HRMS (ESI) calc for $C_9H_{18}NaN_2O_3Br$ ($[M+Na]^+$): *m/z* 303.0315, found: 303.0377.

Di-tert-butyl 2,2'-(4-(2-((2-((tert-butoxycarbonyl)amino)ethyl) amino)-2-oxoethyl)-10-(2-oxo-2-((phenanthridin-6-ylmethyl)amino)ethyl)-1,4,7,10-tetraazacyclododecane-1,7-diyl)diacetate (6).

Di-*tert*-butyl 2,2'-(4-(2-oxo-2-((phenanthridin-6-ylmethyl)amino)ethyl)-1,4,7,10-tetraazacyclododecane-1,7-diyl)diacetate (**4**, 50 mg, 0.077 mmol) and Cs_2CO_3 (50 mg, 0.15 mmol) were added to a solution of *tert*-butyl (2-(2-bromoacetamido)ethyl)carbamate (**5**, 43 mg, 0.15 mmol) in acetonitrile (25 mL). The reaction mixture was heated for 18 h at 82 °C. The reaction mixture was then allowed to cool to room temperature and the solvents were removed under reduced pressure yielding the protected ligand **6** as a yellow

oil which was used immediately in the next step. ^{1}H NMR (500 MHz, $CDCl_3$) δ 8.79 (d, *J* = 8.1 Hz, 1H), 8.71 (d, *J* = 7.8 Hz, 1H), 8.30 (d, *J* = 8.1 Hz, 1H), 8.09 (d, *J* = 7.8 Hz, 1H), 7.93 (t, *J* = 8.1 Hz, 1H), 7.75 (m, 3H), 4.34 (s, 2H), 3.25 (m, 4H), 2.71 (m, 24H), 1.43 (s, 18H), 1.36 (s, 9H); ^{13}C NMR (125 MHz, $CDCl_3$) δ 176.2, 175.5, 174.5, 174.1, 172.0, 144.3, 134.5, 132.5, 130.4, 130.1, 129.1, 128.6, 126.9, 125.7, 125.6, 124.0, 123.6, 118.5, 82.1, 80.1, 80.0, 64.5, 62.6, 59.8, 59.4, 57.7, 57.2, 55.9, 55.4, 53.7, 44.6, 41.8, 41.1, 40.1, 28.9, 28.7, 28.5, 28.4, 28.3; HRMS (ESI) calc for $[C_{45}H_{68}NaN_8O_8]^+$ ($[M+Na]^+$): *m/z* 871.5052, found: 871.5034.

2,2'-(4-(2-((2-Aminoethyl)amino)-2-oxoethyl)-10-(2-oxo-2-((phenanthridin-6-ylmethyl) amino)ethyl)-1,4,7,10-tetraazacyclododecane-1,7-diyl)diacetic acid (7).

Di-*tert*-butyl 2,2'-(4-(2-((2-((*tert*-butoxycarbonyl)amino)ethyl)amino)-2-oxoethyl) -10-(2-oxo-2-((phenanthridin-6-ylmethyl)amino)ethyl)-1,4,7,10-tetraazacyclododecane-1,7-diyl)diacetate (**6**) (65 mg, 0.077 mmol) was dissolved in CH_3OH (5 mL) and concentrated HCl (*aq*) (1 mL) was added. The reaction was stirred for 5 days at room temperature after which the volatiles were removed under reduced pressure. The resulting oil was washed with cold CH_3OH (8 × 5 mL). Yield (42 mg, 79% over two steps). ^{1}H NMR (500 MHz, $CDCl_3$) δ 8.52 (d, 2H), 8.17 (s, 1H), 7.81 (m, 5H), 4.42 (s, 2H), 2.40-3.80 (m, 28H); ^{13}C NMR (125 MHz, $CDCl_3$) δ 176.2, 174.7, 158.3, 156.6, 141.6, 131.6, 130.8, 130.3, 129.2, 128.0, 127.4, 125.0, 124.4, 124.0, 123.7, 123.2,122.4, 63.5, 60.9, 56.7, 56.2, 52.3, 48.4, 45.5, 42.7, 39.5, 39.2, 38.0, 37.7, 36.6, 36.4; HRMS (ESI) calc for $[C_{32}H_{41}Na_2LiN_8O_6]^+$ ($[M+2Na+Li]^+$): *m/z* 687.4049, found: 687.4069.

Eu-DO2A-Phen-Amine (8).

2,2'-(4-(2-((2-Aminoethyl)amino)-2-oxoethyl)-10-(2-oxo-2-((phenanthridin-6-ylmethyl)amino)ethyl)-1,4,7,10-tetraazacyclododecane-1,7-diyl)diacetic acid (**7**) (42 mg, 66 μmol) was dissolved in mQ water (5 mL) and magnetically stirred. $EuCl_3 \bullet 6H_2O$ (25 mg, 66 μmol) was added to the reaction mixture and the pH was adjusted to 8 with LiOH. The reaction mixture was stirred for 76 h at 70 °C, filtered and the solvents were removed under reduced pressure. HRMS (ESI) calc for $[C_{33}H_{46}EuN_8O_6]^+$ ($[M+H]^+$): *m/z* 787.2798, found: 787.2731.

Eu-DNA conjugate (9).

Eu-DO2A-Phen-Amine (**8**, 2 mg, 5 μmol) was dissolved in phosphate buffer saline (80 μL) at pH 8. After stirring for 5 min, the amine was added to the protected aptamer (50 nmol) on beads in DMF (20 μL). The reaction mixture was mixed slowly for 15 h. The supernatant was decanted and the beads were rinsed with mQ water (2 × 1 mL), CH_3OH (2 × 1 mL) and CH_3CN (2 × 1 mL). The beads were dried under reduced pressure for 15 min and 30% NH_3 (*aq*) (750 μL) was added. The mixture was then heated at 65 °C for 5 h. The mixture was decanted and the beads were rinsed with water. The combined supernatants were concentrated under reduced pressure. The DNA conjugate was purified by high performance liquid chromatography (HPLC) using a Zorbax 300SB-C8 9.4 x 250 mm, 5 μm Agilent Technologies) column. Solvents were eluted at a flow rate of 2.5 mL/min with a gradient of 12-14 % acetonitrile in 15 mM ammonium acetate over 35 min. and 90% over 2 min. Conjugates were desalted by passing through NAP-5

columns and the eluent was concentrated. Capillary HPLC-MS (ESI)$^-$ calc for the Eu-DNA conjugate **9** ([M-H]$^-$): *m/z* 10938.7; found: 10938.6 (Figure 4.8).

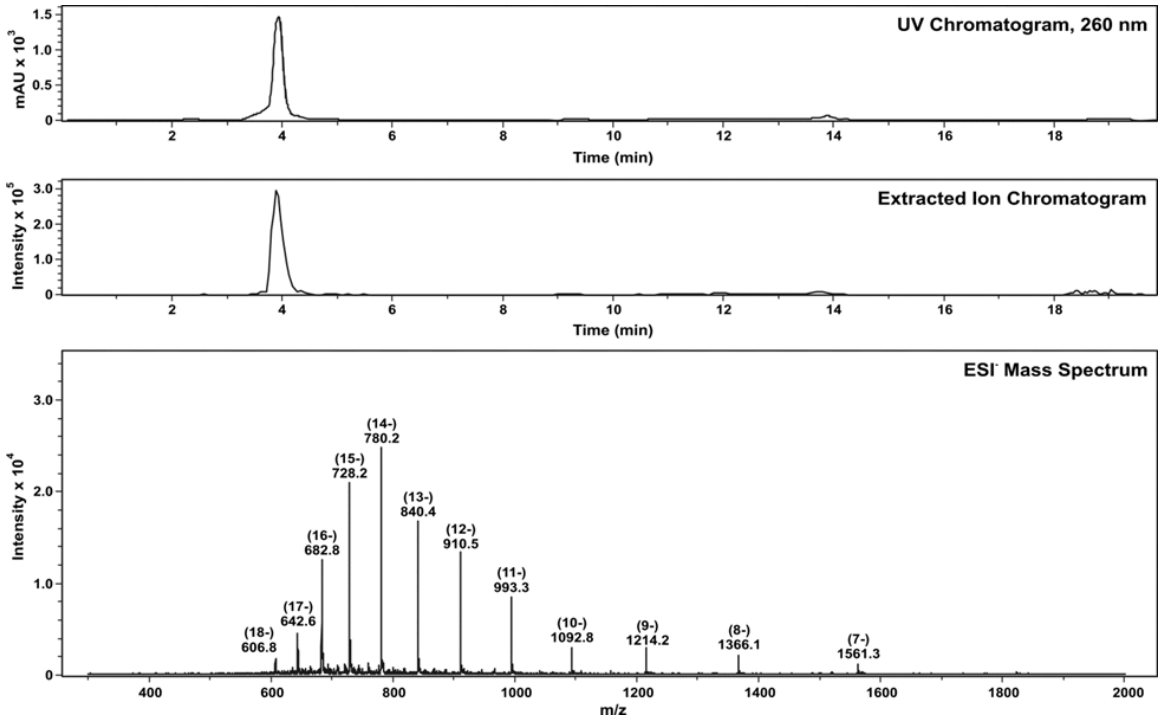

Figure 4.8. HPLC-ESI- mass spectrum of Eu-DNA Conjugate (9)

Eu-AptaSwitch (1)

Eu-DNA conjugate (**9**) was heated with a molar equivalent of the complementary strand (100 μM) in PBS buffer (pH 7.0) at 95°C for 15 min and allowed to cool to room temperature over 15 hours.

5 BACTERIAL DETECTION WITH A LUMINESCENT TROJAN HORSE

5.1 Synopsis

A luminescent siderophore Trojan horse system is presented as a novel diagnostic tool to detect bacteria. Preliminary studies have been performed using a modified enterobactin analog, *N,N′,N″*-(nitrilotris(ethane-2,1-diyl))tris(2,3-bis(benzyloxy) benzamide) (TRENCAM), where TRENCAM has been found to show promising results in bacterial uptake. We hypothesized that the synthetic modifications to TRENCAM do not affect the ability of bacterial receptors to recognize modified TRENCAM. The modified TRENCAM is coupled to a fluorescent dye, resulting in a fluorescent probe that is also metallated with gallium. The mode of action of a siderophore Trojan horse is depicted in Figure 5.1. We hypothesize that our Trojan horses are uptaken by bacteria together with naturally occurring siderophores. When the bacteria, *E. coli* ATCC 25922, were incubated with TRENCAM, this probe was uptaken by the bacteria within 5 min. According to the preliminary data obtained, the limit of detection of our Trojan horse probe in T-media was as low as 10^5 CFU/mL. In addition, the probe was uptaken by bacteria from blood, indicating that even in the presence of other blood cells, the probe is selectively taken up by bacteria.

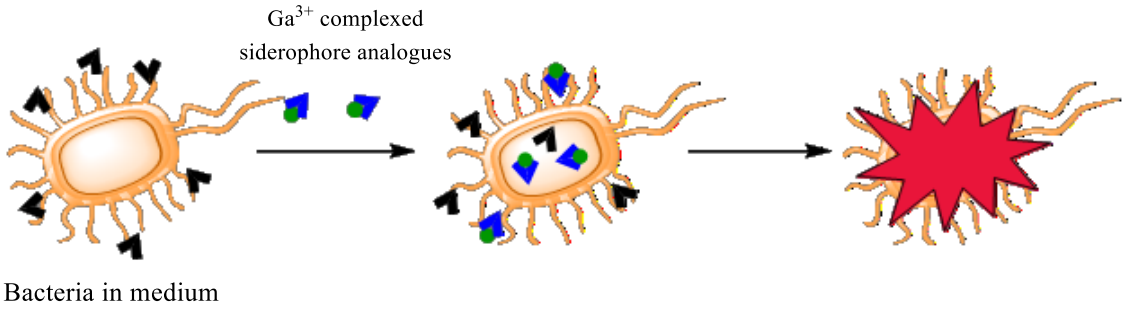

Figure 5.1 Mode of action of a siderophore- Trojan horse

5.2 Introduction

As discussed in Chapter 1, point-of-care (POC) diagnosis of bacterial infections is an unmet need in the medicinal field. Considering the ability of pathogenic bacteria to develop resistance towards antibiotics and the rate at which they develop resistance, rapid identification of bacteria in clinical samples is very important. Because of the emerging threat of antibiotic resistance, the scientific community is acutely aware of a need for novel diagnostic devices. In addition to the methods that have been approved by the food and drug administration (FDA), such as bacterial cultures, nucleic acid amplification techniques and antibody-based techniques, novel biosensors are being developed.[38,33,44,72,286]

Bacterial cultures are the oldest methods available but are still considered to be the gold standard due to their excellent sensitivity and specificity. However, their use is time consuming and hence not suitable for POC settings. Nucleic acid amplification techniques and antibody-based techniques require positive cultures to begin with, and, therefore, those methods do not address the need for shorter time of analysis. Biosensors, on the other hand, were developed to enable rapid diagnostic methods, but most of the

time they end up lacking a good sensitivity and specificity. Therefore, most of the novel biosensors that utilize a number of transducing techniques, such as optical, electrochemical, or mass-based methods, have not yet been approved by the FDA.[33, 44, 287] When developing novel biosensors, the attention of the scientific community has also being focused on pathogen-specific virulent factors such as siderophores. [219,222-225] As it was mentioned in chapter 1, siderophores themselves can be virulent or they can even induce other virulent factors.[115,164,165] Since iron is an essential element required for the growth of almost all bacterial species, with a few exceptions such as *Borrelia burgdorferi,*[100] in order to sequester iron under iron deficit conditions, most of bacteria secrete siderophores, which are small, high affinity iron chelators. Once iron is bound, bacteria have specific receptors to transport this siderophore-bound iron into the cells. Iron uptake pathways have been identified as important nutrient uptake pathways that can be used in developing efficient drug delivery systems based on a Trojan horse strategy. To our knowledge, siderophore Trojan horses have not yet been widely tested for diagnosis purposes. However, Petrik et al. reported a siderophore-Trojan horse system to diagnose a fungal infection, i.e., invasive pulmonary aspergillosis, using Ga^{68}-radiolabled siderophores.[288] Although in the siderophore-antibiotic systems the structure of the siderophore has been modified, it has not been modified in the siderophore-Trojan horse system that was reported by Petrik et al. The only modification in that latter system is in the complexation, i.e., instead or Fe^{3+}, the siderophores used in that study are complexed with Ga^{3+} which is a positron emitter. Therefore, positron emission tomography (PET) imaging has been used as the diagnostic tool. Although this diagnostic method is promising, specificity, selectivity, and toxicity need to be further investigated. Recently,

Hass et al. reported another study on the same topic but the selectivity of the assay was not reported.[289] When siderophores are used in Trojan horse systems for diagnosis purposes, they are used only as the Trojan horse vehicle, and unlike in the case of siderophore-antibiotic conjugates, the modified siderophores are not meant to kill bacteria. Nevertheless, when gallium is utilized as an alternative to iron, Trojan horses become lethal to those iron starving bacteria as gallium does not function inside the cells in the same way as iron.[290]

5.2.1 Siderophore Trojan horses

Siderophore Trojan horse systems are naturally displayed by several microorganisms including both Gram positive and Gram negative bacteria, such as *Actinomyces subtropicus, Streptomyces violaceus, and Streptomyces griseoflavus,* through the production of albomycins, salmycins, and ferrimycins respectively.[291-294] They are also called sideromycins.[295] The siderophore-antibiotic Trojan horse scaffold is mainly comprised of three components, i.e., an antibiotic, a siderophore, and a spacer group that links the former two moieties, as shown in Scheme 5.1.[295-299] All these three factors should be optimized so as to accomplish the target.

Scheme 5.1 Components of siderophore-drug conjugates

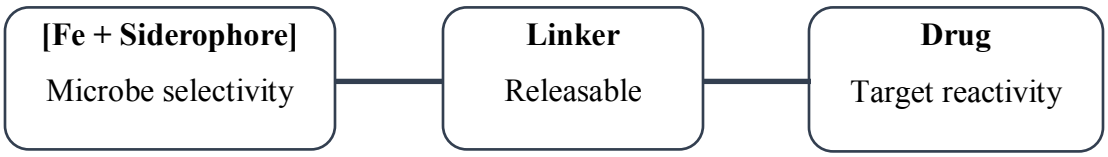

Besides the need for these three functional units, solubility and stability under physiological conditions should also draw attention. Natural siderophore-antibiotic conjugates chelate iron and shuttle it through bacterial membranes with an energy-coupled transport system. The mechanism by which the link between the siderophore and the antibiotic is cleaved, activating the antibiotic inside the bacterial cell, is of utmost importance. One proposed cleavage mechanism is cleavage of an amide linkage by endogenous peptidases, which was shown to release the antibiotic and inhibit an important enzyme involved in bacterial translation process.[300] In the case of another natural siderophore-antibiotic conjugate, cleavage of an ester linkage by intracellular hydrolases releases an antibiotic that induces the depolarization of the inner membrane.[301,302] Studies of sideromycins further reveal that recognition of the siderophore moiety by highly specific TonB-dependent transporters is a crucial step rather than the size of the sideromycin.[27]

Use of heavy metals such as Ga^{3+} for the chelation can also be considered as a siderophore Trojan horse if it is used in the proper context. Miller and coworkers used Ga^{3+} complexed desferrioxamine coupled with antibiotics through a maleimide linker to transport antibiotics into bacteria. The use of Ga^{3+} interrupted the bacterial iron metabolism and inhibited biofilm formation.[290, 303]

The scientific community has been inspired by these fascinating natural roles of sideromycins, leading it to develop synthetic Trojan horses for antibiotic and drug delivery. To this end, siderophores are either synthesized or they are extracted from bacteria culture broths.[27] Especially when stereogenic centers are present and the receptors are found to be stereospecific, extracting siderophores from bacteria seems

more beneficial as the synthesis becomes more complicated. In addition to the synthetic challenges, receptor specificity can also be a challenge when designing a siderophore-antibiotic Trojan horse. In spite of the existence of several promising approaches, only a few highly successful Trojan horses have been developed to date, illustrating the difficulty in using this strategy.

While Gram positive bacteria have only one membrane, Gram negative bacteria have two, i.e., an outer membrane and an inner membrane. In particular, Trojan horses with an antibiotic moiety that targets the cytoplasm have not been very successful with Gram negative bacteria.[304-306] This may be due to differences in the transmembrane transport selectivity of the outer membrane and inner membrane. Notably, outer membrane receptors are more specific than inner membrane transporters. Most of the outer membrane receptors have a specific selectivity, and, therefore, different receptors are responsible for the transport of different siderophores across membranes.[100] In contrast, the inner membrane receptors are not very specific and let several different siderophores pass through the inner membrane. For instance, while ferrichrome is taken up by FhuA and aerobactin is taken up by IutA, these siderophores are shuttled across the inner membrane using the same FhuCBD protein complex.[100] Therefore, a thorough knowledge on the siderophore uptake process is very important when designing a Trojan horse. On the brighter side, although TonB-dependent transporters associated with receptors have been shown to have a greater selectivity, they have also been found to take up compounds larger than the corresponding siderophore, which suggests that the size of the shuttled compound does not play a major role.[27] As an example, the sideromycin microcin E492, which consists of a bulky peptide chain, passes through the outer

membrane by the catechol iron uptake pathway.[307] Another important fact to consider when choosing a siderophore for a Trojan horse is whether that siderophore will be synthesized or extracted from a bacterial strain. Sometimes extraction works well but can yield only a very small amount of the siderophore.[198,308] Moreover, if the receptor recognition moiety is known but extraction or synthesis of the exact siderophore is difficult, a siderophore analogue may be synthesized. TRENCAM is an example of such an analogue; in this case, it is an analogue of enterobactin.[309] Several research groups have reported the synthesis of model complexes for the uptake into bacteria. Such model complexes include catechol, carboxylate and hydroxamate type siderophores (Figure 2.7). Some of those compounds have been used as Trojan horses.[97, 98, 309-315]

When synthesizing such functionalized analogues as vehicles to enter through bacteria, recognition of such vehicles by receptors is an important factor. If the siderophore is modified at a position where it can create a large steric hindrance that would affect receptor recognition, it is very likely that the Trojan horse may not get shuttled into bacteria.[305,316] For example, when functionalizing pyochelin with an antibiotic norfloxacin, N3" functionalization (Figure 5.2 B) has worked better than C5 functionalization (Figure 5.2 A).[305,317] As shown in Figure 5.2, modification of pyochelin with the same fluoroquinolone, norfloxacin but at different positions has given very different results, where C5 modified analogue is not taken up by bacteria while the N3" modified analogue is taken up, indicating that N3" modified analogue does not negatively affect the receptor recognition. Thus, before being built into a Trojan horse, uptake of the model siderophore by the desired bacteria should be verified.

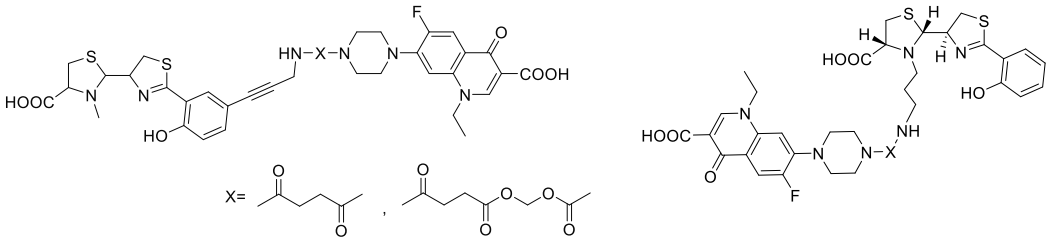

Figure 5.2 Pyochelin modification at different positions

Some siderophores, such as pyoverdines, are composed of a family of siderophores that has a common chromophore but differ in the amino acid chain moiety.[198] Therefore, there can be a few structurally different siderophores belonging to the same siderophore type. For example, pyoverdine (PVD) has three types as PVDI, PVDII and PVDIII, where the difference is in the number, composition and configuration of the amino acids of the oligopeptide chain.[198] Each strain of *Pseudomonas aeruginosa* produces only one of these three pyoverdines and possesses only the receptor for that particular siderophore.[198] Therefore, a single Trojan horse type will not work for all strains of a given bacterial species. Hence, when choosing a siderophore for a Trojan horse, it is better if such specialized siderophores can be avoided. On the other hand, some siderophores can be taken up by several bacterial species.[27] From a therapeutic standpoint this is advantageous because such Trojan horses may be effective for the treatment of co-infections.[27] To the contrary, when Trojan horses are used in the context of diagnosis, a Trojan horse uptaken by many bacterial strains is a disadvantage, as selectivity is lost and specific diagnosis is not possible.

The linker that connects a siderophore and an antibiotic is an important component of a Trojan horse and needs to be optimized.[27] It has to be stable enough to reach the cell without any extracellular hydrolysis, but it also needs to be cleaved once inside the cell. Where exactly this cleavage should take place depends on the drug, and in particular whether the drug is designed to act in the periplasm or cytoplasm.[98]

Considering all siderophore Trojan horses developed to date, it may be concluded that only a limited number of linkers or spacer arms have fulfilled all of the above requirements at least to a certain extent.[27] The fact that antibiotic Trojan horses that target the cytoplasm have not been very promising can be attributed to the failure of the linker to get detached from the antibiotic.[305] It is not clear whether in these cases the linker reduces the binding affinity or whether it hinders the drug from reaching the target. Either way, the activity of the antibiotic is lost. However, hydrolysable spacer groups like methylene-dioxy linkers and thiol-maleimide linkers have shown more promising results as far as the antibiotic activity is concerned.[303,304] Some studies of Trojan horses linked via hydrolysable groups with *tonB* mutants have shown antibacterial activity, suggesting an extracellular hydrolysis and penetration of antibiotic via diffusion.

Miller and co-workers formulated an interesting hypothesis for drug release by studying salmycins that get converted to danoxamines upon drug release.[318,319] They proposed that the reduction of ferric ion to ferrous ion might be initiating an internal cyclization, resulting in the formation of a stable ring and the release of the drug. However, ferric reduction is believed to take place in the cytoplasm. Therefore, in order for this argument to be true, the Trojan horse has to pass through the cytoplasmic membrane, permitting the antibiotic to reach the target. To test this, antibiotics that are

known to be targeting the cytoplasm should be conjugated, and drug uptake profiles should be evaluated. However, additional experiments will provide more conclusive results.

The structure-activity relationship and the target location of a drug determine whether drug release from the linker and the siderophore is necessary for activity or not.[319] For instance, since penicillin binding proteins or transpeptidases are natural targets of β-lactam antibiotics and these proteins reside in the periplasm, such antibiotics do not require to be cleaved from the linker. Therefore, their activity is not affected much by a change in linker.

Studies to date leave a lot open about the understanding of antibiotic activity, linker cleavage, and membrane transporter systems. Moreover, there is no guarantee that bacteria will not develop resistance towards siderophore Trojan horses. Since the uptake of siderophore Trojan horses depends on TonB dependent outer membrane transporters, altering the specificity of these systems can affect the resistance.[299, 320]

5.2.2 Design considerations for siderophore - Trojan horses for diagnosis

When developing a siderophore Trojan horse for the diagnosis of bacteria, not all three main components of a siderophore–antibiotic conjugate are necessarily required. Although there should be a linker between the siderophore and the diagnostic probe, depending on the probe design, a specific linker group as such may or may not be required (Scheme 5.2). For example, if the mode of action of the diagnostic probe is independent of the linker to the siderophore, then the hydrolyzability of the linker is not important.

Scheme 5.2 Components of siderophore-diagnostic probe conjugates

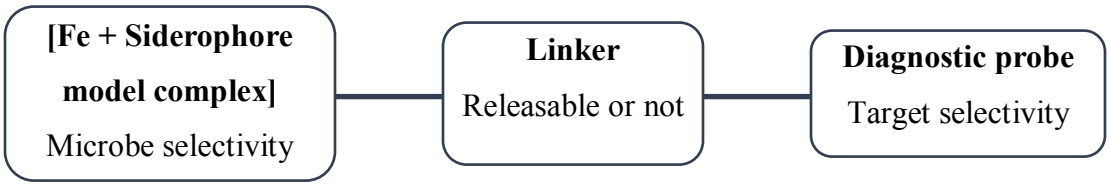

Similar as for siderophore-antibiotic conjugates, for a siderophore-diagnostic probe conjugates a siderophore that has been extracted from bacteria or a synthetic analogue of a siderophore is required. The siderophore part will mainly serve as a vehicle for the diagnostic probe to enter the bacterial cell but not mammalian cells such as blood cells. The nature of the diagnostic probe varies depending on its function. If the probe is a dye, an ability of the dye to pass through the outer membrane (for Gram negative bacteria) is sufficient. However, if the probe is required to pass through the inner membrane, then a siderophore that can pass through the inner membrane should be chosen. For example, pyoverdine does not pass through the inner membrane, while ferrichrome and pyochelin are shuttled through the inner membrane of *P. aeruginosa*.[321-323] Although outer membrane receptor proteins are specific for siderophores, inner membrane proteins are specific for a siderophore class.[324]

Also the linkage between the siderophore and the diagnostic probe should be stable until the conjugate reaches the target, i.e., if the target is in the cytoplasm, the linker should not hydrolyze in the periplasm. For example, if the diagnostic probe is a DNA intercalator that requires access to bacterial DNA in order to exhibit a color change, then the probe needs to remain connected to the siderophore while passing through the inner membrane.

5.2.3 Siderophore Trojan horse design for bacterial diagnosis

In the current study, to test the use of siderophore Trojan horses for bacterial diagnosis, a probe that is an analogue of enterobactin was designed and conjugated to a dye. Studies have shown that while the triscatechol iron center and the amide groups of the coordinated catechol ligands are necessary for receptor recognition, the trilactone ring is not.[103] Therefore, TRENCAM, which has been shown to be successfully shuttled into bacteria, was chosen.[309] While $\log K_{FeL}$ for enterobactin is 52, $\log K_{FeL}$ for TRENCAM is 43.6, which shows that TRENCAM strongly binds iron.[309] Other physical properties of enterobactin and TRENCAM are also comparable. Since enterobactin does not have a functional group to attach a diagnostic probe, a modified enterobactin derivative with functional group suitable for derivatization was required.

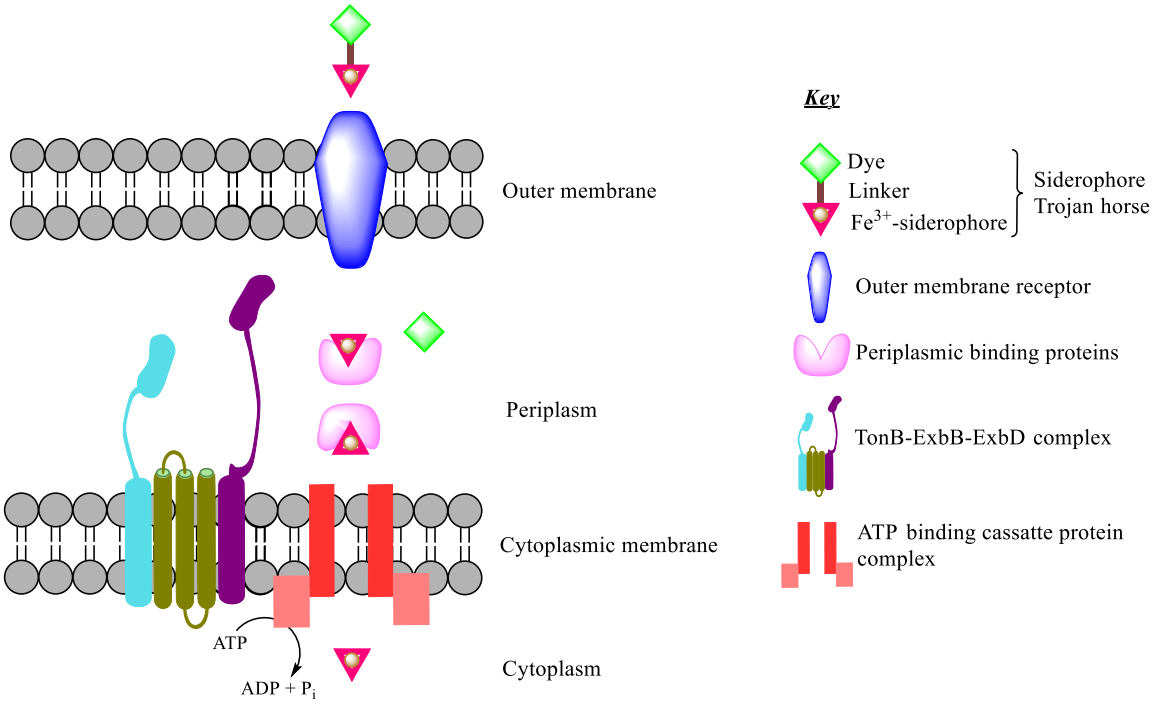

Figure 5.3 Mode of action of luminescent siderophore Trojan horse[325]

Our hypothesis is that, as shown in Figure 5.3, the TRENCAM-dye conjugate will be shuttled by bacterial receptors across membranes, and once inside the periplasm dye may or may not detach from the siderophore, but either way the bacteria will luminesce when excited with a wavelength appropriate for the dye.

5.3 Results and Discussion

5.3.1 Synthesis of a siderophore Trojan horse

An enterobactin Trojan horse was synthesized using the convergent approach outlined in Scheme 5.3. Intermediates **3-2**[326] and **3-5**[327, 328] were synthesized according to previously published reports. A nucleophilic substitution reaction of the secondary amine at the center of *N,N″*-dibenzyloxycarbonyl diethylenetriamine with the alkyl bromide functionality in **3-2** resulted in a tetraamine, **3-3**, which was deprotected to give the intermediate **3-4** with three primary amino groups. The latter were coupled to bisbenzyloxy benzoic acid to give the completely protected ligand **3-6**. The methyl ester in this intermediate was then deprotected under alkaline conditions, and the thus obtained carboxylic acid derivative **3-7** was further coupled to the 5(6)-tamra cadaverine dye. Deprotection by removal of the benzyl groups followed by metallation with gallium(III) yielded the complete enterobactin Trojan horse **3-9**.

Scheme 5.3 Synthesis of Siderophore Trojan horse (3-9)[a]

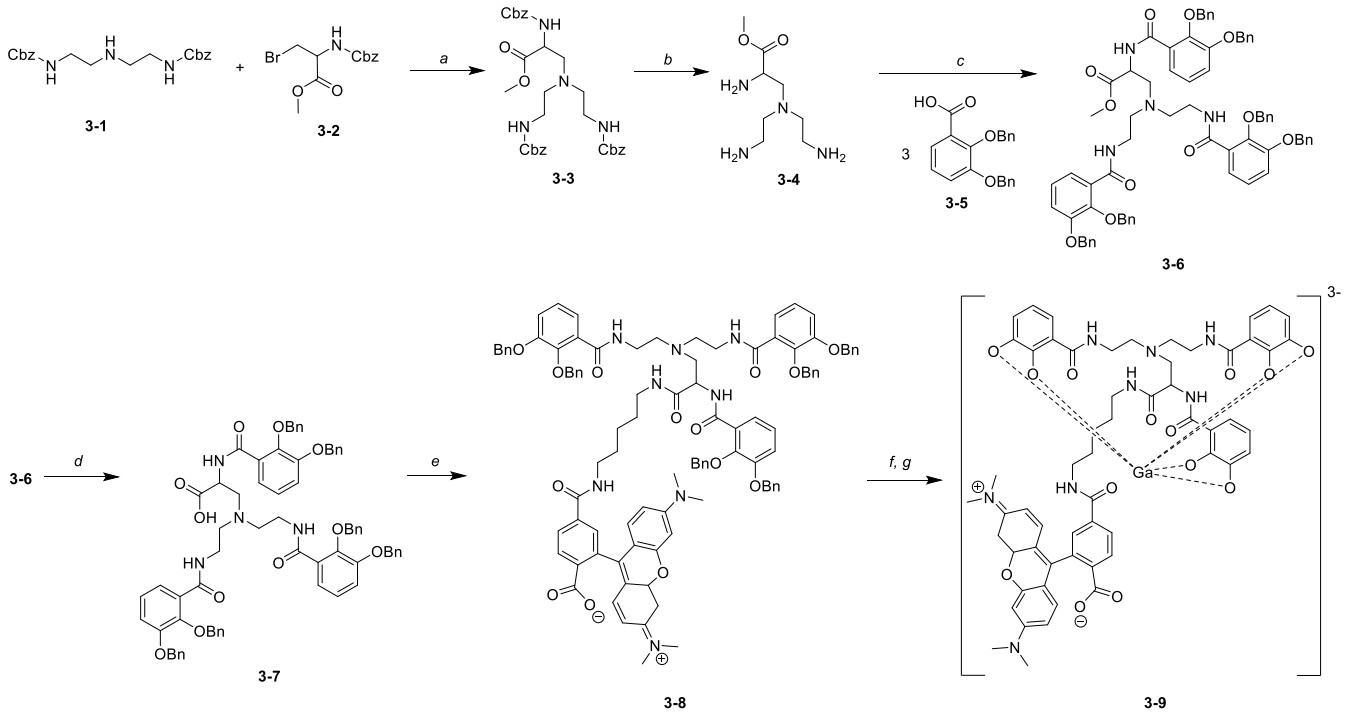

[a]Experimental conditions: (a) Cs_2CO_3, anhydrous acetone, 58 °C, 72 h; (b) H_2, Pd/C, CH_3OH, 24 h; (c) HATU, DIPEA, DMA, r.t., 15 h; (d) KOH, CH_3OH:H_2O =3:1, r.t., 18 h; (e) 5(6)-tamra cadaverine dye, HATU, DIPEA, DMA, r.t., 15 h; (f) H_2, Pd/C, CH_3OH, 3 d; (g) $GaCl_3$, DI water, pH = 7, r.t., 15 h.

The yield for the synthesis of **3-3** was only 40%. This can be attributed to an elimination reaction that may be taking place from the intermediate **3-2** in alkaline medium. It could be an α-halo elimination (**A**) or an elimination followed by an intramolecular rearrangement (**B**) to yield a stable cyclic product, as shown in Scheme 5.4. As one would expect, better leaving groups favored elimination, while poor leaving groups were not active enough for the desired substitution reaction. To this end, bromide was the best leaving group for this reaction. However, the new intermediate *tert*-butyl 4-[(benzyloxycarbonyl)amino]-5-bromopentanoate was synthesized in order to minimize α-halo elimination. Although the use of this intermediate does not result in a stable extended conjugate as it would be the case with **3-2**, α-halo elimination still takes place. The synthesis of the Trojan horse with tert-butyl 4-[(benzyloxycarbonyl)amino]-5-bromopentanoate intermediate is shown in Scheme 5.5, and the progress towards synthesis of the Trojan horse **3-17** is discussed in the experimental section.

Scheme 5.4 Possible mechanisms for the intramolecular elimination reactions

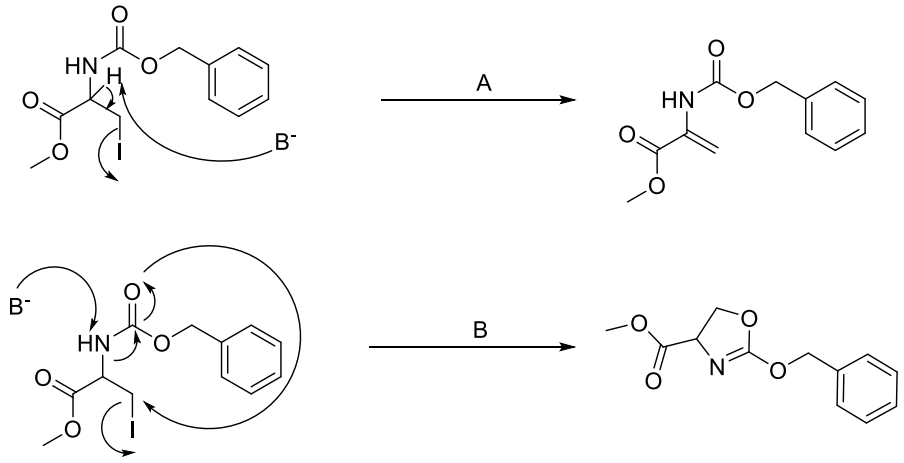

Scheme 5.5 Synthesis of Siderophore Trojan horse (3-17)[b]

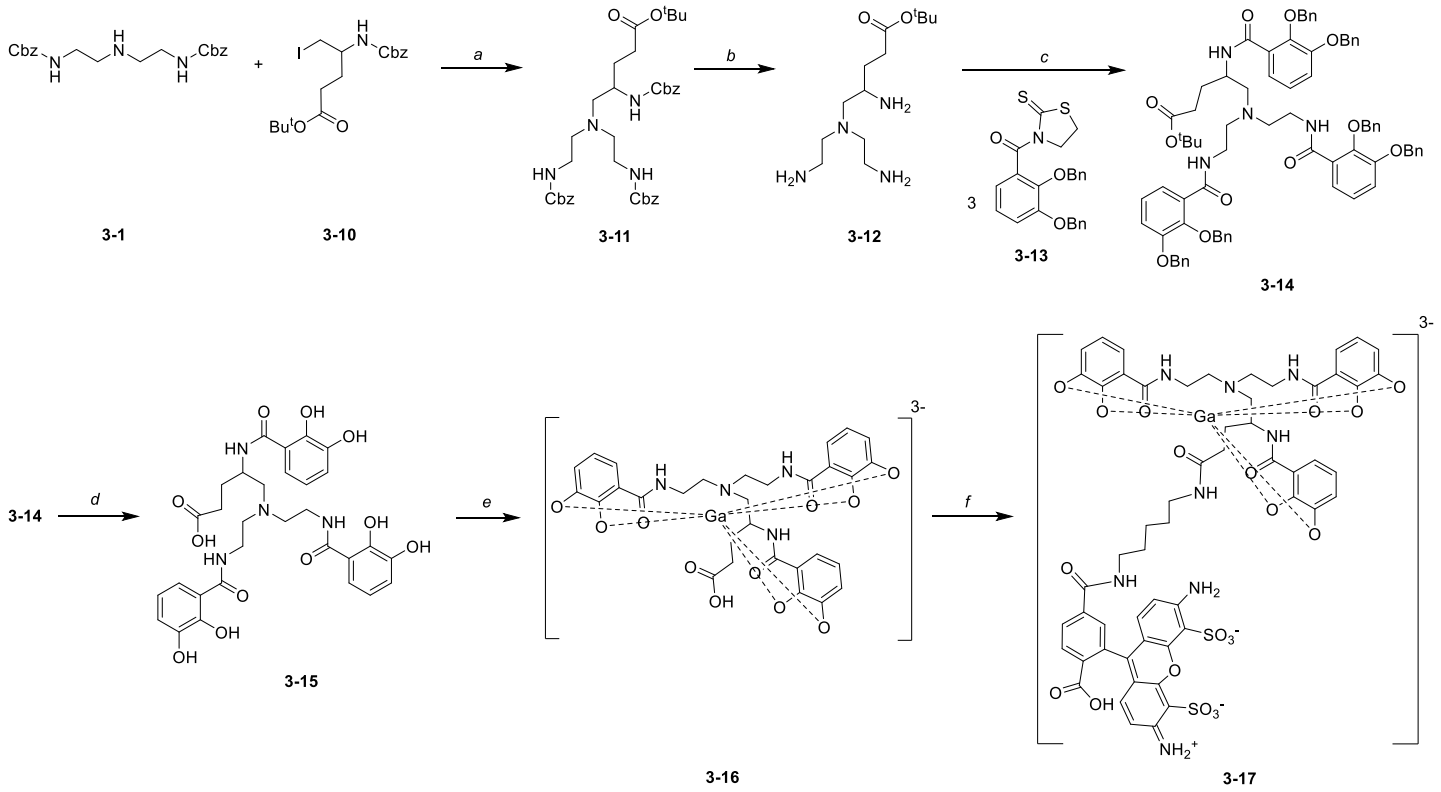

[b]Experimental conditions: (a) Cs_2CO_3, anhydrous acetone, 58 °C, 72 h; (b) H_2, Pd/C, CH_3OH, 24 h; (c) DIPEA, CH_2Cl_2, r.t., 48 h; (d) H_2, Pd/C, CH_3COOH, HCl, H_2O, r.t., 48 h; (e) $GaCl_3$, DI water, pH = 7, r.t., 15 h (f) Alexa fluor 488 dye, HATU, DIPEA, DMA, r.t., 15 h.

5.3.2 Effect of incubation time on probe uptake

In order to evaluate the luminescent Trojan horse **3-8** different concentrations of bacteria (10^6, 10^7, 10^8, 10^9 CFU/mL) were incubated with the Trojan horse probe (12.5 μM) for different lengths of time ranging from 5, 10, and 30 to 60 minutes. After incubation, the bacterial solutions were filtered through 50 kDa filters, and the residues were re-dissolved in phosphate buffered saline (PBS) to measure the fluorescence. Measurement of only the uptaken probe was ensured by washing the residues will still on the filters with PBS. If the probe is uptaken by bacteria, an increase in fluorescence with increasing bacterial concentration and a correlation of the probe uptake with respect to the incubation time is expected. However, fluorescence measurements obtained did not show any correlation due to the turbidity of the solutions. The effect of incubation time for the Trojan horse uptake was determined using a fixed concentration of 10^9 CFU/mL of bacteria. Although fluorescence measurements was not quantifiable with a fluorimeter even after 5 minutes of incubation, probe uptake by a 10^9 CFU/mL bacterial solution was clearly visible to the naked eye (Figure 5.4). However, probe uptake was not visible to the naked eye for the bacterial solutions with lower concentrations than 10^9 CFU/mL (Figure 5.4).

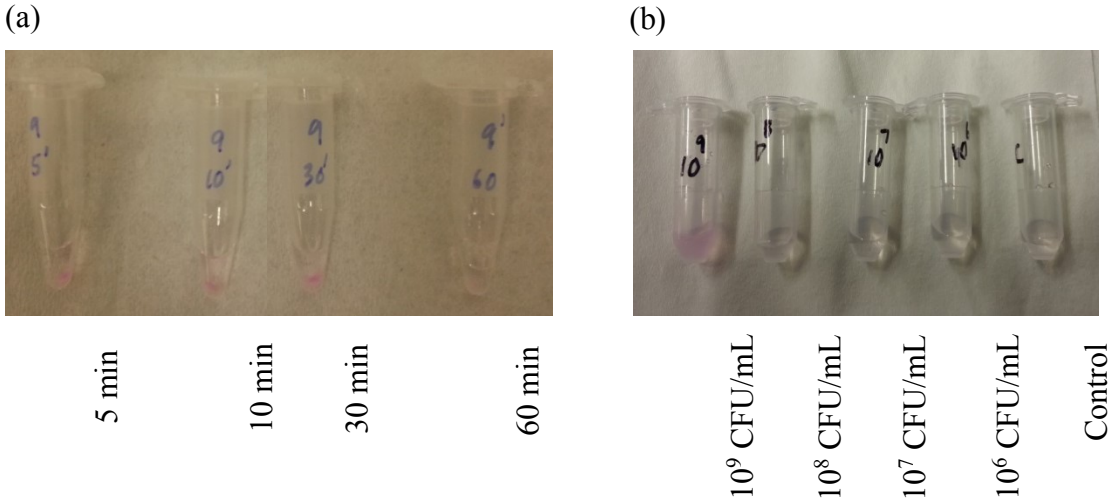

Figure 5.4 (a) Effect of incubation time for Trojan horse probe uptake by bacteria (b) Trojan horse probe uptake by bacteria after 5 minutes of incubation time

Bacterial cells were lysed using alkaline sodium dodecyl sulfate (SDS) solution, centrifuged, and the fluorescence of supernatants was obtained. No correlation was observed even after cell lysis; instead, the sediments after centrifugation were also colored in addition to the supernatant. These results suggest that bacteria have uptaken the Trojan horse probe within 5 min. The coloration of the sediments could be due to incomplete uptake or trapping of the probe within the cellular membranes. Probably because of this fractionation, there is no linear correlation in fluorescence of the supernatant with the increase in concentration of bacteria.

5.3.3 Limit of detection (LOD)

Since it was evident that Trojan horse probes were taken-up in 5 min, in order to find the limit of detection, different concentrations of bacteria (10^5, 10^6, 10^7, 10^8 and 10^9 CFU/mL) were incubated with the probe for 5 min. After incubation, bacterial solutions

were filtered through epifluorescence filters and those filters they were observed under Zeiss Axioplan II microscope (Figure 5.5) after washing the filters with PBS buffer to remove any excess probe. Since the dye is a fluorescent dye, bacteria become fluorescent once they uptake the probe. This preliminary analysis of micrographs revealed that a bacterial concentration of 10^5 CFU/mL could be detected; however, bacterial concentrations below 10^5 CFU/mL were not tested. An increase in fluorescence was observed with increasing concentration of bacteria, as expected. This suggests that a quantitative analysis of bacteria could be performed using a suitable calibration plot.

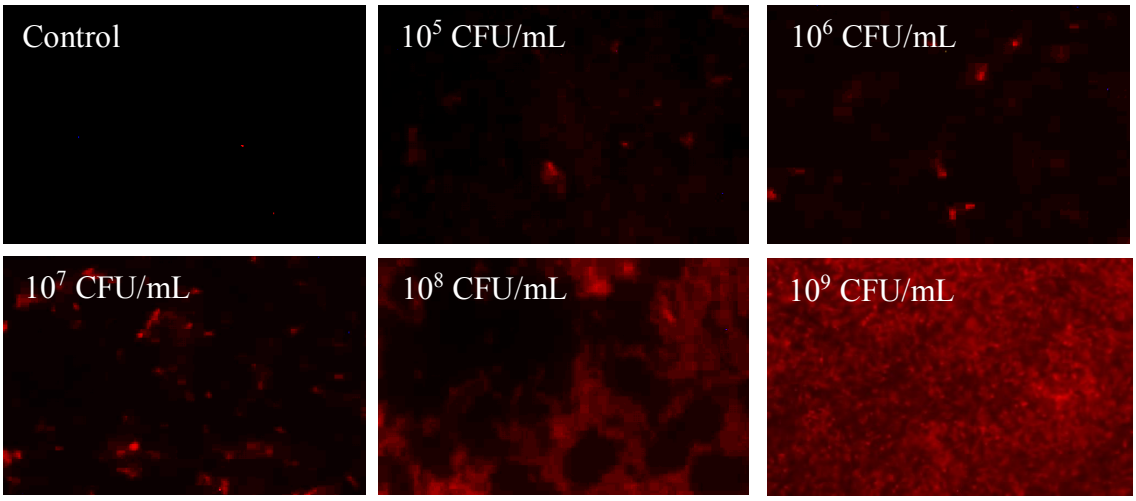

Figure 5.5 Evaluation of limit of detection of E. coli using a Trojan horse probe. *Microscope settings: Capture 1360 x 1024, Gamma 0.35, Contrast 40, Image format 16 bit TIF, Exposure time 600 ms, Gain 2, Zoom 126x*

5.3.4 Detection of antibiotic susceptibility

Bacterial solutions of 10^6 CFU/mL were prepared and treated with different concentrations of bactericidal (ampicillin) and bacteriostatic (tetracycline) antibiotics. After incubation for 2 hours, the Trojan horse probe was introduced and incubation continued for another 5 minutes. If the antibiotic activity was null, the bacterial solutions were projected to have a concentration of 10^8 CFU/mL, as suggested by the growth chart of *E. coli* ATCC 25922 (Figure 5.6). According to this growth chart, a maximum growth of bacteria in T-media (recipe shown in the Experimental Section) can be observed between 8-10 hours. Therefore, it was ensured that at the end of the incubation time the bacteria had not reached a population density where they already started to die.

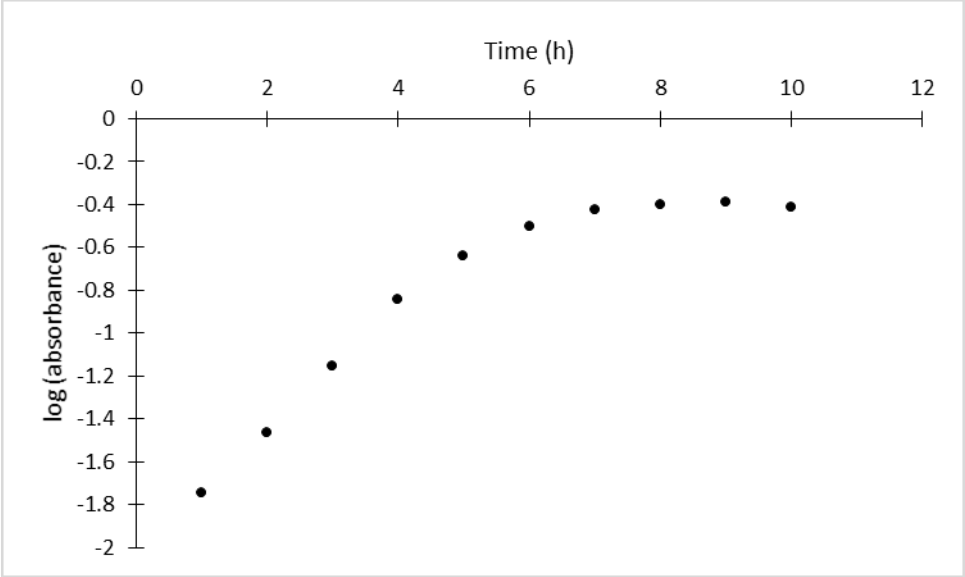

Figure 5.6 E. coli ATCC 25922 growth chart in T-media

Bactericidal antibiotics kill bacteria while bacteriostatic antibiotics slow the proliferation of bacteria. Therefore it is expected that the fluorescence intensity gradually

decreases with an increasing concentration of antibiotic. This trend can be seen when comparing the images taken for maximum and minimum concentrations of ampicillin treated bacterial solutions (Figure 5.7). No trend was observed for tetracycline treated bacteria.

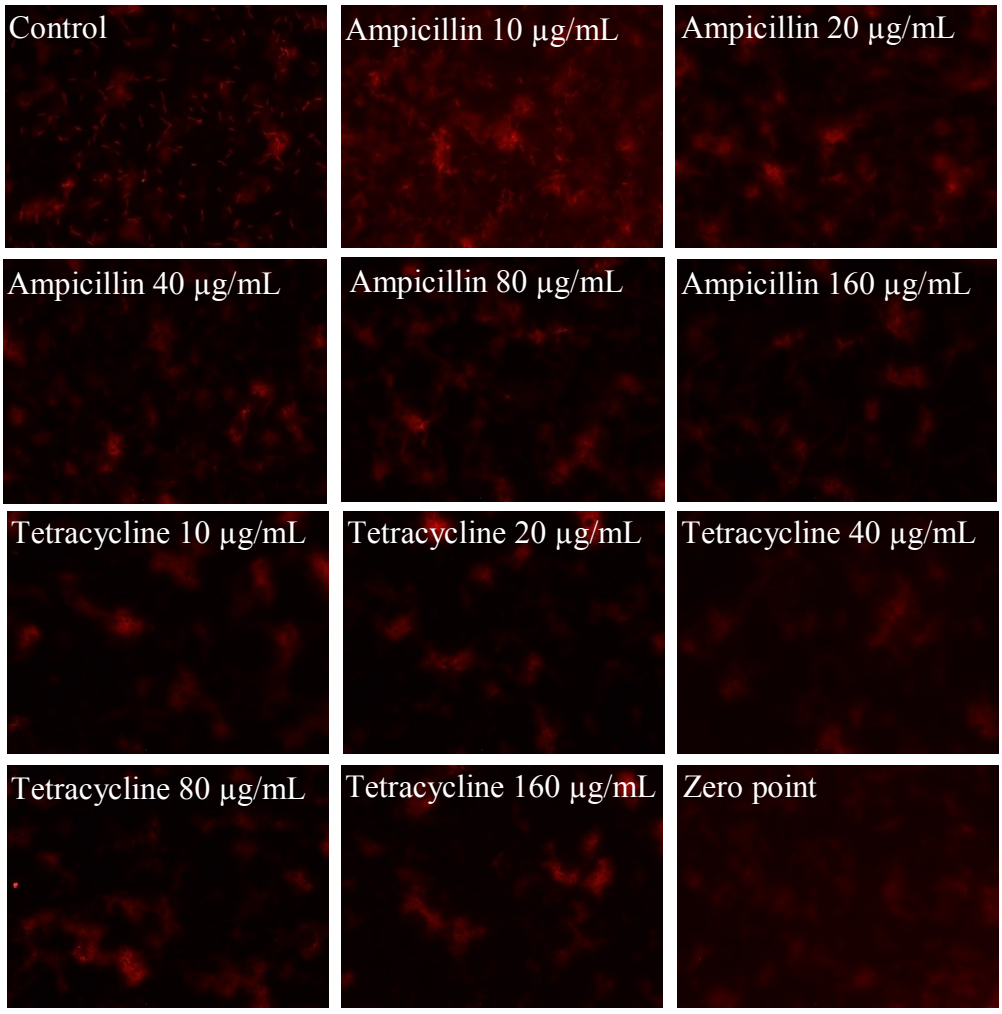

Figure 5.7 Antibiotic susceptibility test. *Microscope settings: Capture 1360 x 1024, Gamma 0.35, Contrast 40, Image format 16 bit TIF, Exposure time 600 ms, Gain 2, Zoom 126x*

An inconsistency with this data is that a maximum fluorescence intensity should have been observed with the control, where no antibiotic is present and the incubation

time was long enough that a bacterial concentration of 10^8 CFU/mL was projected. This is clearly not the case. The fluorescence in the image of the bacterial solution treated with the minimum amount of ampicillin showed a higher fluorescence intensity than the control. Also, in the antibiotic treated bacterial solutions, the bacterial cells are not differentiated as in the control. This might be due to biofilm development by bacteria. It is known that the development of biofilms in some bacteria make bacteria resistant to antibiotics.[329]

5.3.5 Applicability in biological samples

The applicability of Trojan horse probe in biological media was evaluated by testing the probe in mouse blood. Bacteria (10^8 CFU/mL) were spiked into mouse blood and the probe was introduced. After incubating for 5 min, the blood was smeared onto 0.2 μm filters for observation under the microscope. Although the anticoagulant heparin was added to the blood before testing, filtration of blood through 0.2 μm filters was not possible, which explains why the blood was simply smeared onto the filters. Blood without any bacteria was also treated with the probe as a control, and after 5 minutes it was also smeared onto filters and imaged under the microscope. Results are shown in Figure 5.8. They suggest that the Trojan horse probe can selectivity be taken-up by *E. coli* and is not taken-up by mammalian cells such as blood cells. Moreover, the detection of bacteria by the Trojan horse probe is not affected by the presence of other cells.

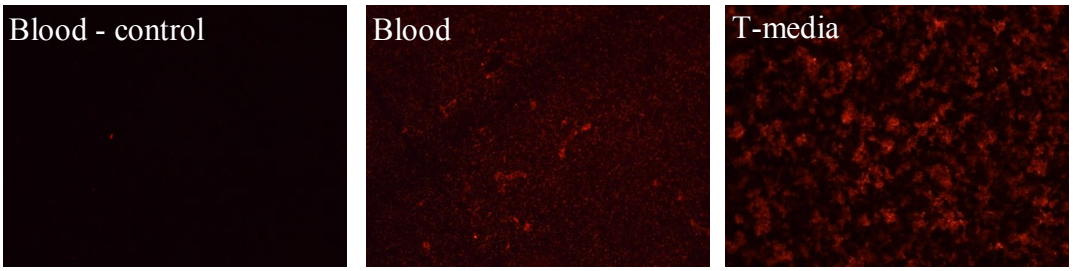

Figure 5.8 Applicability of the Trojan horse probe in mouse blood. *Microscope settings: Capture 1360 x 1024, Gamma 0.35, Contrast 40, Image format 16 bit TIF, Exposure time 600 ms, Gain 2, Zoom 20x*

5.4 Summary and Future Directions

In this work, an enterobactin Trojan horse was developed by coupling a dye to an enterobactin model complex. According to the preliminary results obtained with this luminescent Trojan horse, enterobactin-uptaking bacteria in a concentration of 10^5 CFU/mL can be detected within 5 minutes. This detection limit is appropriate for the detection of pathogens in an infection such as urinary tract infection. However, the current detection limit is not sufficient to detect food poisoning from *E. coli* O157:H7, which is present in blood at concentrations as low as 10 CFU/mL. Some biosensors that have been developed by Gill *et al*. and Settu *et al*. have reported detection limits of 10 CFU/mL in sputum and 7 CFU/mL in urine, respectively, with a time-to-results of about 60 min.[75,86] In comparison, the Trojan horse approach reported in this study is as faster diagnostic method. However, the preliminary data were only obtained in T-media, and the probe was not tested for bacterial concentrations below 10^5 CFU/mL. The limit of detection is restricted not only by the assay but by the imaging technique too. The preliminary data obtained in this study were obtained using a microscope which suffered

with a low signal-to-background noise ratio. If the microscopic data were followed up with fluorescence spectroscopic data, better detection limits could be expected. Although the applicability of the Trojan horse in biological samples was tested using mouse blood, a higher concentration of bacteria (10^8 CFU/mL) was spiked in. According to the preliminary results, the current probe can be used to detect bacteria in blood even in the presence of blood cells without any matrix effects. Nonetheless, it will be necessary to test the selectivity of this Trojan horse in the presence of other bacterial species. Furthermore, the antibiotic susceptibility was tested for ampicillin and tetracycline using the enterobactin Trojan horse, which appeared only promising for ampicillin. Due to biofilm formation in the sample, especially with tetracycline, it was not possible to obtain conclusive evidence from this antibiotic susceptibility test.

Additional control experiments will provide more conclusive results regarding the use of this Trojan horse for diagnostic purposes. Studies have shown, while receptor FepA is responsible for enterobactin uptake, receptors Cir and Fiu are responsible for uptaking the degradation products of enterobactin. For control experiments with siderophore-antibiotic conjugates, several groups have reported that *fepA* mutant *E. coli* strain H873 did not show a significant difference in uptaking the tested siderophore-antibiotic conjugate, however *fepA, cir, fiu* triple mutant *E. coli* strain H1876 showed a significant difference.[98,330] Therefore, in order to evaluate this TRENCAM Trojan horse, testing with *E. coli* strain H1876 will serve as a good negative control.

Although TRENCAM has been identified as an enterobactin model complex that can be taken up by bacteria, the modified TRENCAM complex used in this study has not been tested for its ability to to be uptaken into bacteria. Therefore, testing the uptake

profile of the modified TRENCAM is an important control experiment. In addition, the dye itself has also not been tested for bacterial uptake. Such a control experiment would also be very informative, as for example if bacteria do not uptake the probe, but the dye merely colors the bacteria from the surface; if that is so, then the dye alone will also color the surface of bacteria.

Microscope images as obtained in this study provide only qualitative estimates. However, if a constant area were analyzed, quantitative results could be obtained for evenly distributed samples. To obtain quantitative data, an area should be defined and an image processing algorithm such as an intensity histogram could be used.

The Trojan horse described in this study has been tested in mouse blood. However, testing the probe in other biological fluids such as urine and cerebrospinal fluid or in stools may help assess the universality of the probe, that is, whether the probe will be useful in other sterilized and non-sterilized clinical samples.

In future, if this siderophore Trojan horse strategy is implemented for bacterial diagnosis, care should be taken to choose pathogen specific siderophores. Otherwise, xenosiderophore uptake by bacteria may produce false positive results, which in turn can lead to wrong diagnosis.

5.5 Experimental Procedures

General Considerations

Unless otherwise noted, starting materials were obtained from commercial suppliers and used without further purification. Water was distilled and further purified by a Millipore cartridge system (resistivity 18.2 MΩ). Flash chromatography was

performed on Salicycle Silica Gel (230-400 mesh) or Brockmann activated aluminium oxide (neutral, 60 mesh). ^{1}H NMR spectra were recorded on a Varian 300 or Varian 500 at 300 MHz or 500 MHz respectively, and ^{13}C NMR spectra on a Varian 300 at 75 MHz at the LeClaire-Dow Instrumentation Facility at the Department of Chemistry, University of Minnesota, Twin-Cities. The residual solvent peak was used as an internal reference. Data for ^{1}H NMR are recorded as follow: chemical shift (δ, ppm), multiplicity (s, singlet; br s, broad singlet; d, doublet; t, triplet; q, quartet; m, multiplet), integration, coupling constant (Hz). Data for ^{13}C NMR are reported in terms of chemical shift (δ, ppm). Mass spectra (LR = low resolution; HR = high resolution; ESI = electrospray ionization) were recorded on a Bruker BioTOF II at the Waters Center of Innovation for Mass Spectrometry at the Department of Chemistry, University of Minnesota, Twin-Cities.

Benzyl phenyl carbonate

Phenyl chloroformate (2.51 mL, 20 mmol) was added to a mixture of benzyl alcohol (2.07 mL, 20 mmol), pyridine (2.00 mL, 25 mmol) and DCM (50 mL) in a 250 mL 3-necked flask equipped with a condenser over a period of 1 h. The reaction mixture was stirred for an additional 3 h, and water was added. The organic phase was washed with 2 M aq H_2SO_4, dried over $MgSO_4$, filtered, and concentrated under reduced pressure. The crude product was distilled in vacuum to get the desired product. ^{1}H NMR ($CDCl_3$): δ = 5.32 (s, 2 H), 7.18-7.48 (m, 10 H), LRMS (ESI) calc. for $[C_{14}H_{12}NaO_3]^+$ ($[M+Na]^+$) : m/z 251.0791, found: 251.1114.

Dibenzyl (azanediylbis(ethane-2,1-diyl))dicarbamate (3-1)

Benzyl phenyl carbonate (434 μL, 2.2 mmol) was added to a solution of diethylenetriamine (108 μL, 1.0 mmol) in DCM (25 mL). The reaction mixture was stirred overnight at room temperature and poured into a phosphate buffer (40 mL; 0.025 M K_2HPO_4 and 0.025 M NaH_2PO_4). The pH was adjusted to 3 with 2 M aq. H_2SO_4, and the mixture was extracted with DCM (2 × 50 mL). The aqueous phase was made strongly alkaline with aq. NaOH (9 M), and extracted with DCM (3 × 50 mL). The organic phase was dried over $MgSO_4$, filtered and concentrated under reduced pressure. ^{1}H NMR ($CDCl_3$): δ = 1.275 (s, 1 H), 2.665 (s, 4 H), 3.211 (s, 4H), 5.066 (s, 4 H), 5.460 (s, 2 H), 7.240 - 7.299 (m, 10 H). LRMS (ESI) calc. for $[C_{20}H_{26}N_3O_4]^+$ ($[M+H]^+$): m/z 372.1994, found: 372.2415.

Methyl 2-(((benzyloxy)carbonyl)amino)-3-bromopropanoate (3-2)

Under cooling in an ice bath, a solution of LiBr (440 mg, 10 mmol) in dry acetone (30 mL) was added slowly to a solution of serine tosylate(*S*)-2-(benzyloxycarbonylamino)-3-(*p*-toluolsulfonyl)methylpropionate (1.02 g, 5.0 mmol) in dry acetone (40 mL). After the addition was complete, the reaction mixture was warmed up to room temperature and stirred for 2 h whereby lithium tosylate precipitated. To complete the substitution reaction, the mixture was heated under reflux for 1 h. Insoluble material was filtered off and the solution was concentrated under reduced pressure. The thus obtained almost colorless oil was dissolved again in $CHCl_3$, filtered to remove salts and purified by silica column chromatography. ^{1}H NMR ($CDCl_3$): δ = 3.762 – 3.854 (m,

5H), 4.883 (t, *J* =7.0 Hz, 1H), 5.182 (m, 2H), 6.093 (s, 1H), 7.342 - 7.410 (m, 5H). HRMS (ESI) calc. for $[C_{12}H_{14}NBrNaO_4]^+$ ($[M+K]^+$): m/z 338.0019, found: 338.0181.

Methyl 2-(((benzyloxy)carbonyl)amino)-3-(bis(2-(((benzyloxy)carbonyl)amino)ethyl) amino)propanoate (3-3)

A solution of the methyl 2-(((benzyloxy)carbonyl)amino)-3-bromopropanoate, **3-2** (106 mg, 0.34 mmol) in acetone (10 mL) was added to a solution of dibenzyl (azanediylbis(ethane-2,1-diyl))dicarbamate (250 mg, 0.67 mmol) and Cs_2CO_3 (132 mg, 0.40 mmol). The reaction mixture was heated to reflux under N_2 for 48 h and filtered. The filtrate was evaporated to dryness and purified by silica column chromatography. ^{1}H NMR ($CDCl_3$): δ 2.61 – 2.70 (m, 6 H), 3.14 - 3.23 (m, 3 H), 3.46 – 3.72 (m, 3 H), 4.99 – 5.15 (m, 5 H), 5.48 (s, 7 H), 7.27 - 7.34 (m, 15 H). LRMS (ESI) calc. for $[C_{32}H_{39}N_4O_8]^+$ ($[M+H]^+$): m/z 607.27, found: 607.20.

Methyl 2-amino-3-(bis(2-aminoethyl)amino)propanoate (3-4)

Methyl 2-(((benzyloxy)carbonyl)amino)-3-(bis(2-(((benzyloxy)carbonyl) amino) ethyl) amino) propanoate, **3-3** (26 mg, 0.03 mmol) was dissolved in anhydrous methanol (50 mL) and Pd on activated C (10 % w/w, 10 mg) was added. The reaction flask was purged thrice with H_2 gas, pressurized to 3 bar with H_2, and mechanically shaken in a Parr hydrogenator for 24 h. The catalyst was filtered off, and the solvent was removed under reduced pressure to yield methyl 2-amino-3-(bis(2-aminoethyl)amino)propanoate, **3-4** as a pale yellow oil. ^{1}H NMR (500 MHz, $CDCl_3$) δ: 2.20 -2.25 (m, 1 H), 2.74 - 2.86

(m, 3 H), 3.24 - 3.40 (m, 3 H), 3.67 - 3.92 (m, 6 H), 5.070 (s, 1 H). LRMS (ESI) calc. for $[C_8H_{21}N_4O_2]^+$ ($[M+H]^+$): m/z 205.17, found: 205.01.

Benzyl 2,3-bis(benzyloxy)benzoate

Benzyl chloride (1.33 mL, 11.6 mmol) and K_2CO_3 (1.71 g, 12.4 mmol) were added to a solution of dihydroxybenzoic acid (500 mg, 3.24 mmol) in DMF (30 mL). The resulting mixture was then heated to reflux at 120 °C under N_2 and stirred overnight. The reaction mixture was filtered, and the filtrate was evaporated under reduced pressure to give a brown oil. The crude oil was purified on a silica column using DCM as the eluent. Evaporation of the solvent gave a colorless oil, which was immediately used in the next step. Yield: 1.36 g (96%).

2,3-Bis(benzyloxy)benzoic acid (3-5)

6 M NaOH (6 mL) was added to a solution of benzyl 2,3-bis(benzyloxy)benzoate (1.32 g, 3.11 mmol) in MeOH (10 mL). The mixture was stirred overnight at room temperature under N_2. The solvent was evaporated under reduced pressure and the product was extracted into DCM and washed with 6 M HCl. The organic phase was collected, dried over anhydrous $MgSO_4$, and evaporated under reduced pressure to give a white solid. The white crude product was dissolved in water, and slowly acidified with concentrated hydrochloric acid. The white solid precipitated out at pH 1, was filtered off, and the residue was lyophilized. The lyophilized product was purified with a silica column with a gradient from 100% CH_2Cl_2 to 5% CH_3OH/ 95% CH_2Cl_2, yielding 2,3-bis(benzyloxy)benzoic acid, **3-5**, as a pure white solid. Yield: 97 %. ^{1}H NMR ($CDCl_3$):δ

= 5.21 (s, 2H), 5.28 (s, 2 H), 7.18 (m, 1 H), 7.35 (m, 9 H), 7.46 (m, 2 H), 7.68 (d, *J* = 7.5 Hz, 1 H).

Methyl 2-(bis(2-(2,3-bis(benzyloxy)benzamido)ethyl)amino)-3-(2,3-bis(benzyloxy)benz-amido)propanoate (3-6)

2,3-Bis(benzyloxy)benzoic acid, **3-5** (220 mg, 0.66 mmol) was dissolved in DMA (5 mL). HATU (250 mg, 0.66 mmol) was added and stirred for 15 min. Methyl 2-amino-3-(bis(2-aminoethyl)amino)propanoate, **3-4** (37 mg, 0.18 mmol), and DIPEA (126 μL, 0.72 mmol) were dissolved in DMA (5 mL) separately for 15 min. and added to the activated acid mixture. The reaction was allowed to proceed overnight and then extracted with ethyl acetate (x3). The solvent was evaporated under reduced pressure, and silica column purification was performed to remove any excess HATU.

2-(Bis(2-(2,3-bis(benzyloxy)benzamido)ethyl)amino)-3-(2,3-bis(benzyloxy) benzamido)propanoic acid (3-7)

Methyl 2-(bis(2-(2,3-bis(benzyloxy)benzamido)ethyl)amino)-3-(2,3-bis(benzyl oxy)benz-amido)propanoate, **3-6** (25 mg, 22 μmol), was dissolved in MeOH:H_2O (3:1 mixture) and 3 pellets of KOH were added. After overnight stirring at room temperature, the solvent was evaporated, and the residue was dissolved in water, acidified with dilute HCl, and extracted with DCM (x3). The extract was dried with $MgSO_4$ and the solvent was evaporated to obtain the deprotected acid complex, **3-7,** which was used in the next step.

4-((5-(2-(bis(2-(2,3-bis(benzyloxy)benzamido)ethyl)amino)-3-(2,3-bis(benzyloxy)benz-amido)propanamido)pentyl)carbamoyl)-2-(6-(dimethylamino)-3-(dimethyliminio)-4,4a-dihydro-3H-xanthen-9-yl)benzoate (3-8)

2-(Bis(2-(2,3-bis(benzyloxy)benzamido)ethyl)amino)-3-(2,3-bis(benzyloxy) benzamido) propanoic acid, **3-7** (8 mg, 7.02 μmol), was dissolved in DMA (2 mL), and HATU (3 mg, 8.43 μmol) was added. The dye, 5(6)-TAMRA cadaverine (5 mg, 8.43 μmol), and DIPEA (4 μL, 21 μmol) were dissolved separately in DMA and then added to the complex mixture after stirring for 15 min. The reaction was allowed to proceed overnight and then extracted with ethyl acetate (×3). The organic layer was evaporated under reduced pressure and the next step was performed.

4-((5-(2-(bis(2-(2,3-dihydroxybenzamido)ethyl)amino)-3-(2,3-dihydroxybenzamido)pro-panamido)pentyl)carbamoyl)-2-(6-(dimethylamino)-3-(dimethyliminio)-4,4a-dihydro-3H-xanthen-9-yl)benzoate

4-((5-(2-(bis(2-(2,3-bis(benzyloxy)benzamido)ethyl)amino)-3-(2,3 bis(benzyloxy) benzaido)propanamido)pentyl)carbamoyl)-2-(6-(dimethylamino)-3-(dimethyliminio)-4,4a-dihydro-3*H*-xanthen-9-yl)benzoate, **3-8** (10 mg, 6 μmol) was dissolved in anhydrous methanol (10 mL) and Pd on activated C (10 % w/w, 2 mg) was added. The reaction flask was purged thrice with H_2 gas, pressurized to 4 bar with H_2, and mechanically shaken in a Parr hydrogenator for 3 h. The catalyst was filtered off, and the solvent was removed under reduced pressure to yield the complete final ligand.

Gallium(III) 4-((5-(2-(bis(2-(2,3-dioxidobenzamido)ethyl)amino)-3-(2,3-dioxidobenzamido)propanamido)pentyl)carbamoyl)-2-(6-(dimethylamino)-3-(dimethyliminio)-4,4a-dihydro-3H-xanthen-9-yl)benzoate (3-9)

4-((5-(2-(bis(2-(2,3-dihydroxybenzamido)ethyl)amino)-3-(2,3-dihydroxybenzamido)propanamido)pentyl)carbamoyl)-2-(6-(dimethylamino)-3-(dimethyliminio)-4,4a-dihydro-3*H*-xanthen-9-yl)benzoate (10 mg, 9 μmol) was dissolved in DI water (10 mL), $GaCl_3$ (2 mg, 9 μmol) was added, and the pH was adjusted to 7 with KOH. The resulting solution was stirred overnight, and solvent was evaporated under reduced pressure. A dark purple solid, **3-9** was obtained.

Progress towards synthesis of 6-amino-9-(5-((5-(5-(bis(2-(2,3-dihydroxybenzamido) ethyl)amino)-4-(2,3-dihydroxybenzamido)pentanamido)pentyl)carbamoyl)-2-carboxyphenyl)-3-iminio-3*H*-xanthene-4,5-disulfonate (3-17)

Tert-butyl 4-(((benzyloxy)carbonyl)amino)-5-hydroxypentanoate

2-Mercaptopyridine (91 mg, 8.1 mmol) was added to a stirred solution of Z-L-glutamic acid 5-*tert*-butyl ester (2.5 g, 7.4 mmol) and DCC (1.7 g, 8.4 mmol) in EtOAc (75 mL). Stirring was continued for 4 h, at which time the precipitate was filtered off and the solvent was removed under reduced pressure. The residue was dissolved in 1,4-dioxane (50 mL), cooled to 0 °C and treated with $NaBH_4$ (1 g). When the reaction was completed after 1.5 h, as monitored by TLC, it was quenched slowly by adding 2% $KHSO_4$ (aq). The mixture was extracted with Et_2O (3 × 50 mL). The combined organic layers were washed with 5% $NaHCO_3$ (2 × 25 mL) and brine, dried with $MgSO_4$, and

concentrated under vacuum. The crude product was purified by silica column chromatography eluting with a gradient of 100% hexanes to 40% EtOAc/ 60% hexanes to give the product as colorless oil. Yield: 1.29 g (54 %). ^{1}H NMR ($CDCl_3$): δ 7.34 (s, 5H), 5.17 (d, *J* = 7.5 Hz, 1H), 5.09 (s, 2H), 3.61 (m, 3H), 2.36 (m, 2H), 1.87 – 1 .72 (m, 2 H), 1.43 (s, 9H). LRMS (ESI) calc. for $[C_{17}H_{25}NNaO_5]^+$ ($[M+Na]^+$): m/z 346.16, found: 346.14.

Tert-butyl 4-(((benzyloxy)carbonyl)amino)-5-iodopentanoate (3-10)

PPh_3 (2.09 g, 7.98 mmol), I_2 (1.01 g, 7.98 mmol), and imidazole (906 mg, 13.0 mmol) were dissolved in anhydrous CH_2Cl_2 (15 mL) and stirred for 30 min. under N_2 at room temperature. This solution was added to a solution of *tert*-butyl 4-(((benzyloxy)carbonyl)amino)-5-hydroxypentanoate (860 mg, 2.66 mmol) dissolved in dry CH_2Cl_2 (5 mL) and stirred for 3 h. The solvent was evaporated under reduced pressure. The obtained yellow solid was purified by silica column chromatography. Yield: 910 mg (79%). ^{1}H NMR ($CDCl_3$): δ = 1.43 (s, 9H), 1.82 (m, 2H), 2.29 (m, 2H), 3.28 (m, 1H), 3.39 (m, 1H), 3.50 (m, 1H), 5.09 (s, 2H), 5.13 (s, 1H), 7.26 - 7.35 (m, 5H). LRMS (ESI) calc. for $[C_{17}H_{24}INNaO_4]^+$ ($[M+Na]^+$): m/z 456.08, found: 456.10.

Tert-butyl 4-(((benzyloxy)carbonyl)amino)-5-bromopentanoate

Tert-butyl 4-(((benzyloxy)carbonyl)amino)-5-hydroxypentanoate (446 mg, 1.70 mmol), and CBr_4 (493 mg, 1.46 mmol) were dissolved in anhydrous CH_2Cl_2 (10 mL). PPh_3 (400 mg, 1.24 mmol) was added at 0 °C. The reaction was stirred for 1 h at room temperature. Diethyl ether (~10 mL) was added, the precipitate was filtered off, and the

filtrate was evaporated under reduced pressure. The thus obtained yellow solid was purified by silica column chromatography. Yield: 190 mg (40%). ^{1}H NMR ($CDCl_3$): δ = 1.38 (s, 9H), 1.82 (m, 2H), 2.25 (m, 2H), 3.41 (m, 1H), 3.48 (m, 1H), 3.84 (m, 1H), 5.04 (s, 2H), 5.16 (s, 1H), 7.26 - 7.32 (m, 5H). LRMS (ESI) calc. for $[C_{17}H_{24}BrNNaO_4]^+$ ($[M+Na]^+$): m/z 409.08, found: 409.08.

Tert-butyl 4-(((benzyloxy)carbonyl)amino)-5-(bis(2-(((benzyloxy)carbonyl)amino)ethyl) amino)pentanoate (3-11)

A solution of the *tert*-butyl 4-(((benzyloxy)carbonyl)amino)-5-iodopentanoate, **3-10** (84 mg, 0.19 mmol), in acetone (10 mL) was added to a solution of dibenzyl (azanediylbis(ethane-2,1-diyl))dicarbamate (72 mg, 0.19 mmol) and Cs_2CO_3 (126 mg, 0.39 mmol) was added. The reaction mixture was heated to reflux for 72 h. The solid was filtered off, and the filtrate was evaporated under reduced pressure. The thus obtained yellow oil was purified over a silica column. Yield: 30 mg (23 %). ^{1}H-NMR (CD_3OD) δ: 7.26 -7.25 (m, 15 H), 5.05 (s, 6 H), 3.65 (m, 1 H), 3.16 (m, 4 H), 2.62 (m, 2 H), 2.52 (m, 2 H), 2.40 (m, 2H), 2.24 (m, 2H), 1 83 (m, 1H), 1.48 (m, 1H), 1.40 (s, 9 H). ^{13}C-NMR (CD_3OD) δ: 173.17, 157.70, 157.54, 136.94, 128.01, 127.64, 127.52, 127.49, 127.43, 80.17, 66.08, 60.13, 59.25, 53.53, 38.44, 31.60, 27.66, 27.14. HRMS (ESI) calc. for $[C_{37}H_{49}N_4O_8]^+$ ($[M+H]^+$): m/z 677.3545, found: 677.3619.

Tert-butyl 4-amino-5-(bis(2-aminoethyl)amino)pentanoate (3-12)

Tert-butyl4-(((benzyloxy)carbonyl)amino)-5-(bis(2-(((benzyloxy)carbonyl) amino)ethyl) amino)pentanoate, **3-11** (30 mg, 0.04 mmol) was dissolved in anhydrous

methanol (15 mL) and Pd on activated C (10 % w/w, 10 mg) was added. The reaction flask was purged thrice with H_2 gas, pressurized to 3 bar with H_2, and mechanically shaken in a Parr hydrogenator for 48 h. The catalyst was filtered off, and the solvent was removed under reduced pressure. Yield: 12 mg (100 %). ^{1}H-NMR (CD_3OD) δ: 2.88 (m, 1 H), 2.82 (m, 4 H), 2.60 (m, 2 H), 2.44 (m, 2 H), 2.30 (m, 4 H), 1.71 (m, 1 H), 1.54 (m, 1H), 1.45 (s, 9H). ^{13}C-NMR (CD_3OD) δ: 172.73, 79.92, 61.91, 56.70, 48.59, 39.09, 32.15, 30.58, 27.82 HRMS (ESI) calc. for $[C_{13}H_{31}N_4O_2]^+$ ($[M+H]^+$): m/z 275.2420, found: 275.2422.

(2,3-Bis(benzyloxy)phenyl)(2-thioxothiazolidin-3-yl)methanone (3-13)

2,3-Bisbenzyloxybenzoic acid (500 mg, 1.5 mmol) was suspended in anhydrous toluene (3 mL). 0.1 mL of anhydrous DMF was added to the flask and purged with N_2 (g). Oxalyl chloride (393 μL, 3.0 mmol) was added to the mixture under N_2 (g). After 2.5 h, the mixture was filtered off and the filtrate was evaporated under reduced pressure. The thus obtained yellow oil was thoroughly dried in a vacuum oven. The yellow oil was dissolved in anhydrous THF (1.5 mL). 2-Mercaptathiazoline (540 mg, 1.5 mmol) and triethylamine (3 mL) were mixed in anhydrous THF (1.5 mL). Mercaptathiazoline solution was slowly added to the THF solution of acid chloride. A precipitate formed, and the reaction was stirred overnight. The precipitate was filtered, and the filtrate was evaporated under reduced pressure. The residue was dissolved in DCM and extracted with 1 M KOH (4 × 25 mL) and brine (2 × 25 mL). The thus obtained yellow organic phase was dried with Mg_2SO_4 and the solvent evaporated under reduced pressure. The resulted yellow oil was purified over a silica column (100% DCM). Yield: 433 mg

(67%). ^{1}H NMR ($CDCl_3$): δ 2.84 (t, *J* = 5 Hz, 2H), 4.33 (t, *J* = 5 Hz, 2H), 5.12 (s, 4H), 6.95 (m, 1H), 7.08 (m, 2H), 7.34 (m, 10H).

Tert-butyl 5-(bis(2-(2,3-bis(benzyloxy)benzamido)ethyl)amino)-4-(2,3-bis(benzyloxy) benzamido)pentanoate (3-14)

(2,3-Bis(benzyloxy)phenyl)(2-thioxothiazolidin-3-yl)methanone, **3-13** (100 mg, 0.23 mmol), and *tert*-butyl 4-amino-5-(bis(2-aminoethyl)amino)pentanoate, **3-12** (21 mg, 76 μmol) were dissolved in CH_2Cl_2 (5 mL) and the solution stirred two days at room temperature. After one day, because the starting material was still present, DIPEA (0.5 mL) was added. After two days, the solvent was evaporated and the resulting product purified by silica column chromatography. Yield: 56 mg (51%). ^{1}H NMR ($CDCl_3$):δ = 1.35 (s, 9H), 1.36 (m, 1H), 1.71 (m, 1H), 2.07 (m, 2H), 2.11 (m, 1H), 2.22 (m, 1H), 2.41 (m, 4H), 3.17 (m, 4H), 3.95 (m, 1H), 5.08 (m, 12H), 7.04 (m, 6H), 7.23 - 7.47 (m, 33H), 7.65 (m, 1H), 7.75 (m, 2 H). ^{13}C-NMR ($CDCl_3$) δ: 172.25, 165.21, 164.74, 151.60, 146.62, 137.01, 128.70, 128.68, 128.65, 128.59, 128.50, 128.44, 128.39, 128.14, 128.10, 127.72, 127.68, 127. 42, 124.12, 123.97, 122.92, 122.54, 116.37, 79.83, 76.05, 71.01, 58.63, 47.61, 37.30, 32.11, 28.04, 27.83. HRMS (ESI) calc. for $[C_{76}H_{78}N_4NaO_{11}]^+$ ($[M+Na]^+$): m/z 1245.5700, found: 1245.5742.

5-(Bis(2-(2,3-dihydroxybenzamido)ethyl)amino)-4-(2,3-dihydroxybenzamido)pentanoic acid (3-15)

Tert-butyl5-(bis(2-(2,3-bis(benzyloxy)benzamido)ethyl)amino)-4-(2,3-bis (benzyloxy)benzamido)pentanoate, **3-14** (30 mg, 25 μmol), was dissolved in glacial

acetic acid (10 mL), and HCl (2 mL) and water (5 mL) were added. Pd on activated C (10 % w/w, 10 mg) was added. The reaction flask was purged thrice with H_2 gas, pressurized to 4 bar with H_2, and mechanically shaken in a Parr hydrogenator for 48 h. The catalyst was filtered off, washed with CH_3OH (5 × 5 mL), and the solvent was removed under reduced pressure. Analysis of NMR and mass spectrometric data suggested a mixture of the desired product, **3-15**, (LRMS (ESI) calc. for $[C_{30}H_{35}N_4O_{11}]^+$ ($[M+H]^+$): m/z 627.23, found: 627.29)) and the methyl ester of the product (LRMS (ESI) calc. for $[C_{31}H_{37}N_4O_{11}]^+$ ($[M+H]^+$): m/z 641.25, found: 641.31).

T-media

T-media is a combination of medium A and medium B (supplemental medium). All compounds of medium A were dissolved in milli Q water (0.97 L), as shown in Table 5.1. The pH was adjusted to pH 7.4 with dilute HCl and the resulting solution was autoclaved for 20 min. The proteins shown in Table 5.2 were dissolved in milli Q water (0.30 L) separately and added to medium A once it had cooled to room temperature.

Table 5.1 T-media preparation (Medium A)

Medium A	Amount (g)
NaCl	5.8
KCl	3.7
$CaCl_2$	0.133
$MgCl_2 \cdot 6H_2O$	0.1
NH_4Cl	1.1
KH_2PO_4	0.272
Tris	12.1
Na_2SO_4	0.142
$MnCl_2$ (100 mM)	10 uL
Casamino acids	0.5

Table 5.2 T-media preparation (Medium B)

Medium B	Amount (mg)
leucine	50
proline	50
tryptophan	50
thiamine HCl	5
glucose	2000

6 REFERENCES

1. http://medical-dictionary.thefreedictionary.com/Commensal+bacteria - accessed on 02/02/15.

2. Mortality, G. B. D.; Causes of Death, C., Global, regional, and national age-sex specific all-cause and cause-specific mortality for 240 causes of death, 1990-2013: a systematic analysis for the Global Burden of Disease Study 2013. *Lancet* **2015,** *385*, 117-171.

3. Magill, S. S.; Edwards, J. R.; Bamberg, W.; Beldavs, Z. G.; Dumyati, G.; Kainer, M. A.; Lynfield, R.; Maloney, M.; McAllister-Hollod, L.; Nadle, J.; Ray, S. M.; Thompson, D. L.; Wilson, L. E.; Fridkin, S. K., Multistate Point-Prevalence Survey of Health Care–Associated Infections. *New Engl. J. Med.* **2014,** *370*, 1198-1208.

4. http://www.buzzle.com/articles/pathogenic-diseases.html - accessed on 02/02/15.

5. O'Connor, S. M.; Taylor, C. E.; Hughes, J. M., Emerging Infectious Determinants of Chronic Diseases. *Emerg. Infect. Dis.* **2006,** *12*, 1051-1057.

6. http://www.bacteriamuseum.org/index.php/main-exhibits/pathogenic-bacteria/pathogenicity - accessed on 02/02/15.

7. Chen, L.; Xiong, Z.; Sun, L.; Yang, J.; Jin, Q., VFDB 2012 update: toward the genetic diversity and molecular evolution of bacterial virulence factors. *Nucleic Acids Res.* **2012,** *40*, D641-D645.

8. www.cdc.gov/drugresistance/threat-report-2013/ - accessed on 02/02/15.

9. http://www.cdc.gov/abcs/reports-findings/survreports/hib13.html - accessed on 02/02/15.

10. Watt, J. P.; Wolfson, L. J.; O'Brien, K. L.; Henkle, E.; Deloria-Knoll, M.; McCall, N.; Lee, E.; Levine, O. S.; Hajjeh, R.; Mulholland, K.; Cherian, T., Burden of disease caused by *Haemophilus influenzae* type b in children younger than 5 years: global estimates. *Lancet* **2009,** *374*, 903-911.

11. http://www.cdc.gov/nchs/data/hus/2013/039.pdf - accessed on 03/06/15.

12. http://www.who.int/bulletin/archives/77%288%29651.pdf - accessed on 03/04/15.

13. Majowicz, S. E.; Musto, J.; Scallan, E.; Angulo, F. J.; Kirk, M.; O'Brien, S. J.; Jones, T. F.; Fazil, A.; Hoekstra, R. M., The Global Burden of Nontyphoidal *Salmonella* Gastroenteritis. *Clin. Infect. Dis.* **2010,** *50*, 882-889.

14. http://www.cdc.gov/abcs/reports-findings/survreports/leg12.html - accessed on 02/02/15.

15. http://www.nalco.com/eu/services/about-legionella.htm -accessed on 03/04/15.

16. http://www.cdc.gov/meningococcal/global.html - accessed on 03/04/15.

17. http://whqlibdoc.who.int/publications/2011/9789241502450_eng.pdf?ua=1 - accessed on 03/04/15.

18. http://apps.who.int/iris/bitstream/10665/112738/1/9789240692671_eng.pdf?ua=1 - accessed on 03/06/15.

19. http://www.cdc.gov/abcs/reports-findings/survreports/mrsa12.html - accessed on 02/02/15.

20. http://www.cdc.gov/abcs/reports-findings/survreports/spneu13.html - accessed on 02/02/15.

21. http://www.who.int/immunization/topics/pneumococcal_disease/en/ - accessed on 03/04/15.

22. http://www.cdc.gov/abcs/reports-findings/survreports/gbs13.html - accessed on 02/02/15.

23. http://www.cdc.gov/abcs/reports-findings/survreports/gas13.html - accessed on 02/02/15.

24. Safar, A.; Lennon, D.; Stewart, J.; Trenholme, A.; Drinkovic, D.; Peat, B.; Taylor, S.; Read, K.; Roberts, S.; Voss, L., Invasive Group A Streptococcal Infection and Vaccine Implications. *Emerg. Infect. Dis.* **2011,** *17*, 983-989.

25. www.cdc.gov/HAI/pdfs/hai/Scott_CostPaper.pdf -accessed on 02/04/15.

26. http://www.cdc.gov/drugresistance/ - accessed on 02/07/15.

27. Mislin, G. L. A.; Schalk, I. J., Siderophore-dependent iron uptake systems as gates for antibiotic Trojan horse strategies against Pseudomonas aeruginosa. *Metallomics* **2014,** *6*, 408-420.

28. Daniel, A. T.; Shaohua, Z.; Emily, T.; Sherry, A.; Aparna, S.; Mary, J. B.; Patrick, F. M., Antimicrobial Drug Resistance in *Escherichia coli* from Humans and Food Animals, United States, 1950–2002. *Emerg. Infect. Dis.* **2012,** *18*, 741.

29. Watanabe, T., Infective Heredity Of Multiple Drug Resistance In Bacteria. *Bacteriol. Rev.* **1963,** *27*, 87-115.

30. Urdea, M.; Penny, L. A.; Olmsted, S. S.; Giovanni, M. Y.; Kaspar, P.; Shepherd, A.; Wilson, P.; Dahl, C. A.; Buchsbaum, S.; Moeller, G.; Hay Burgess, D. C., Requirements for high impact diagnostics in the developing world. *Nature* **2006**, 73-79.

31. Su, W.; Gao, X.; Jiang, L.; Qin, J., Microfluidic platform towards point-of-care diagnostics in infectious diseases. *J. Chromatogr. A* **2015,** *1377*, 13-26.

32. Mabey, D.; Peeling, R. W.; Ustianowski, A.; Perkins, M. D., Tropical infectious diseases: Diagnostics for the developing world. *Nat. Rev. Micro.* **2004,** *2*, 231-240.

33. Tokel, O.; Inci, F.; Demirci, U., Advances in Plasmonic Technologies for Point of Care Applications. *Chem. Rev.* **2014,** *114*, 5728-5752.

34. Heijnen, L. M., G., Method for rapid detection of viable Escherichia coli in water using real-time NASBA. *Water Research* **2009,** *43*, 3124-3132.

35. Wildeboer, D.; Amirat, L.; Price, R. G.; Abuknesha, R. A., Rapid detection of *Escherichia coli* in water using a hand-held fluorescence detector. *Water Res.* **2010,** *44*, 2621-2628.

36. Caruso, G.; Crisafi, E.; Mancuso, M., Development of an enzyme assay for rapid assessment of *Escherichia coli* in seawaters. *J. Appl. Microbiol.* **2002,** *93*, 548-556.

37. http://www.accessdata.fda.gov/cdrh_docs/reviews/k082068.pdf - accessed on 02/12/15.

38. Ginocchio, C. C., Strengths and Weaknesses of FDA-Approved/Cleared Diagnostic Devices for the Molecular Detection of Respiratory Pathogens. *Clin. Infect. Dis.* **2011,** *52*, S312-S325.

39. http://www.cdc.gov/nhsn/PDFs/pscManual/7pscCAUTIcurrent.pdf -accessed on 03/10/15.

40. http://www.cdc.gov/nhsn/PDFs/pscManual/6pscVAPcurrent.pdf - accessed on 03/10/15.

41. Carrol, E. D.; Guiver, M.; Nkhoma, S.; Mankhambo, L. A.; Marsh, J.; Balmer, P.; Banda, D. L.; Jeffers, G.; White, S. A.; Molyneux, E. M.; Molyneux, M. E.; Smyth, R. L.; Hart, C. A.; Group, T. I. S., High Pneumococcal DNA Loads Are Associated With Mortality in Malawian Children With Invasive Pneumococcal Disease. *Pediatr. Infect. Dis. J.* **2007,** *26*, 416-422.

42. Van Dorst, B.; Cremers, A.; Jans, K.; Van Domburg, T.; Steegen, K.; Huang, C.; Dorrer, C.; Lagae, L.; Ferwerda, G.; Stuyver, L. J., Integration of clinical point-of-care requirements in a DNA microarray genotyping test. *Biosens. Bioelectron.* **2014,** *61*, 605-611.

43. Operario, D. J.; Houpt, E., Defining the Etiology of Diarrhea: Novel Approaches. *Curr. Opin. Infect. Dis.* **2011,** *24*, 464-471.

44. Singh, R.; Mukherjee, M. D.; Sumana, G.; Gupta, R. K.; Sood, S.; Malhotra, B. D., Biosensors for pathogen detection: A smart approach towards clinical diagnosis. *Sensor. Actuator.* **2014,** *197*, 385-404.

45. Ndao, M., Diagnosis of Parasitic Diseases: Old and New Approaches. *Interdiscipl. Persp. Infect. Dis.* **2009,** *2009*, Article ID 278246.

46. Guerra, R. L.; Hooper, N. M.; Baker, J. F.; Alborz, R.; Armstrong, D. T.; Maltas, G.; Kiehlbauch, J. A.; Dorman, S. E., Use of the amplified *Mycobacterium tuberculosis* direct test in a public health laboratory*: Test performance and impact on clinical care. *Chest* **2007,** *132* (3), 946-951.

47. Pusterla, N.; Madigan, J. E.; Leutenegge, C. M., Real-Time Polymerase Chain Reaction: A Novel Molecular Diagnostic Tool for Equine Infectious Diseases. *J. Vet. Intern. Med.* **2006,** *20*, 3–12.

48. Jordan, J. A.; Durso, M. B., Real-Time Polymerase Chain Reaction for Detecting Bacterial DNA Directly from Blood of Neonates Being Evaluated for Sepsis. *J. Mol. Diagn.* **2005,** *7*, 575-581.

49. Fortin, N. Y.; Mulchandani, A.; Chen, W., Use of Real-Time Polymerase Chain Reaction and Molecular Beacons for the Detection of *Escherichia coli* O157:H7. *Anal. Biochem.* **2001,** *289*, 281-288.

50. Catalina, L.-S.; Jorge, F. C.; Nicolas, V.-S.; Rocío, T.; Velazquez, F. R.; Javier, T.; Phillip, I. T.; Teresa, E.-G., Single Multiplex Polymerase Chain Reaction To Detect Diverse Loci Associated with Diarrheagenic *Escherichia coli*. *Emerg. Infect. Dis.* **2003,** *9*, 127.

51. Numazaki, K.; Chiba, S.; Moroboshi, T.; Kudoh, T.; Yamanaka, T.; Nakao, T., Comparison of enzyme linked immunosorbent assay and enzyme linked fluorescence immunoassay for detection of antibodies against *Chlamydia trachomatis*. *J. Clin. Pathol.* **1985,** *38*, 345-350.

52. http://www.nmihi.com/p/pyuria.htm -accessed on 03/11/15.

53. http://www.mdguidelines.com/pyuria - accessed on 03/11/15.

54. Schmelcher, M.; Loessner, M. J., Application of bacteriophages for detection of foodborne pathogens. *Bacteriophage* **2014,** *4*, e28137.

55. Fan, S. T.; Teoh-Chan, C. H.; Lau, K. F., Evaluation of central venous catheter sepsis by differential quantitative blood culture. *Eur. J. Clin. Microbiol. Infect. Dis.* **1989,** *8*, 142-144.

56. Isaacman, D. J.; Karasic, R. B.; Reynolds, E. A.; Kost, S. I., Effect of number of blood cultures and volume of blood on detection of bacteremia in children. *J. Pediatr.* **1996,** *128*, 190-195.

57. Schelonka, R. L.; Chai, M. K.; Yoder, B. A.; Hensley, D.; Brockett, R. M.; Ascher, D. P., Volume of blood required to detect common neonatal pathogens. *J. Pediatr.* **1996,** *129*, 275-278.

58. Wang, S.; Inci, F.; Chaunzwa, T. L.; Ramanujam, A.; Vasudevan, A.; Subramanian, S.; Chi Fai Ip, A.; Sridharan, B.; Gurkan, U. A.; Demirci, U., Portable microfluidic chip for detection of *Escherichia coli* in produce and blood. *Int. J. Nanomed.* **2012,** *7*, 2591-2600.

59. Sanderson, M. W.; Sreerama, S.; Nagaraja, T. G., Sensitivity of Direct Plating for Detection of High Levels of *E. coli* O157:H7 in Bovine Fecal Samples. *Curr. Microbiol.* **2007,** *55*, 158-161.

60. Wade, W., Unculturable bacteria—the uncharacterized organisms that cause oral infections. *J. Roy. Soc. Med.* **2002,** *95*, 81-83.

61. Galikowska, E.; Kunikowska, D.; Tokarska-Pietrzak, E.; Dziadziuszko, H.; Łoś, J. M.; Golec, P.; Węgrzyn, G.; Łoś, M., Specific detection of *Salmonella enterica* and *Escherichia coli* strains by using ELISA with bacteriophages as recognition agents. *Eur. J. Clin. Microbiol. Infect. Dis.* **2011,** *30*, 1067-1073.

62. Notomi, T.; Okayama, H.; Masubuchi, H.; Yonekawa, T.; Watanabe, K.; Amino, N.; Hase, T., Loop-mediated isothermal amplification of DNA. *Nucleic acids research* **2000,** *28*.

63. http://www.harrisonconsultant.com/yahoo_site_admin/assets/docs/FDA_Approved_Molecular_Assays.324145127.pdf -accessed on 03/11/15.

64. Norén, T.; Alriksson, I.; Andersson, J.; Åkerlund, T.; Unemo, M., Rapid and Sensitive Loop-Mediated Isothermal Amplification Test for *Clostridium difficile* Detection Challenges Cytotoxin B Cell Test and Culture as Gold Standard. *J. Clin. Microbiol.* **2011,** *49*, 710-711.

65. http://www.reeis.usda.gov/web/crisprojectpages/0188151-detection-of-viable-enterohemorrhagic-escherichia-coli-using-pcr-and-rt-pcr.html - accessed on 02/13/15.

66. Hogardt, M.; Trebesius, K.; Geiger, A. M.; Hornef, M.; Rosenecker, J.; Heesemann, J., Specific and Rapid Detection by Fluorescent In Situ Hybridization of Bacteria in Clinical Samples Obtained from Cystic Fibrosis Patients. *J. Clin. Microbiol.* **2000,** *38*, 818-825.

67. http://www.cdc.gov/lyme/diagnosistesting/LabTest/TwoStep/EIA/index.html-accessed on 03/11/15.

68. Lv, L.-L.; Liu, B.-C.; Zhang, C.-X.; Tang, Z.-M.; Zhang, L.; Lu, Z.-H., Construction of an antibody microarray based on agarose-coated slides. *Electrophoresis* **2007,** *28*, 406-413.

69. Shabani, A.; Zourob, M.; Allain, B.; Marquette, C. A.; Lawrence, M. F.; Mandeville, R., Bacteriophage-Modified Microarrays for the Direct Impedimetric Detection of Bacteria. *Anal. Chem.* **2008,** *80*, 9475-9482.

70. Wammanda, R. D.; Aikhionbare, H. A.; Ogala, W. N., Use of nitrite dipstick test in the screening for urinary tract infection in children. *West Afr. J. Med.* **2000,** *19*, 206-208.

71. Vollmer, T.; Hinse, D.; Kleesiek, K.; Dreier, J., The Pan Genera Detection Immunoassay: a Novel Point-of-Issue Method for Detection of Bacterial Contamination in Platelet Concentrates. *J. Clin. Microbiol.* **2010,** *48*, 3475-3481.

72. Velusamy, V.; Arshak, K.; Korostynska, O.; Oliwa, K.; Adley, C., An overview of foodborne pathogen detection: In the perspective of biosensors. *Biotechnol. Adv.* **2010,** *28*, 232-254.

73. Vo-Dinh, T.; Cullum, B., Biosensors and biochips: advances in biological and medical diagnostics. *Fresenius J. Anal. Chem.* **2000,** *366*, 540–551.

74. Li, C.-z.; Vandenberg, K.; Prabhulkar, S.; Zhu, X.; Schneper, L.; Methee, K.; Rosser, C. J.; Almeide, E., Paper based point-of-care testing disc for multiplex whole cell bacteria analysis. *Biosens. Bioelectron.* **2011,** *26*, 4342-4348.

75. Gill, P.; Ghalami, M.; Ghaemi, A.; Mosavari, N.; Abdul-Tehrani, H.; Sadeghizadeh, M., Nanodiagnostic Method for Colorimetric Detection of *Mycobacterium tuberculosis* 16S rRNA. *NanoBiotechnol.* **2008,** *4*, 28-35.

76. Ho, J.-a.; Zeng, S.-C.; Tseng, W.-H.; Lin, Y.-J.; Chen, C.-h., Liposome-based immunostrip for the rapid detection of *Salmonella*. *Anal. Bioanal. Chem.* **2008,** *391*, 479-485.

77. Hwang, K.-Y.; Jeong, S.-Y.; Kim, Y.-R.; Namkoong, K.; Lim, H.-K.; Chung, W.-S.; Kim, J.-H.; Huh, N., Rapid detection of bacterial cell from whole blood: Integration of DNA sample preparation into single micro-PCR chip. *Sensor. Actuator.* **2011,** *154*, 46-51.

78. Liu, T.; Lu, Y.; Gau, V.; Liao, J.; Wong, P., Rapid Antimicrobial Susceptibility Testing with Electrokinetics Enhanced Biosensors for Diagnosis of Acute Bacterial Infections. *Ann. Biomed. Eng.* **2014,** *42*, 2314-2321.

79. Besant, J. D.; Das, J.; Sargent, E. H.; Kelley, S. O., Proximal Bacterial Lysis and Detection in Nanoliter Wells Using Electrochemistry. *ACS Nano* **2013,** *7*, 8183–8189.

80. Kuralay, F.; Campuzano, S.; Haake, D. A.; Wang, J., Highly sensitive disposable nucleic acid biosensors for direct bioelectronic detection in raw biological samples. *Talanta* **2011,** *85*, 1330-1337.

81. Cai, D.; Xiao, M.; Xu, P.; Xu, Y.-C.; Du, W., An integrated microfluidic device utilizing dielectrophoresis and multiplex array PCR for point-of-care detection of pathogens. *Lab Chip* **2014,** *14*, 3917-3924.

82. Lim, D. V., Detection of Microorganisms and Toxins with Evanescent Wave Fiber-Optic Biosensors. *Proc. IEEE* **2003,** *91*, 902–907.

83. Ouyang, M.; Mohan, R.; Lu, Y.; Liu, T.; Mach, K. E.; Sin, M. L. Y.; McComb, M.; Joshi, J.; Gau, V.; Wong, P. K.; Liao, J. C., An AC electrokinetics facilitated biosensor cassette for rapid pathogen identification. *Analyst* **2013,** *138*, 3660-3666.

84. Liao, J. C.; Mastali, M.; Gau, V.; Suchard, M. A.; Møller, A. K.; Bruckner, D. A.; Babbitt, J. T.; Li, Y.; Gornbein, J.; Landaw, E. M.; McCabe, E. R. B.; Churchill, B. M.; Haake, D. A., Use of Electrochemical DNA Biosensors for Rapid Molecular Identification of Uropathogens in Clinical Urine Specimens. *J. Clin. Microbiol.* **2006,** *44*, 561-570.

85. Wu, J.; Campuzano, S.; Halford, C.; Haake, D. A.; Wang, J., Ternary Surface Monolayers for Ultrasensitive (Zeptomole) Amperometric Detection of Nucleic Acid Hybridization without Signal Amplification. *Anal. Chem.* **2010,** *82*, 8830-8837.

86. Settu, K.; Chen, C.-J.; Liu, J.-T.; Chen, C.-L.; Tsai, J.-Z., Impedimetric method for measuring ultra-low *E. coli* concentrations in human urine. *Biosens. Bioelectron.* **2015,** *66*, 244-250.

87. Lillehoj, P. B.; Kaplan, C. W.; He, J.; Shi, W.; Ho, C.-M., Rapid, Electrical Impedance Detection of Bacterial Pathogens Using Immobilized Antimicrobial Peptides. *J. Lab. Autom.* **2014,** *19*, 42-49.

88. Lu, X.; Samuelson, D. R.; Xu, Y.; Zhang, H.; Wang, S.; Rasco, B. A.; Xu, J.; Konkel, M. E., Detecting and Tracking Nosocomial Methicillin-Resistant

Staphylococcus aureus Using a Microfluidic SERS Biosensor. *Anal. Chem.* **2013,** *85*, 2320-2327.

89. Gopala, J.; Narayan, J. L.; Hui-Fen, W., TiO2 nanoparticle assisted mass spectrometry as biosensor of *Staphylococcus aureus*, key pathogen in nosocomial infections from air, skin surface and human nasal passage. *Biosens. Bioelectron.* **2011,** *27*, 201–206.

90. Mahmoudian, L.; Kaji, N.; Tokeshi, M.; Nilsson, M.; Baba, Y., Rolling Circle Amplification and Circle-to-circle Amplification of a Specific Gene Integrated with Electrophoretic Analysis on a Single Chip. *Anal. Chem.* **2008,** *80*, 2483-2490.

91. Jassal, M. S.; Nedeltchev, G. G.; Lee, J.-H.; Choi, S. W.; Atudorei, V.; Sharp, Z. D.; Deretic, V.; Timmins, G. S.; Bishai, W. R., (13)[C]-Urea Breath Test as a Novel Point-of-Care Biomarker for Tuberculosis Treatment and Diagnosis. *PLoS One* **2010,** *5*, e12451.

92. Campuzano, S.; Pedrero, M.; García, J.; García, E.; García, P.; Pingarrón, J., Development of amperometric magnetogenosensors coupled to asymmetric PCR for the specific detection of *Streptococcus pneumoniae*. *Anal. Bioanal. Chem.* **2011,** *399*, 2413-2420.

93. Fronczek, C. F.; Park, T. S.; Harshman, D. K.; Nicolini, A. M.; Yoon, J.-Y., Paper microfluidic extraction and direct smartphone-based identification of pathogenic nucleic acids from field and clinical samples. *RSC Adv.* **2014,** *4*, 11103-11110.

94. Mach, K. E.; Du, C. B.; Phull, H.; Haake, D. A.; Shih, M.-C.; Baron, E. J.; Liao, J. C., Multiplex Pathogen Identification for Polymicrobial Urinary Tract Infections Using Biosensor Technology: A Prospective Clinical Study. *J. Urol.* **2009,** *182*, 2735-2741.

95. Shriver-Lake, L.; Golden, J.; Bracaglia, L.; Ligler, F., Simultaneous assay for ten bacteria and toxins in spiked clinical samples using a microflow cytometer. *Anal. Bioanal. Chem.* **2013,** *405*, 5611-5614.

96. Lam, B.; Fang, Z.; Sargent, E. H.; Kelley, S. O., Polymerase Chain Reaction-Free, Sample-to-Answer Bacterial Detection in 30 Minutes with Integrated Cell Lysis. *Anal. Chem.* **2012,** *84*, 21-25.

97. Souto, A.; Montaos, M. A.; Balado, M.; Osorio, C. R.; Rodríguez, J.; Lemos, M. L.; Jiménez, C., Synthesis and antibacterial activity of conjugates between norfloxacin and analogues of the siderophore vanchrobactin. *Bioorgan. Med. Chem.* **2013,** *21*, 295-302.

98. Ji, C.; Miller, P. A.; Miller, M. J., Iron Transport-Mediated Drug Delivery: Practical Syntheses and In Vitro Antibacterial Studies of Tris-Catecholate Siderophore–Aminopenicillin Conjugates Reveals Selectively Potent Antipseudomonal Activity. *J. Am. Chem. Soc.* **2012,** *134*, 9898-9901.

99. Chakraborty, R., Iron Uptake in Bacteria with Emphasis on *E. coli* and *Pseudomonas*. In *SpringerBriefs in Molecular Science*, Chakraborty, R.; Braun, V.; Hantke, K.; Cornelis, P., Eds. Springer: **2013**, 1-29.

100. Braun, V., Iron uptake mechanisms and their regulation in pathogenic bacteria. *Int. J. Med. Microbiol.* **2001,** *291*, 67-79.

101. Fardeau, S.; Mullié, C.; Dassonville-Klimpt, A.; Audic, N.; Sasaki, A.; Sonnet, P., Bacterial iron uptake: a promising solution against multidrug resistant bacteria In *Science against microbial pathogens: communicating current research and technological advances* A.Mendez-Vilas, Ed. **2011**.

102. Krewulak, K. D.; Vogel, H. J., Structural biology of bacterial iron uptake. *Biochim. Biophys. Acta* **2008,** *1778*, 1781-1804.

103. Raymond, K. N.; Dertz, E. A.; Kim, S. S., Enterobactin: An archetype for microbial iron transport. *Proc. Natl. Acad. Sci. USA* **2003,** *100*, 3584-3588.

104. Braun, V.; Killmann, H., Bacterial solutions to the iron-supply problem. *Trends Biochem. Sci.* **1999,** *24*, 104-109.

105. Wandersman, C., Stojiljkovic, I., Bacterial heme sources: the role of heme, hemoprotein receptors and hemophores. *Curr. Opin. Microbiol.* **2000,** *3*, 215–220

106. Caza, M.; Kronstad, J., Shared and distinct mechanisms of iron acquisition by bacterial and fungal pathogens of humans. *Front. Cell. Infec. Microbiol.* **2013,** *3*.

107. Koczura, R.; Kaznowski, A., The Yersinia high-pathogenicity island and iron-uptake systems in clinical isolates of *Escherichia coli*. *J. Med. Microbiol.* **2003,** *52*, 637-642.

108. Otto, B. R.; van Dooren, S. J. M.; Nuijens, J. H.; Luirink, J.; Oudega, B., Characterization of a Hemoglobin Protease Secreted by the Pathogenic *Escherichia coli* Strain EB1. *J. Exp. Med.* **1998,** *188*, 1091-1103.

109. Dall´Agnol, M.; Martinez, M. B., Uptake of iron from different compounds by enteroinvasive *Escherichia coli*. *Rev. Microbiol.* **1999,** *30*, 149-152.

110. Braun, V., Iron uptake by *Escherichia coli*. *Front. Biosci.* **2003,** *8*, S1409-S1421.

111. Cornelissen, C. N.; Kelley, M.; Hobbs, M. M.; Anderson, J. E.; Cannon, J. G.; Cohen, M. S.; Sparling, P. F., The transferrin receptor expressed by gonococcal strain FA1090 is required for the experimental infection of human male volunteers. *Mol. Microbiol.* **1998,** *27*, 611-616.

112. Fischbach, M. A.; Lin, H.; Zhou, L.; Yu, Y.; Abergel, R. J.; Liu, D. R.; Raymond, K. N.; Wanner, B. L.; Strong, R. K.; Walsh, C. T.; Aderem, A.; Smith, K. D., The pathogen-associated iroA gene cluster mediates bacterial evasion of lipocalin 2. *Proc. Natl. Acad. Sci. USA* **2006,** *103*, 16502-16507.

113. Chu, B. C.; Garcia-Herrero, A.; Johanson, T. H.; Krewulak, K. D.; Lau, C. K.; Peacock, R. S.; Slavinskaya, Z.; Voge, H. J., Siderophore uptake in bacteria and the battle for iron with the host; a bird's eye view. *Biometals* **2010,** *23*, 601-611.

114. Vokes, S. A.; Reeves, S. A.; Torres, A. G.; Payne, S. M., The aerobactin iron transport system genes in *Shigella flexneri* are present within a pathogenicity island. *Mol. Microbiol.* **1999,** *33*, 63-73.

115. Holden, V. I.; Bachman, M., Diverging Roles of Bacterial Siderophores During Infection. *Metallomics* **2015**.

116. Mokracka, J.; Koczura, R.; Kaznowski, A., Yersiniabactin and other siderophores produced by clinical isolates of *Enterobacter* spp. and *Citrobacter* spp. *FEMS Immun. Med. Microbiol.* **2004,** *40*, 51-55.

117. Mokracka, J.; Cichoszewska, E.; Kaznowski, A., Siderophore production by Gram-negative rods isolated from human polymicrobial infections. *Biological Lett.* **2011,** *48*, 147–157.

118. Fischbach, M. A.; Lin, H.; Liu, D. R.; Walsh, C. T., How pathogenic bacteria evade mammalian sabotage in the battle for iron. *Nat. Chem. Biol.* **2006,** *2*, 132-138.

119. Hider, R. C.; Kong, X., Chemistry and biology of siderophores. *Nat. Prod. Rep.* **2010,** *27*, 637-657.

120. Bister, B.; Bischoff, D.; Nicholson, G.; Valdebenito, M.; Schneider, K.; Winkelmann, G.; Hantke, K.; Süssmuth, R., The structure of salmochelins: C-glucosylated enterobactins of *Salmonella enterica*. *Biometals* **2004,** *17*, 471-481.

121. Valdebenito, M.; Crumbliss, A. L.; Winkelmann, G.; Hantke, K., Environmental factors influence the production of enterobactin, salmochelin, aerobactin, and yersiniabactin in *Escherichia coli* strain Nissle 1917. *Int. J. Med. Microbiol.* **2006,** *296,* 513–520.

122. Karch, H.; Tarr, P. I.; Bielaszewska, M., Enterohaemorrhagic *Escherichia coli* in human medicine. *Int. J. Med. Microbiol.* **2005,** *295*, 405-418.

123. Bach, S.; de Almeida, A.; Carniel, E., The Yersinia high-pathogenicity island is present in different members of the family Enterobacteriaceae. *FEMS Microbiol. Lett.* **2000,** *183*, 289-294.

124. Schubert, S.; Cuenca, S.; Fischer, D.; Heesemann, J., High-Pathogenicity Island of *Yersinia pestis* in Enterobacteriaceae Isolated from Blood Cultures and Urine Samples: Prevalence and Functional Expression. *J. Infect. Dis.* **2000,** *182*, 1268-1271.

125. Heesemann, J.; Hantke, K.; Vocke, T.; Saken, E.; Rakin, A.; Stojiljkovic, I.; Berner, R., Virulence of *Yersinia enterocolitica* is closely associated with siderophore production, expression of an iron-repressible outer membrane polypeptide of 65 000 Da and pesticin sensitivity. *Mol. Microbiol.* **1993,** *8*, 397-408.

126. Perry, R. D.; Brubaker, R. R., Accumulation of iron by yersiniae. *J. Bacteriol.* **1979,** *137*, 1290-1298.

127. Rabsch, W.; Voigt, W.; Reissbrodt, R.; Tsolis, R. M.; Bäumler, A. J., *Salmonella typhimurium* IroN and FepA Proteins Mediate Uptake of Enterobactin but Differ in Their Specificity for Other Siderophores. *J. Bacteriol.* **1999,** *181*, 3610-3612.

128. Morton, D. J.; Turman, E. J.; Hensley, P. D.; VanWagoner, T. M.; Seale, T. W.; Whitby, P. W.; Stull, T. L., Identification of a siderophore utilization locus in nontypeable *Haemophilus influenzae*. *BMC Microbiol.* **2010,** *10*, 113-113.

129. Proschak, A.; Lubuta, P.; Grün, P.; Löhr, F.; Wilharm, G.; De Berardinis, V.; Bode, H. B., Structure and Biosynthesis of Fimsbactins A–F, Siderophores from *Acinetobacter baumannii* and *Acinetobacter baylyi*. *ChemBioChem* **2013,** *14*, 633-638.

130. Dorsey, C. W.; Tomaras, A. P.; Connerly, P. L.; Tolmasky, M. E.; Crosa, J. H.; Actis, L. A., The siderophore-mediated iron acquisition systems of *Acinetobacter baumannii* ATCC 19606 and *Vibrio anguillarum* 775 are structurally and functionally related. *Microbiology* **2004,** *150*, 3657-3667.

131. Cianciotto, N., Iron Acquisition by *Legionella pneumophila*. *Biometals* **2007,** *20*, 323-331.

132. Hollander, A.; Mercante, A. D.; Shafer, W. M.; Cornelissen, C. N., The Iron-Repressed, AraC-Like Regulator MpeR Activates Expression of fetA in *Neisseria gonorrhoeae*. *Infect. Immun.* **2011,** *79*, 4764-4776.

133. Register, K. B.; Ducey, T. F.; Brockmeier, S. L.; Dyer, D. W., Reduced Virulence of a *Bordetella bronchiseptica* Siderophore Mutant in Neonatal Swine. *Infect. Immun.* **2001,** *69*, 2137-2143.

134. Seedorf, H.; Fricke, W. F.; Veith, B.; Brüggemann, H.; Liesegang, H.; Strittmatter, A.; Miethke, M.; Buckel, W.; Hinderberger, J.; Li, F.; Hagemeier, C.; Thauer, R. K.; Gottschalk, G., The genome of *Clostridium kluyveri,* a strict anaerobe with unique metabolic features. *Proc. Natl. Acad. Sci. USA* **2008,** *105*, 2128-2133.

135. Mariotti, P.; Malito, E.; Biancucci, M.; Surdo, P. L.; Mishra, R. P. N.; Nardi-Dei, V.; Savino, S.; Nissum, M.; Spraggon, G.; Grandi, G.; Bagnoli, F.; Bottomley, M. J., Structural and functional characterization of the *Staphylococcus aureus* virulence factor and vaccine candidate FhuD2. *Biochem. J.* **2013,** *449*, 683–693.

136. Courcol, R. J.; Trivier, D.; Bissinger, M. C.; Martin, G. R.; Brown, M. R., Siderophore production by *Staphylococcus aureus* and identification of iron-regulated proteins. *Infect. Immun.* **1997,** *65*, 1944-1948.

137. Konetschny-Rapp, S.; Jung, G.; Meiwes, J.; ZÄHner, H., Staphyloferrin A: a structurally new siderophore from staphylococci. *Eur. J. Biochem.* **1990,** *191*, 65-74.

138. Dale, S. E.; Doherty-Kirby, A.; Lajoie, G.; Heinrichs, D. E., Role of Siderophore Biosynthesis in Virulence of *Staphylococcus aureus*: Identification and Characterization of Genes Involved in Production of a Siderophore. *Infect. Immun.* **2004,** *72*, 29-37.

139. Sebulsky, M. T.; Heinrichs, D. E., Identification and Characterization of fhuD1 and fhuD2, Two Genes Involved in Iron-Hydroxamate Uptake in *Staphylococcus aureus*. *J. Bacteriol.* **2001,** *183*, 4994-5000.

140. Retamales, J.; González-Contreras, A.; Salazar, S.; Toranzo, A. E.; Avendaño-Herrera, R., Iron utilization and siderophore production by *Streptococcus phocae* isolated from diseased Atlantic salmon (*Salmo salar*). *Aquaculture* **2012,** *364–365*, 305-311.

141. Ge, R.; Sun, X., Iron acquisition and regulation systems in *Streptococcus* species. *Metallomics* **2014,** *6*, 996-1003.

142. May, J. J.; Wendrich, T. M.; Marahiel, M. A., The dhb Operon of *Bacillus subtilis* Encodes the Biosynthetic Template for the Catecholic Siderophore 2,3-Dihydroxybenzoate-Glycine-Threonine Trimeric Ester Bacillibactin. *J. Biol. Chem.* **2001,** *276*, 7209-7217.

143. Miethke, M.; Klotz, O.; Linne, U.; May, J. J.; Beckering, C. L.; Marahiel, M. A., Ferri-bacillibactin uptake and hydrolysis in *Bacillus subtilis*. *Mol. Microbiol.* **2006,** *61*, 1413-1427.

144. Snow, G. A., Mycobactin. A growth factor for *Mycobacterium johnei.* Part III. Degradation and tentative structure. *J. Chem. Soc.* **1954,** 4080-4093.

145. Crosa, J. H.; Walsh, C. T., Genetics and Assembly Line Enzymology of Siderophore Biosynthesis in Bacteria. *Microbiol. Mol. Biol. R.* **2002,** *66*, 223-249.

146. McHugh, J. P.; Rodríguez-Quiñones, F.; Abdul-Tehrani, H.; Svistunenko, D. A.; Poole, R. K.; Cooper, C. E.; Andrews, S. C., Global Iron-dependent Gene Regulation in *Escherichia coli*: A New Mechanism For Iron Homeostasis. *J. Biol. Chem.* **2003,** *278*, 29478-29486.

147. Anzaldi, L. L.; Skaar, E. P., Overcoming the Heme Paradox: Heme Toxicity and Tolerance in Bacterial Pathogens. *Infect. Immun.* **2010,** *78*, 4977-4989.

148. Ratledge, C.; Dover, L. G., Iron Metabolism In Pathogenic Bacteria. *Annu. Rev. Microbiol.* **2000,** *54*, 881-941.

149. Boukhalfa, H.; Crumbliss, A. L., Chemical aspects of siderophore mediated iron transport. *Biometals* **2002,** *15*, 325–339.

150. Miethke, M.; Marahiel, M. A., Siderophore-Based Iron Acquisition and Pathogen Control. *Microbiol. Mol. Biol. R.* **2007,** *71*, 413–451.

151. Grass, G., Iron Transport in *Escherichia Coli*: All has not been said and Done. *Biometals* **2006,** *19*, 159-172.

152. Carrano, C. J.; Drechsel, H.; Kaiser, D.; Jung, G.; Matzanke, B.; Winkelmann, G.; Rochel, N.; Albrecht-Gary, A. M., Coordination Chemistry of the Carboxylate Type Siderophore Rhizoferrin: The Iron(III) Complex and Its Metal Analogs. *Inorg. Chem.* **1996,** *35*, 6429-6436.

153. Harris, W. R.; Carrano, C. J.; Raymond, K. N., Coordination chemistry of microbial iron transport compounds. 16. Isolation, characterization, and formation constants of ferric aerobactin. *J. Am. Chem. Soc.* **1979,** *101*, 2722-2727.

154. Crumbliss, A. L.; Harrington, J. M., Iron sequestration by small molecules: Thermodynamic and kinetic studies of natural siderophores and synthetic model compounds. In *Adv. Inorg. Chem.*, Rudi van, E.; Colin, D. H., Eds. Academic Press: **2009**; Vol. 61, 179-250.

155. Anderegg, G.; L'Eplattenier, F.; Schwarzenbach, G., Hydroxamatkomplexe III. Eisen(III)-Austausch zwischen Sideraminen und Komplexonen. Diskussion der Bildungskonstanten der Hydroxamatkomplexe. *Helv. Chim. Acta* **1963,** *46*, 1409-1422.

156. Carrano, C. J.; Cooper, S. R.; Raymond, K. N., Coordination chemistry of microbial iron transport compounds. 11. Solution equilibriums and electrochemistry of ferric rhodotorulate complexes. *J. Am. Chem. Soc.* **1979,** *101*, 599-604.

157. Telford, J. R.; Raymond, K. N., Coordination Chemistry of the Amonabactins, Bis(catecholate) Siderophores from *Aeromonas hydrophila1*. *Inorg. Chem.* **1998,** *37*, 4578-4583.

158. Kaufmann, G. F.; Sartorio, R.; Lee, S.-H.; Rogers, C. J.; Meijler, M. M.; Moss, J. A.; Clapham, B.; Brogan, A. P.; Dickerson, T. J.; Janda, K. D., Revisiting quorum sensing: Discovery of additional chemical and biological functions for 3-oxo-N-acylhomoserine lactones. *Proc. Natl. Acad. Sci. USA* **2005,** *102*, 309-314.

159. Gare´naux, A. l.; Caza, M. l.; Dozois, C. M., The Ins and Outs of siderophore mediated iron uptake by extra-intestinal pathogenic *Escherichia coli*. *Vet. Microbiol.* **2011,** *153*, 89–98.

160. Andrews, S. C.; Robinson, A. K.; Rodríguez-Quiñones, F., Bacterial iron homeostasis. *FEMS Microbiol. Rev.* **2003,** *27*, 215-237.

161. Higgs, P. I.; Larsen, R. A.; Postle, K., Quantification of known components of the *Escherichia coli* TonB energy transduction system: TonB, ExbB, ExbD and FepA. *Mol. Microbiol.* **2002,** *44*, 271-281.

162. Wandersman, C.; Delepelaire, P., Bacterial Iron Sources: From Siderophores to Hemophores. *Annu. Rev. Microbiol.* **2004,** *58*, 611-647.

163. Grigg, J. C.; Cooper, J. D.; Cheung, J.; Heinrichs, D. E.; Murphy, M. E. P., The *Staphylococcus aureus* Siderophore Receptor HtsA Undergoes Localized Conformational Changes to Enclose Staphyloferrin A in an Arginine-rich Binding Pocket. *J. Biol. Chem.* **2010,** *285*, 11162-11171.

164. West, S. A.; Buckling, A., Cooperation, virulence and siderophore production in bacterial parasites. *P. Roy. Soc. Lond. B Bio.* **2003,** *270*, 37-44.

165. Lamont, I. L.; Beare, P. A.; Ochsner, U.; Vasil, A. I.; Vasil, M. L., Siderophore-mediated signaling regulates virulence factor production in *Pseudomonas aeruginosa*. *P. Natl. Acad. Sci. USA* **2002,** *99*, 7072-7077.

166. Vagarali, M.; Karadesai, S.; Patil, C.; Metgud, S.; Mutnal, M., Haemagglutination and siderophore production as the urovirulence markers of uropathogenic *Escherichia coli*. *Indian J. Med. Microbi.* **2008,** *26*, 68-70.

167. Johnson, T. J.; Kariyawasam, S.; Wannemuehler, Y.; Mangiamele, P.; Johnson, S. J.; Doetkott, C.; Skyberg, J. A.; Lynne, A. M.; Johnson, J. R.; Nolan, L. K., The Genome Sequence of Avian Pathogenic *Escherichia coli* Strain O1:K1:H7 Shares Strong Similarities with Human Extraintestinal Pathogenic *E. coli* Genomes. *J. Bacteriol.* **2007,** *189*, 3228-3236.

168. O'brien, I. G.; Gibson, F., The Structure Of Enterochelin And Related 2,3-Dihydroxy-N-Benzoylserine Conjugates From *Escherichia Coli*. *Biochim. Biophys. Acta* **1970,** *215*, 393-402.

169. Pollack, J. R.; Neilands, J. B., Enterobactin, An Iron Transport Comkxind From *Salmonella typhimurium*. *Biochem. Bioph. Res. Co.* **1970,** *38*, 989-992.

170. Karpishin, T. B.; Raymond, K. N., The First Structural Characterization of a Metal–Enterobactin Complex: $[V(enterobactin)]^{2-}$. *Angew. Chem. Int. Edit.* **1992,** *31*, 466-468.

171. Karpishin, T. B.; Dewey, T. M.; Raymond, K. N., Coordination chemistry of microbial iron transport. 49. The vanadium(IV) enterobactin complex: structural, spectroscopic, and electrochemical characterization. *J. Am. Chem. Soc.* **1993,** *115*, 1842-1851.

172. Thulasiraman, P.; Newton, S. M. C.; Xu, J.; Raymond, K. N.; Mai, C.; Hall, A.; Montague, M. A.; Klebba, P. E., Selectivity of Ferric Enterobactin Binding and Cooperativity of Transport in Gram-Negative Bacteria. *J. Bacteriol.* **1998,** *180*, 6689-6696.

173. Ecker, D. J.; Matzanke, B. F.; Raymond, K. N., Recognition and transport of ferric enterobactin in *Escherichia coli*. *J. Bacteriol.* **1986,** *167*, 666-673.

174. Loomis, L. D.; Raymond, K. N., Solution equilibria of enterobactin and metal-enterobactin complexes. *Inorg. Chem.* **1991,** *30*, 906-911.

175. Furman, M.; Fica, A.; Saxena, M.; Di Fabio, J. L.; Cabello, F. C., *Salmonella typhi* iron uptake mutants are attenuated in mice. *Infect. Immun.* **1994,** *62*, 4091-4094.

176. Benjamin, W. H.; Turnbough, C. L.; Posey, B. S.; Briles, D. E., The ability of *Salmonella typhimurium* to produce the siderophore enterobactin is not a virulence factor in mouse typhoid. *Infect. Immun.* **1985,** *50*, 392-397.

177. Flo, T. H.; Smith, K. D.; Sato, S.; Rodriguez, D. J.; Holmes, M. A.; Strong, R. K.; Akira, S.; Aderem, A., Lipocalin 2 mediates an innate immune response to bacterial infection by sequestrating iron. *Nature* **2004,** *432*, 917-921.

178. Bachman, M. A.; Miller, V. L.; Weiser, J. N., Mucosal Lipocalin 2 Has Pro-Inflammatory and Iron-Sequestering Effects in Response to Bacterial Enterobactin. *PLoS Pathog.* **2009,** *5*, e1000622.

179. Hantke, K.; Nicholson, G.; Rabsch, W.; Winkelmann, G., Salmochelins, siderophores of *Salmonella enterica* and uropathogenic *Escherichia coli* strains, are recognized by the outer membrane receptor IroN. *Proc. Natl. Acad. Sci. USA* **2003,** *100*, 3677-3682.

180. Feldmann, F.; Sorsa, L. J.; Hildinger, K.; Schubert, S., The Salmochelin Siderophore Receptor IroN Contributes to Invasion of Urothelial Cells by Extraintestinal Pathogenic *Escherichia coli* In Vitro. *Infect. Immun.* **2007,** *75*, 3183-3187.

181. Nègre, V. L.; Bonacorsi, S.; Schubert, S.; Bidet, P.; Nassif, X.; Bingen, E., The Siderophore Receptor IroN, but Not the High-Pathogenicity Island or the Hemin Receptor ChuA, Contributes to the Bacteremic Step of *Escherichia coli* Neonatal Meningitis. *Infect. Immun.* **2004,** *72*, 1216-1220.

182. Peigne, C.; Bidet, P.; Mahjoub-Messai, F.; Plainvert, C.; Barbe, V.; Médigue, C.; Frapy, E.; Nassif, X.; Denamur, E.; Bingen, E.; Bonacorsi, S., The Plasmid of *Escherichia coli* Strain S88 (O45:K1:H7) That Causes Neonatal Meningitis Is Closely Related to Avian Pathogenic *E. coli* Plasmids and Is Associated with High-Level Bacteremia in a Neonatal Rat Meningitis Model. *Infect. Immun.* **2009,** *77*, 2272-2284.

183. Gao, Q.; Wang, X.; Xu, H.; Xu, Y.; Ling, J.; Zhang, D.; Gao, S.; Liu, X., Roles of iron acquisition systems in virulence of extraintestinal pathogenic *Escherichia coli*: salmochelin and aerobactin contribute more to virulence than heme in a chicken infection model. *BMC Microbiol.* **2012,** *12*, 143-143.

184. Dozois, C. M.; Fairbrother, J. M.; Harel, J.; Bossé, M., pap-and pil-related DNA sequences and other virulence determinants associated with *Escherichia coli* isolated from septicemic chickens and turkeys. *Infect. Immun.* **1992,** *60*, 2648-2656.

185. Lafont, J. P.; Dho, M.; D'Hauteville, H. M.; Bree, A.; Sansonetti, P. J., Presence and expression of aerobactin genes in virulent avian strains of *Escherichia coli*. *Infect. Immun.* **1987,** *55*, 193-197.

186. Garcia, E. C.; Brumbaugh, A. R.; Mobley, H. L. T., Redundancy and Specificity of *Escherichia coli* Iron Acquisition Systems during Urinary Tract Infection. *Infect. Immun.* **2011,** *79*, 1225-1235.

187. Arisoy, M.; Aysev, D.; Ekim, M.; Özel, D.; Köse, S. K.; Özsoy, E. D.; Akar, N., Detection of virulence factors of *Escherichia coli* from children by multiplex polymerase chain reaction. *Int. J. Clin. Pract.* **2006,** *60*, 170-173.

188. Demir, M.; Kaleli, I., Production by *Escherichia coli* isolates of siderophore and other virulence factors and their pathogenic role in a cutaneous infection model. *Clin. Microbiol. Infec.* **2004,** *10*, 1011-1014.

189. Russo, T. A.; Olson, R.; MacDonald, U.; Metzger, D.; Maltese, L. M.; Drake, E. J.; Gulick, A. M., Aerobactin Mediates Virulence and Accounts for Increased Siderophore Production under Iron-Limiting Conditions by Hypervirulent (Hypermucoviscous) *Klebsiella pneumoniae*. *Infect. Immun.* **2014,** *82*, 2356-2367.

190. Williams, P. H.; Carbonetti, N. H., Iron, siderophores, and the pursuit of virulence: independence of the aerobactin and enterochelin iron uptake systems in *Escherichia coli*. *Infect. Immun.* **1986,** *51*, 942-947.

191. Lawlor, M. S.; O'Connor, C.; Miller, V. L., Yersiniabactin Is a Virulence Factor for *Klebsiella pneumoniae* during Pulmonary Infection. *Infect. Immun.* **2007,** *75*, 1463-1472.

192. Fetherston, J. D.; Kirillina, O.; Bobrov, A. G.; Paulley, J. T.; Perry, R. D., The Yersiniabactin Transport System Is Critical for the Pathogenesis of Bubonic and Pneumonic Plague. *Infect. Immun.* **2010,** *78*, 2045-2052.

193. Miller, M. C.; Parkin, S.; Fetherston, J. D.; Perry, R. D.; DeMoll, E., Crystal structure of ferric-yersiniabactin, a virulence factor of *Yersinia pestis*. *J. Inorg. Biochem.* **2006,** *100*, 1495–1500.

194. Perry, R. D.; Balbo, P. B.; Jones, H. A.; Fetherston, J. D.; DeMoll, E., Yersiniabactin from *Yersinia pestis:* biochemical characterization of the siderophore and its role in iron transport and regulation. *Microbiology* **1999,** *145*, 1181-1190.

195. Bearden, S. W.; Fetherston, J. D.; Perry, R. D., Genetic organization of the yersiniabactin biosynthetic region and construction of avirulent mutants in *Yersinia pestis*. *Infect. Immun.* **1997,** *65*, 1659-68.

196. Bearden, S. W.; Perry, R. D., The Yfe system of *Yersinia pestis* transports iron and manganese and is required for full virulence of plague. *Mol. Microbiol.* **1999,** *32*, 403-414.

197. Paauw, A.; Leverstein-van Hall, M. A.; van Kessel, K. P. M.; Verhoef, J.; Fluit, A. C., Yersiniabactin Reduces the Respiratory Oxidative Stress Response of Innate Immune Cells. *PLoS One* **2009,** *4*, e8240.

198. Cornelis, P.; Hohnadel, D.; Meyer, J. M., Evidence for different pyoverdine-mediated iron uptake systems among *Pseudomonas aeruginosa* strains. *Infect. Immun.* **1989,** *57*, 3491-3497.

199. Albrecht-Gary, A.-M.; Blanc, S.; Rochel, N.; Ocaktan, A. Z.; Abdallah, M. A., Bacterial Iron Transport: Coordination Properties of Pyoverdin PaA, a Peptidic Siderophore of *Pseudomonas aeruginosa*. *Inorg. Chem.* **1994,** *33*, 6391-6402.

200. Lamont, I. L.; Beare, P. A.; Ochsner, U.; Vasil, A. I.; Vasil, M. L., Siderophore-mediated signaling regulates virulence factor production in *Pseudomonas aeruginosa*. *Proc. Natl. Acad. Sci.* **2002,** *99*, 7072-7077.

201. Peek, M. E.; Bhatnagar, A.; McCarty, N. A.; Zughaier, S. M., Pyoverdine, the Major Siderophore in *Pseudomonas aeruginosa*, Evades NGAL Recognition. *Interdiscipl. Persp. Infect. Dis.* **2012,** *2012*.

202. Thomas, M. S., Iron acquisition mechanisms of the *Burkholderia cepacia* complex. *Biometals* **2007,** *20*, 431-452.

203. Brandel, J.; Humbert, N.; Elhabiri, M.; Schalk, I. J.; Mislin, G. L. A.; Albrecht-Gary, A.-M., Pyochelin, a siderophore of *Pseudomonas aeruginosa*: Physicochemical characterization of the iron(iii), copper(ii) and zinc(ii) complexes. *Dalton Trans.* **2012,** *41*, 2820-2834.

204. Cox, C. D., Effect of pyochelin on the virulence of *Pseudomonas aeruginosa*. *Infect. Immun.* **1982,** *36*, 17-23.

205. Quadri, L. E. N.; Sello, J.; Keating, T. A.; Weinreb, P. H.; Walsh, C. T., Identification of a *Mycobacterium tuberculosis* gene cluster encoding the biosynthetic enzymes for assembly of the virulence-conferring siderophore mycobactin. *Chem. Biol.* **1998,** *5*, 631-645.

206. Ratledge, C., Iron, mycobacteria and tuberculosis. *Tuberculosis* **2004,** *84*, 110-130.

207. Reddy, P. V.; Puri, R. V.; Chauhan, P.; Kar, R.; Rohilla, A.; Khera, A.; Tyagi, A. K., Disruption of Mycobactin Biosynthesis Leads to Attenuation of *Mycobacterium tuberculosis* for Growth and Virulence. *J. Infect. Dis.* **2013,** *208*, 1255-1265.

208. Arnow, L. E., Colorimetric Determination Of The Components Of 3,4-Dihydroxyphenylalaninetyrosine Mixtures. *J. Biol. Chem.* **1937,** *118*, 531-537.

209. Barnum, D. W., Spectrophotometric determination of catechol, epinephrine, dopa, dopamine and other aromatic vic-diols. *Anal. Chim. Acta* **1977,** *89*, 157-166.

210. Rioux, C.; Jordan, D. C.; Rattray, J. B. M., Colorimetric determination of catechol siderophores in microbial cultures. *Anal. Biochem.* **1983,** *133*, 163-169.

211. Csaky, T. Z., On the Estimation of Bound Hydroxylamine in Biological Materials. *Acta Chem. Scand.* **1948,** *2*, 450–454.

212. Atkin, C. L.; Neilands, J. B.; Phaff, H. J., Rhodotorulic Acid from Species of *Leucosporidium, Rhodosporidium, Rhodotorula, Sporidiobolus,* and *Sporobolomyces*, and a New Alanine-Containing Ferrichrome from *Cryptococcus melibiosum*. *J. Bacteriol.* **1970,** *103*, 722-733.

213. Schwyn, B.; Neilands, J. B., Universal chemical assay for the detection and determination of siderophores. *Anal. Biochem.* **1987,** *160*, 47-56.

214. Ames-Gottfred, N. P.; Christie, B. R.; Jordan, D. C., Use of the Chrome Azurol S Agar Plate Technique To Differentiate Strains and Field Isolates of *Rhizobium leguminosarum* biovar *trifolii*. *Appl. Environ. Microb.* **1989,** *55*, 707-710.

215. Milagres, A. M. F.; Machuca, A.; Napoleão, D., Detection of siderophore production from several fungi and bacteria by a modification of chrome azurol S (CAS) agar plate assay. *J. Microbiol. Meth.* **1999,** *37*, 1-6.

216. Machuca, A.; Milagres, A. M. F., Use of CAS-agar plate modified to study the effect of different variables on the siderophore production by *Aspergillus*. *Lett. Appl. Microbiol.* **2003,** *36*, 177-181.

217. Shin, S. H.; Lim, Y.; Lee, S. E.; Yang, N. W.; Rhee, J. H., CAS agar diffusion assay for the measurement of siderophores in biological fluids. *J. Microbiol. Meth.* **2001,** *44*, 89-95.

218. Pérez-Miranda, S.; Cabirol, N.; George-Téllez, R.; Zamudio-Rivera, L. S.; Fernández, F. J., O-CAS, a fast and universal method for siderophore detection. *J. Microbiol. Meth.* **2007,** *70*, 127-131.

219. Sankaranarayanan, R.; Alagumaruthanayagam, A.; Sankaran, K., A new fluorimetric method for the detection and quantification of siderophores using Calcein Blue, with potential as a bacterial detection tool. *Appl. Microbiol. Biot.* **2015**, 1-11.

220. Glickstein, H.; Ben El, R.; Shvartsman, M.; Cabantchik, Z. I., Intracellular labile iron pools as direct targets of iron chelators: a fluorescence study of chelator action in living cells. *Blood* **2005,** *106*, 3242-3250.

221. Marenco, M.; Fowley, C.; Hyland, B.; Galindo-Riaño, D.; Sahoo, S.; Callan, J., A New Fluorescent Sensor for the Determination of Iron(III) in Semi-Aqueous Solution. *J. Fluoresc.* **2012,** *22*, 795-798.

222. Doorneweerd, D. D.; Henne, W. A.; Reifenberger, R. G.; Low, P. S., Selective Capture and Identification of Pathogenic Bacteria Using an Immobilized Siderophore. *Langmuir* **2010,** *26*, 15424-15429.

223. Kim, Y.; Lyvers, D. P.; Wei, A.; Reifenberger, R. G.; Low, P. S., Label-free detection of a bacterial pathogen using an immobilized siderophore, deferoxamine. *Lab Chip* **2012,** *12*, 971-976.

224. Wolfenden, M. L.; Sakamuri, R. M.; Anderson, A. S.; Prasad, L.; Schmidt, J. G.; Mukundan, H., Determination of bacterial viability by selective capture using surface-bound siderophores. *Adv. Biol. Chem.* **2012,** *2*, 396-402.

225. Sakamuri, R. M.; Wolfenden, M. S.; Anderson, A. S.; Swanson, B. I.; Schmidt, J. S.; Mukundan, H., Novel optical strategies for biodetection. *Proc. of SPIE* **2013,** *8812*, 881209-881209-7.

226. Bugdahn, N.; Peuckert, F.; Albrecht, A. G.; Miethke, M.; Marahiel, M. A.; Oberthür, M., Direct Identification of a Siderophore Import Protein Using Synthetic Petrobactin Ligands. *Angew. Chem. Int. Edit.* **2010,** *49*, 10210-10213.

227. Nutiu, R.; Li, Y. F., Structure-Switching Signaling Aptamers. *J. Am. Chem. Soc.* **2003,** *125*, 4771-4778.

228. Sefah, K.; Phillips, J. A.; Xiong, X.; Meng, L.; Van Simaeys, D.; Chen, H.; Martin, J.; Tan, W., Nucleic acid aptamers for biosensors and bio-analytical applications. *Analyst* **2009,** *134*, 1765-1775.

229. Catherine, A. T.; Shishido, S. N.; Robbins-Welty, G. A.; Diegelman-Parente, A., Rational design of a structure-switching DNA aptamer for potassium ions. *FEBS Open Bio* **2014,** *4*, 788-795.

230. Stojanovic, M. N.; de Prada, P.; Landry, D. W., Fluorescent Sensors Based on Aptamer Self-Assembly. *J. Am. Chem. Soc.* **2000,** *122*, 11547-11548.

231. Stojanovic, M. N.; de Prada, P.; Landry, D. W., Aptamer-Based Folding Fluorescent Sensor for Cocaine. *J. Am. Chem. Soc.* **2001,** *123*, 4928-4931.

232. Hamaguchi, N.; Ellington, A.; Stanton, M., Aptamer Beacons for the Direct Detection of Proteins. *Anal. Biochem.* **2001,** *294*, 126-131.

233. Merino, E. J.; Weeks, K. M., Fluorogenic Resolution of Ligand Binding by a Nucleic Acid Aptamer. *J. Am. Chem. Soc.* **2003,** *125*, 12370-12371.

234. Thibon, A.; Pierre, V. C., Principles of responsive lanthanide-based luminescent probes for cellular imaging. *Anal. Bioanal. Chem.* **2009,** *394*, 107-20.

235. Bunzli, J.-C. G.; Piguet, C., Taking advantage of luminescent lanthanide ions. *Chem. Soc. Rev.* **2005,** *34*, 1048-1077.

236. Liu, J. W.; Cao, Z. H.; Lu, Y., Functional Nucleic Acid Sensors. *Chem. Rev.* **2009,** *109*, 1948-1998.

237. Li, T.; Dong, S. J.; Wang, E., A Lead(II)-Driven DNA Molecular Device for Turn-On Fluorescence Detection of Lead(II) Ion with High Selectivity and Sensitivity. *J. Am. Chem. Soc.* **2010,** *132*, 13156-13157.

238. Qin, H.; Ren, J.; Wang, J.; Luedtke, N. W.; Wang, E., G-Quadruplex-Modulated Fluorescence Detection of Potassium in the Presence of a 3500-Fold Excess of Sodium Ions. *Anal. Chem.* **2010,** *82*, 8356-8360.

239. Lv, L.; Guo, Z.; Wang, J.; Wang, E., G-quadruplex as signal transducer for biorecognition events. *Curr. Pharm. Des.* **2012,** *18*, 2076-95.

240. He, H.-Z.; Pui-Yan Ma, V.; Leung, K.-H.; Shiu-Hin Chan, D.; Yang, H.; Cheng, Z.; Leung, C.-H.; Ma, D.-L., A label-free G-quadruplex-based switch-on fluorescence assay for the selective detection of ATP. *Analyst* **2012,** *137*, 1538-1540.

241. Jiang, Y.; Fang, X.; Bai, C., Signaling Aptamer/Protein Binding by a Molecular Light Switch Complex. *Anal. Chem.* **2004,** *76*, 5230-5235.

242. Wang, J.; Jiang, Y.; Zhou, C.; Fang, X., Aptamer-Based ATP Assay Using a Luminescent Light Switching Complex. *Anal. Chem.* **2005,** *77*, 3542-3546.

243. Cuisong, Z.; Yaxin, J.; Shuang, H.; Baocheng, M.; Xiaohong, F.; Menglong, L., Detection of oncoprotein platelet-derived growth factor using a fluorescent signaling complex of an aptamer and TOTO. *Anal. Bioanal. Chem.* **2006,** *384*, 1175-1180.

244. Babu, E.; Singaravadivel, S.; Manojkumar, P.; Krishnasamy, S.; Gnana kumar, G.; Rajagopal, S., Aptamer-based label-free detection of PDGF using ruthenium(II) complex as luminescent probe. *Anal. Bioanal. Chem.* **2013,** *405*, 6891-5.

245. Li, B.; Wei, H.; Dong, S., Sensitive detection of protein by an aptamer-based label-free fluorescing molecular switch. *Chem. Commun.* **2007,** 73-75.

246. Choi, M. S.; Yoon, M.; Baeg, J. O.; Kim, J., Label-free dual assay of DNA sequences and potassium ions using an aptamer probe and a molecular light switch complex. *Chem. Commun.* **2009,** 7419-7421.

247. Pan, L.; Huang, Y.; Wen, C.; Zhao, S., Label-free fluorescence probe based on structure-switching aptamer for the detection of interferon gamma. *Analyst* **2013,** *138*, 6811-6.

248. Luo, Y.; Wu, P.; Hu, J.; He, S.; Hou, X.; Xu, K., An oligonucleotide-based label-free fluorescent sensor: highly sensitive and selective detection of Hg^{2+} in aqueous samples. *Anal. Methods* **2012,** *4*, 1310-1314.

249. Chiang, C. K.; Huang, C. C.; Liu, C. W.; Chang, H. T., Oligonucleotide-Based Fluorescence Probe for Sensitive and Selective Detection of Mercury(II) in Aqueous Solution. *Anal. Chem.* **2008,** *80*, 3716-21.

250. Kong, L.; Xu, J.; Xu, Y. Y.; Xiang, Y.; Yuan, R.; Chai, Y. Q., A universal and label-free aptasensor for fluorescent detection of ATP and thrombin based on SYBR Green I dye. *Biosens. Bioelectron.* **2013,** *42*, 193-197.

251. Thibon, A.; Pierre, V. C., Principles of responsive lanthanide-based luminescent probes for cellular imaging. *Anal. Bioanal. Chem.* **2009,** *394*, 107-120.

252. Weitz, E. A.; Chang, J. Y.; Rosenfield, A. H.; Doan, P.; Pierre, V. C., Molecular Recognition and the Basis for Selective Time-Gated Luminescent Detection of ATP and GTP. *Chem. Sci.* **2013,** *4*, 4052-4060.

253. Plush, S. E.; Gunnlaugsson, T., Solution studies of trimetallic lanthanide luminescent anion sensors: towards ratiometric sensing using an internal reference channel. *Dalton Trans.* **2008,** 3801-4.

254. Law, G.-L.; Pal, R.; Palsson, L. O.; Parker, D.; Wong, K.-L., Responsive and reactive terbium complexes with an azaxanthone sensitiser and one naphthyl group: applications in ratiometric oxygen sensing *in vitro* and in regioselective cell killing. *Chem. Commun.* **2009,** 7321-7323.

255. Smith, D. G.; McMahon, B. K.; Pal, R.; Parker, D., Live cell imaging of lysosomal pH changes with pH responsive ratiometric lanthanide probes. *Chem. Commun.* **2012,** *48*, 8520-8522.

256. Nutiu, R.; Li, Y., Structure-Switching Signaling Aptamers: Transducing Molecular Recognition into Fluorescence Signaling. *Chem. Eur. J.* **2004,** *10*, 1868-1876.

257. Nutiu, R.; Li, Y., Structure-Switching Signaling Aptamers. *J. Am. Chem. Soc.* **2003,** *125*, 4771-4778.

258. Friedman, A. E.; Chambron, J. C.; Sauvage, J. P.; Turro, N. J.; Barton, J. K., Molecular "Light Switch" for DNA : $Ru(bpy)_2(dppz)^{2+}$. *J. Am. Chem. Soc.* **1990,** *112*, 4960-4962.

259. Holmlin, R. E.; Yao, J. A.; Barton, J. K., Dipyridophenazine Complexes of Os(II) as Red-Emitting DNA Probes: Synthesis, Characterization, and Photophysical Properties. *Inorg. Chem.* **1999,** *38*, 174-189.

260. Chan, D. S.-H.; Lee, H.-M.; Che, C.-M.; Leung, C.-H.; Ma, D.-L., A selective oligonucleotide-based luminescent switch-on probe for the detection of nanomolar mercury(II) ion in aqueous solution. *Chem. Commun.* **2009,** 7479-7481.

261. Liu, H.-K.; Sadler, P. J., Metal Complexes as DNA Intercalators. *Acc. Chem. Res.* **2011,** *44*, 349-359.

262. Larsen, R. W.; Jasuja, R.; Hetzler, R. K.; Muraoka, P. T.; Andrada, V. G.; Jameson, D. M., Spectroscopic and Molecular Modeling Studies of Caffeine Complexes with DNA Intercalators. *Biophys. J.* **1996,** *70*, 443-452.

263. Smolensky, E. D.; Peterson, K. L.; Weitz, E. A.; Lewandowski, C.; Pierre, V. C., Magnetoluminescent Light Switches - Dual Modality in DNA Detection. *J. Am. Chem. Soc.* **2013,** *135*, 8966-8972.

264. Weitz, E. A.; Chang, J. Y.; Rosenfield, A. H.; Pierre, V. C., A Selective Luminescent Probe for the Direct Time-Gated Detection of Adenosine Triphosphate. *J. Am. Chem. Soc.* **2012,** *134*, 16099-16102.

265. Bobba, G.; Bretonniere, Y.; Frias, J. C.; Parker, D., Enantiopure lanthanide complexes incorporating a tetraazatriphenylene sensitiser and three naphthyl groups: exciton coupling, intramolecular energy transfer, efficient singlet oxygen formation and perturbation by DNA binding. *Org. Biomol. Chem.* **2003,** *1*, 1870-1872.

266. Bobba, G.; Dickins, R. S.; Kean, S. D.; Mathieu, C. E.; Parker, D.; Peacock, R. D.; Siligardi, G.; Smith, M. J.; Gareth Williams, J. A.; Geraldes, C. F. G. C., Chiroptical, ESMS and NMR spectroscopic study of the interaction of enantiopure lanthanide complexes with selected self-complementary dodecamer oligonucleotides. *J. Chem. Soc. Perkin Trans. 2* **2001,** 1729-1737.

267. Bobba, G.; Frias, J. C.; Parker, D., Highly emissive, nine-coordinate enantiopure lanthanide complexes incorporating tetraazatriphenylenes as probes for DNA. *Chem. Commun.* **2002,** 890-891.

268. Bobba, G.; Kean, S. D.; Parker, D.; Beeby, A.; Baker, G., DNA binding studies of cationic lanthanide complexes bearing a phenanthridinium group. *J. Chem. Soc. Perkin Trans. 2*. **2001,** (9), 1738-1741.

269. Cacheris, W. P.; Quay, S. C.; Rocklage, S. M., The Relationship between Thermodynamics and the Toxicity of Gadolinium Complexes. *Magn. Res. Imag.* **1990,** *8*, 467-481.

270. Hermann, P.; Kotek, J.; Kubicek, V.; Lukes, I., Gadolinium(iii) complexes as MRI contrast agents: ligand design and properties of the complexes. *Dalton Trans.* **2008,** 3027-3047.

271. Wang, Z.; Heon Lee, J.; Lu, Y., Highly sensitive "turn-on" fluorescent sensor for Hg^{2+} in aqueous solution based on structure-switching DNA. *Chem. Commun.* **2008,** 6005-6007.

272. Kovacs, Z.; Sherry, A. D., pH-controlled selective protection of polyaza macrocycles. *Synthesis* **1997,** 759.

273. Moreau, J.; Guillon, E.; Pierrard, J. C.; Rimbault, J.; Port, M.; Aplincourt, M., Complexing Mechanism of the Lanthanide Cations Eu^{3+}, Gd^{3+}, and Tb^{3+} with 1,4,7,10-tetrakis(carboxymethyl)-1,4,7,10-tetraazacyclododecane (dota) - Characterization of Three Successive Complexing Phases: Study of the Thermodynamic and Structural Properties of the Complexes by Potentiometry, Luminescence Spectroscopy, and EXAFS. *Chem. Eur. J.* **2004,** *10*, 5218-5232.

274. Magda, D.; Wright, M.; Crofts, S.; Lin, A.; Sessler, J. L., Metal Complex Conjugates of Antisense DNA Which Display Ribozyme-Like Activity. *J. Am. Chem. Soc.* **1997,** *119*, 6947-6948.

275. Holmlin, R. E.; Dandliker, P. J.; Barton, J. K., Synthesis of Metallointercalator-DNA Conjugates on a Solid Support. *Bioconjugate Chem.* **1999,** *10*, 1122-1130.

276. Gaballah, S. T.; Kerr, C. E.; Eaton, B. E.; Netzel, T. L., Synthesis of 5-(2,2'-bipyridinyl and 2,2'-bipyridinediiumyl)-2'-deoxyuridine nucleosides: precursors to metallo-DNA conjugates. *Nucleosides Nucleotides Nucleic Acids* **2002,** *21*, 547-60.

277. Hara, K.; Kitamura, M.; Inoue, H., Synthesis and hybridization studies on oligonucleotide-metal complex conjugates. *Nucleic Acids Symp. Ser. (Oxf)* **2004,** 217-8.

278. Ihara, T.; Kitamura, Y.; Okada, K.; Tazaki, M.; Jyo, A., Asymmetric cooperativity in tandem hybridization of the DNA conjugates bearing chiral metal complexes. *Nucleic Acids Symp. Ser. (Oxf)* **2005,** 229-30.

279. Graf, N.; Goritz, M.; Kramer, R., A Metal-Ion-Releasing Probe for DNA detection by Catalytic Signal Amplification. *Angew. Chem. Int. Ed. Engl.* **2006,** *45*, 4013-5.

280. Kitamura, Y.; Ihara, T.; Tsujimura, Y.; Osawa, Y.; Jyo, A., Colorimetric allele analysis based on the DNA-directed cooperative formation of luminous lanthanide complexes. *Nucleic Acids Symp. Ser. (Oxf)* **2006,** 105-6.

281. Dubey, I. Y., Dubey,L. V.,Piletska,E. V.,Piletsky, S. A., Metal complexes of 1,4,7-triazacyclononane and their oligonucleotide conjugates as chemical nucleases. *Ukrainica Bioorganica Acta* **2007,** *5*, 11-19.

282. Andersen, C. S.; Yan, H.; Gothelf, K. V., Bridging One Helical Turn in Double-Stranded DNA by Templated Dimerization of Molecular Rods. *Angew. Chem. Int. Ed. Engl.* **2008,** *47*, 5569-72.

283. Ghosh, S.; Pignot-Paintrand, I.; Dumy, P.; Defrancq, E., Design and synthesis of novel hybrid metal complex-DNA conjugates: key building blocks for multimetallic linear DNA nanoarrays. *Org. Biomol. Chem.* **2009,** *7*, 2729-37.

284. Ihara, T.; Kitamura, Y.; Tsujimura, Y.; Jyo, A., DNA Analysis Based on the Local Structural Disruption to the Duplexes Carrying a Luminous Lanthanide Complex. *Anal. Sci.* **2011,** *27*, 585-590.

285. Hurtado, R. R.; Harney, A. S.; Heffern, M. C.; Holbrook, R. J.; Holmgren, R. A.; Meade, T. J., Specific Inhibition of the Transcription Factor Ci by a Cobalt(III) Schiff Base-DNA Conjugate. *Mol. Pharm.* **2012,** *9*, 325-33.

286. Cullum, T. V.-D. B., Biosensors and biochips: advances in biological and medical diagnostics. *Fresenius J Anal Chem* **2000,** *366*, 540–551.

287. Ivnitski, D.; Abdel-Hamid, I.; Atanasov, P.; Wilkins, E., Biosensors for detection of pathogenic bacteria. *Biosens. Bioelectron.* **1999,** *14*, 599-624.

288. Petrik, M.; Haas, H.; Dobrozemsky, G.; Lass-Flörl, C.; Helbok, A.; Blatzer, M.; Dietrich, H.; Decristoforo, C., 68Ga-Siderophores for PET Imaging of Invasive Pulmonary Aspergillosis: Proof of Principle. *J. Nucl. Med.* **2010,** *51*, 639-645.

289. Haas, H.; Petrik, M.; Decristoforo, C., An Iron-Mimicking, Trojan Horse-Entering Fungi—Has the Time Come for Molecular Imaging of Fungal Infections? *PLoS Pathog.* **2015,** *11*, e1004568.

290. Nagoba, B.; Vedpathak, D., Medical Applications of Siderophores. *Eur. J. Gen. Med.* **2011,** *8*, 229-235.

291. Gause, G. F., Recent Studies on Albomycin, a New Antibiotic. *Br. Med. J.* **1955,** *2*, 1177-1179.

292. Fiedler, H. P.; Walz, F.; Döhle, A.; Zähner, H., Albomycin: Studies on fermentation, isolation and quantitative determination. *Appl. Microbiol. Biotechnol.* **1985,** *21*, 341-347.

293. Vértesy, L.; Aretz, W.; Fehlhaber, H.-W.; Kogler, H., Salmycin A–D, Antibiotika aus *Streptomyces violaceus,* DSM 8286, mit Siderophor-Aminoglycosid-Struktur. *Helvetica Chimica Acta* **1995,** *78*, 46-60.

294. de Lima Procópio, R. E.; da Silva, I. R.; Martins, M. K.; de Azevedo, J. L.; de Araújo, J. M., Antibiotics produced by *Streptomyces*. *Braz. J. Infect. Dis.* **2012,** *16*, 466-471.

295. Braun, V.; Pramanik, A.; Gwinner, T.; Köberle, M.; Bohn, E., Sideromycins: tools and antibiotics. *Biometals* **2009,** *22*, 3-13.

296. Bickel, H.; Gäumann, E.; Keller-Schierlein, W.; Prelog, V.; Vischer, E.; Wettstein, A.; Zähner, H., Über eisenhaltige Wachstumsfaktoren, die Sideramine, und ihre Antagonisten, die eisenhaltigen Antibiotika Sideromycine. *Experientia* **1960,** *16*, 129-133.

297. Destoumieux-Garzón, D.; Peduzzi, J.; Thomas, X.; Djediat, C.; Rebuffat, S., Parasitism of Iron-siderophore Receptors of *Escherichia coli* by the Siderophore-peptide Microcin E492m and its Unmodified Counterpart. *Biometals* **2006,** *19*, 181-191.

298. Nolan, E. M.; Walsh, C. T., Investigations of the MceIJ-Catalyzed Posttranslational Modification of the Microcin E492 C-Terminus: Linkage of Ribosomal and Nonribosomal Peptides To Form "Trojan Horse" Antibiotics†. *Biochemistry* **2008,** *47*, 9289-9299.

299. Górska, A.; Sloderbach, A.; Marszałł, M. P., Siderophore–drug complexes: potential medicinal applications of the 'Trojan horse' strategy. *Trends Pharmacol. Sci.* **2014,** *35*, 442-449.

300. Braun, V.; Günthner, K.; Hantke, K.; Zimmermann, L., Intracellular activation of albomycin in *Escherichia coli* and *Salmonella typhimurium*. *J. Bacteriol.* **1983,** *156*, 308-315.

301. Destoumieux-Garzón, D.; Thomas, X.; Santamaria, M.; Goulard, C.; Barthélémy, M.; Boscher, B.; Bessin, Y.; Molle, G.; Pons, A.-M.; Letellier, L.; Peduzzi, J.; Rebuffat, S., Microcin E492 antibacterial activity: evidence for a TonB-dependent inner membrane permeabilization on *Escherichia coli*. *Mol. Microbiol.* **2003,** *49*, 1031-1041.

302. de Lorenzo, V.; Pugsley, A. P., Microcin E492, a low-molecular-weight peptide antibiotic which causes depolarization of the *Escherichia coli* cytoplasmic membrane. *Antimicrob. Agents Ch.* **1985,** *27*, 666-669.

303. Juárez-Hernández, R. l. E.; Miller, P. A.; Miller, M. J., Syntheses of Siderophore−Drug Conjugates Using a Convergent Thiol−Maleimide System. *ACS Med. Chem. Lett.* **2012,** *3*, 799−803.

304. Rivault, F.; Liébert, C.; Burger, A.; Hoegy, F.; Abdallah, M. A.; Schalk, I. J.; Mislin, G. L. A., Synthesis of pyochelin–norfloxacin conjugates. *Bioorgan. Med. Chem. Lett.* **2007,** *17*, 640-644.

305. Noel, S.; Gasser, V.; Pesset, B.; Hoegy, F.; Rognan, D.; Schalk, I. J.; Mislin, G. L. A., Synthesis and biological properties of conjugates between fluoroquinolones and a N3 "-functionalized pyochelin. *Org. Biomol. Chem.* **2011,** *9*, 8288-8300.

306. Hennard, C.; Truong, Q. C.; Desnottes, J.-F. o.; Paris, J.-M.; Moreau, N. J.; Abdallah, M. A., Synthesis and Activities of Pyoverdin-Quinolone Adducts: A Prospective Approach to a Specific Therapy Against *Pseudomonas aeruginosa*. *J. Med. Chem.* **2001,** *44*, 2139-2151.

307. Strahsburger, E.; Baeza, M.; Monasterio, O.; Lagos, R., Cooperative uptake of microcin E492 by receptors FepA, Fiu, and Cir and inhibition by the siderophore enterochelin and its dimeric and trimeric hydrolysis products. *Antimicrob. Agents Ch.* **2005,** *49*, 3083-3086.

308. S.Wendenbaum, P. D., A.Dell, J.M.Meyer, M.A.Abdallah, The Structure of Pyoverdine Pa, The Siderophore of *Pseudomonas Aeruginosa*. *Tetrahedron Lett.* **1983,** *24*, 4877-4880.

309. Rodgers, S. J.; Lee, C.-W.; Ng, C. Y.; Raymond, K. N., Ferric Ion Sequestering Agents. 15. Synthesis, Solution Chemistry, and Electrochemistry of a New Cationic Analogue of Enterobactin. *Inorg. Chem.* **1987,** *26*, 1622-1625.

310. Santos, M. A.; Gaspar, M.; Simões Gonçalves, M. L. S.; Amorim, M. T., Siderophore analogues. A new macrocyclic bis-(amine, amide, hydroxamate) ligand. Synthesis, solution chemistry, electrochemistry and molecular mechanics calculations for the iron complex. *Inorganica Chimica Acta* **1998,** *278*, 51-60.

311. Mies, K. A.; Gebhardt, P.; Möllmann, U.; Crumbliss, A. L., Synthesis, siderophore activity and iron(III) chelation chemistry of a novel mono-hydroxamate, bis-catecholate siderophore mimic: Nα,-Nε-Bis[2,3-dihydroxybenzoyl]-l-lysyl-(γ-N-methyl-N-hydroxyamido)-l-glutamic acid. *J. Inorg. Biochem.* **2008,** *102*, 850-861.

312. Wencewicz, T. A.; Miller, M. J., Biscatecholate-Monohydroxamate Mixed Ligand Siderophore-Carbacephalosporin Conjugates are Selective Sideromycin Antibiotics that Target *Acinetobacter baumannii*. *J. Med. Chem.* **2013,** *56*, 4044-4052.

313. Zheng, T.; Bullock, J. L.; Nolan, E. M., Siderophore-Mediated Cargo Delivery to the Cytoplasm of *Escherichia coli* and *Pseudomonas aeruginosa*: Syntheses of Monofunctionalized Enterobactin Scaffolds and Evaluation of Enterobactin–Cargo Conjugate Uptake. *J. Am. Chem. Soc.* **2012,** *134*, 18388-18400.

314. Wencewicz, T. A.; Long, T. E.; Möllmann, U.; Miller, M. J., Trihydroxamate Siderophore–Fluoroquinolone Conjugates Are Selective Sideromycin Antibiotics that Target *Staphylococcus aureus*. *Bioconjugate Chem.* **2013,** *24*, 473-486.

315. Milner, S. J.; Seve, A.; Snelling, A. M.; Thomas, G. H.; Kerr, K. G.; Routledge, A.; Duhme-Klair, A.-K., Staphyloferrin A as siderophore-component in fluoroquinolone-based Trojan horse antibiotics. *Org. Biomol. Chem.* **2013,** *11*, 3461-3468.

316. Yoganathan, S.; Sit, C. S.; Vederas, J. C., Chemical synthesis and biological evaluation of gallidermin-siderophore conjugates. *Org. Biomol. Chem.* **2011,** *9*, 2133-2141.

317. Rivault, F.; Schons, V.; Liebert, C.; Burger, A.; Salcr, E.; Abdallah, M. A.; Schalk, I. J.; Mislin, G. L. A., Synthesis of functionalized analogs of pyochelin, a siderophore of *Pseudomonas aeruginosa* and *Burkholderia cepacia*. *Tetrahedron* **2006,** *62*, 2247-2254.

318. Roosenberg, J. M.; Lin, Y. M.; Lu, Y.; Miller, M. J., Studies and syntheses of siderophores, microbial iron chelators, and analogs as potential drug delivery agents. *Curr. Med. Chem.* **2000,** *7*, 159-197.

319. Wencewicz, T.; Möllmann, U.; Long, T.; Miller, M., Is drug release necessary for antimicrobial activity of siderophore-drug conjugates? Syntheses and biological studies of the naturally occurring salmycin "Trojan Horse" antibiotics and synthetic desferridanoxamine-antibiotic conjugates. *Biometals* **2009,** *22*, 633-648.

320. Ferguson, A. D.; Coulton, J. W.; Diederichs, K.; Welte, W.; Braun, V.; Fiedler, H.-P., Crystal structure of the antibiotic albomycin in complex with the outer membrane transporter FhuA. *Protein Sci.* **2000,** *9*, 956-963.

321. Poole, K.; Neshat, S.; Krebes, K.; Heinrichs, D. E., Cloning and nucleotide sequence analysis of the ferripyoverdine receptor gene fpvA of *Pseudomonas aeruginosa*. *J. Bacteriol.* **1993,** *175*, 4597-4604.

322. Schalk, I. J.; Kyslik, P.; Prome, D.; van Dorsselaer, A.; Poole, K.; Abdallah, M. A.; Pattus, F., Copurification of the FpvA Ferric Pyoverdin Receptor of *Pseudomonas aeruginosa* with Its Iron-Free Ligand: Implications for Siderophore-Mediated Iron Transport. *Biochemistry* **1999,** *38*, 9357-9365.

323. Greenwald, J.; Hoegy, F.; Nader, M.; Journet, L.; Mislin, G. L. A.; Graumann, P. L.; Schalk, I. J., Real Time Fluorescent Resonance Energy Transfer Visualization of Ferric Pyoverdine Uptake in *Pseudomonas aeruginosa*: A Role For Ferrous Iron. *J. Biol. Chem.* **2007,** *282*, 2987-2995.

324. Mollmann, U.; Heinisch, L.; Bauernfeind, A.; Kohler, T.; Ankel-Fuchs, D., Siderophores as drug delivery agents: application of the "Trojan Horse" strategy. *Biometals* **2009,** *22*, 615-624.

325. Fernandes, P.; de Carvalho, C. C. C. R., Siderophores as "Trojan Horses": tackling multidrug resistance? *Front. Microbiol.* **2014,** *5*.

326. Meyer, C.; Scherer, M.; Schonberg, H.; Ruegger, H.; Loss, S.; Gramlich, V.; Grutzmacher, H., Coordination chemistry of phosphanyl amino acids: solid state and solution structures of neutral and cationic rhodium complexes. *Dalton Trans.* **2006,** 137-148.

327. Rastetter, W. H.; Erickson, T. J.; Venuti, M. C., Synthesis of Iron Chelators - Enterobactin, Enantioenterobactin, and a Chiral Analog. *J. Org. Chem.* **1981,** *46*, 3579-3590.

328. Agrawal, A.; DeSoto, J.; Fullagar, J. L.; Maddali, K.; Rostami, S.; Richman, D. D.; Pommier, Y.; Cohen, S. M., Probing chelation motifs in HIV integrase inhibitors. *Proc. Natl. Acad. Sci. USA* **2012,** *109*, 2251-2256.

329. Dunne, W. M., Bacterial adhesion: Seen any good biofilms lately? *Clin. Microbiol. Rev.* **2002,** *15*, 155.

330. Wittmann, S.; Schnabelrauch, M.; Scherlitz-Hofmann, I.; Mollmann, U.; Ankel-Fuchs, D.; Heinisch, L., New synthetic siderophores and their beta-lactam conjugates based on diamino acids and dipeptides. *Bioorgan. Med. Chem.* **2002,** *10*, 1659-1670.